Łukasz Rajchel

Metoda oddziałujących gęstości monomerowych i jej zastosowanie do kompleksów van der Waalsa

Praca doktorska wykonana w Pracowni Chemii Kwantowej
Wydziału Chemii Uniwersytetu Warszawskiego
pod kierunkiem prof. dr. hab. Grzegorza Chałasińskiego

Warszawa

MMX

Łukasz Rajchel

A DFT Approach to van der Waals Complexes via Interacting Monomer Densities

A dissertation submitted in partial fulfillment of the requirements
for the degree of Doctor of Philosophy in Chemistry
Thesis supervisor: prof. Grzegorz Chałasiński

Warsaw

mmx

Contents

Podziękowania

- *Przede wszystkim gorąco dziękuję mojemu nieocenionemu promotorowi, prof. Grzegorzowi Chałasińskiemu z Pracowni Chemii Kwantowej Wydziału Chemii UW, a także prof. Małgorzacie Szczęśniak z Wydziału Chemii Oakland University (USA), de facto będącej moim drugim promotorem, za wszelką pomoc udzieloną mi w czasie pracy zarówno w Polsce, jak i USA.*

- *Współkwantowcom z Pracowni Chemii Kwantowej (Konradowi, Monice, Wojtkowi, Piotrkowi, Filipowi, Edycie, Markowi, Leonidowi, Massimo, i młodszym — Michałowi i Marcinowi) dziękuję serdecznie za wspaniałą atmosferę w Pracowni i za wyśmienite towarzystwo, zarówno w samej Pracowni, jak i na szlakach Polski i Słowacji.*

- *Współoaklandowcom z Wydziału Chemii Oakland University (Gosi, Krysi, Adamowi i Piotrkowi) — za pomoc i takoż doborowe towarzystwo w czasie moich licznych pobytów na tamtejszym Wydziale.*

- *Piotrkowi Pieniążkowi, guru SF-EOM, za wprowadzenie mnie w tajniki tejże metody w czasie mojego pobytu na Wydziale Chemii Uniwersytetu Południowej Kalifornii.*

- *Wreszcie — dziękuję moim Rodzicom i Siostrze za całą okazaną mi pomoc.*

Motto

- Dyspersjo! Energio moja! ty jesteś jak zdrowie;
  Ile cię trzeba cenić, ten tylko się dowie,
  Kto cię stracił.

  (A. Mickiewicz, *Pan Tadeusz*, *Inwokacja*[1])

- Gdybym mówił językami ludzi i aniołów, a dyspersji bym nie miał,
  stałbym się jak miedź brzęcząca albo cymbał brzmiący.
  (...)
  Dyspersja nie zazdrości,
  nie szuka poklasku,
  (...)
  nie cieszy się z niesprawiedliwości,
  lecz współweseli się z indukcją, elektrostatyką i wymianą.

  (Św. Paweł z Tarsu, *Pierwszy list do Koryntian*[1])

[1]Oba powyższe cytaty, jak to zazwyczaj bywa w chemii kwantowej, są zaledwie *przybliżeniami* tych dokładnych w pierwszym rzędzie.

Chapter 1

Introduction

1.1 Significance of Intermolecular Forces

Interactions between closed-shell atoms and molecules are considerably weaker than typical chemical bonds (tens kJ/mol vs. hundreds kJ/mol), yet they govern a wide spectrum of chemical and physical phenomena: from protein structure, solvation and self-assembly to the properties of materials. A molecular-level description of these phenomena requires knowledge of intermolecular interaction potentials which can be obtained either from the analysis of experimental data or from direct computations based on the first principles. Present-day *ab initio* methods are capable of describing these interactions with great accuracy even for systems as large as benzene dimer [1] or the water octamer (see e.g. the exhaustive bibliography in Ref. 2).

Physically speaking, intermolecular interactions are of electromagnetic nature and are due to the electrostatic interactions between charged particles constituting the interacting molecules: electrons and nuclei. Qualitative understanding of these interactions has progressed due in large measure to the developments in the perturbation theory of intermolecular forces [3] which recognizes the interaction energy as a composite of the four fundamental building blocks: electrostatic, exchange, induction, and dispersion. These terms have different physical origins and their importance varies from case to case. On the one hand, assembling the interaction energy from these building blocks has a great interpretative and predictive power. On the other, any reliable method of quantitative modeling of complex systems, e.g. via molecular dynamics or Monte Carlo simulations must give proper account of each of these components.

1.2 Calculation of Intermolecular Interactions

For a two-body system, interaction energy is defined as the difference between the dimer's and isolated monomers' energies:[1]

$$E_{\text{int}} = E_{\text{AB}} - E_{\text{A}} - E_{\text{B}}, \tag{1.1}$$

All calculations of intermolecular interaction energies are performed in the Born-Oppenheimer approximation, usually on a grid covering some representative geometries of the dimer. The relative orientation of the monomers' body-fixed coordinate systems is depicted by the intermolecular vector **R**.

In general, there are two main-stream tools for calculating intermolecular forces: supermolecular method and perturbational approach and both have their advantages and downsides. Supermolecular approach is in general easily applicable at any intermolecular distance and nowadays it is virtually a black-box method, implemented in almost all electronic structure software packages. However, it relies on the cancellation of errors in calculations of Eq. (1.1) terms and is plagued by the notorious basis-set superposition error (BSSE) [4]. Moreover, the result of the method is just a single number representing the whole intermolecular interaction energy that gives no physical insight into the nature of the interaction, measuring only its strength. The perturbational method, on the other hand, yields a decomposition of E_{int} into well-defined physical contributions and the calculation is free of the BSSE. Nevertheless, the perturbation method remains more complex and more difficult to apply, and there are just a few programs with its implementation (Molpro [5], SAPT2008 [6]).

1.2.1 Supermolecular Approach

In a supermolecular approach, interaction energy is calculated directly from Eq. (1.1) using a suitable *ab initio* method, e.g. HF, MP2, MRCI, CCSD(T). Owing to its usual usage simplicity, the method is the most common tool in the field. See Refs. 7 for an exhaustive review on the supermolecular approach.

1.2.2 Perturbative Methods

As we will need a few concepts introduced in the perturbation theory hereafter, we need to elaborate on the method in more detail.

Perturbative methods are based on the assumption that the interaction energy is small relative to total system energy which is reflected in the following

[1] See Appendix A for the summary of acronyms and Appendix B for the details on the notation used throughout the Thesis.

partitioning of the AB dimer hamiltonian:

$$\begin{aligned}\hat{H} &= \sum_{i\in AB}\left(-\frac{1}{2}\Delta_{\mathbf{r}_i} - \sum_{\alpha\in\mathcal{AB}}\frac{Z_\alpha}{|\mathbf{r}_i-\mathbf{R}_\alpha|}\right) + \sum_{i<j\in AB}\frac{1}{r_{ij}} + \sum_{\alpha<\beta\in\mathcal{AB}}\frac{Z_\alpha Z_\beta}{R_{\alpha\beta}} = \\ &= \hat{H}_\mathrm{A} + \hat{H}_\mathrm{B} + \hat{V}. \end{aligned} \tag{1.2}$$

Thus, monomer A's hamiltonian reads

$$\begin{aligned}\hat{H}_\mathrm{A} &= \sum_{i\in A}\left(-\frac{1}{2}\Delta_{\mathbf{r}_i} + \hat{v}_\mathrm{A}^\mathrm{ne}(\mathbf{r}_i)\right) + \sum_{i<j\in A}\frac{1}{r_{ij}} + \sum_{\alpha<\beta\in\mathcal{A}}\frac{Z_\alpha Z_\beta}{R_{\alpha\beta}} = \\ &= \sum_{i\in A}\hat{h}_\mathrm{A}(\mathbf{r}_i) + \hat{V}_\mathrm{A}^\mathrm{ee} + V_\mathrm{A}^\mathrm{nn}, \end{aligned} \tag{1.3}$$

where the nuclear potential of monomer A is

$$\hat{v}_\mathrm{A}^\mathrm{ne}(\mathbf{r}) = -\sum_{\alpha\in\mathcal{A}}\frac{Z_\alpha}{|\mathbf{r}-\mathbf{R}_\alpha|} \tag{1.4}$$

and the nuclear-nuclear repulsion part is simply a constant in clamped-nuclei approximation. From (1.2) and (1.3), the interaction operator is readily found to be

$$\hat{V} = \sum_{i\in A}\sum_{k\in B}\frac{1}{r_{ik}} - \sum_{i\in A}\sum_{\beta\in\mathcal{B}}\frac{Z_\beta}{|\mathbf{r}_i-\mathbf{R}_\beta|} - \sum_{k\in B}\sum_{\alpha\in\mathcal{A}}\frac{Z_\alpha}{|\mathbf{r}_k-\mathbf{R}_\alpha|} + \sum_{\alpha\in\mathcal{A}}\sum_{\beta\in\mathcal{B}}\frac{Z_\alpha Z_\beta}{R_{\alpha\beta}}. \tag{1.5}$$

To emphasize that $\hat{V}$ is a perturbation, the total hamiltonian is assumed in the form

$$\hat{H} = \hat{H}_\mathrm{A} + \hat{H}_\mathrm{B} + \lambda\hat{V} = \hat{H}_0 + \lambda\hat{V} \tag{1.6}$$

with $\lambda \in \langle 0;1\rangle$ being some scaling parameter, which when equated to unity restores the physical description of a system. It is also assumed that the unperturbed hamiltonian wavefunctions are known:

$$\begin{cases}\hat{H}_\mathrm{A}\psi_\mathrm{A}^0 = E_\mathrm{A}^0\psi_\mathrm{A}^0 \\ \hat{H}_\mathrm{B}\psi_\mathrm{B}^0 = E_\mathrm{B}^0\psi_\mathrm{B}^0\end{cases}, \tag{1.7}$$

and the dimer function is simply their product,

$$\psi_0 = \psi_\mathrm{A}^0\psi_\mathrm{B}^0. \tag{1.8}$$

However, such an approach, termed polarization perturbation theory, suffers from the lack of the exchange antisymmetry between monomer functions. As a remedy,

the function may be antisymmetrized, as is the case for the symmetry-adapted perturbation theory (SAPT) [3]:

$$\psi_0' = \hat{\mathscr{A}}\psi_\mathrm{A}^0\psi_\mathrm{B}^0. \tag{1.9}$$

The function (1.9) is no longer an eigenfunction of $\hat{H}_0$, however, the exchange effects are properly included and the method yields correct energies even at the repulsive part of the potential energy curve. The first-order SAPT energy is

$$E^{(1)} = \frac{\langle\psi_0|\hat{V}\hat{\mathscr{A}}|\psi_0\rangle}{\langle\psi_0|\hat{\mathscr{A}}\psi_0\rangle} = E_\mathrm{elst}^{(1)} + E_\mathrm{exch}^{(1)} \tag{1.10}$$

and it contains electrostatic and exchange-repulsion interaction energies. Second order energy is a sum of induction and dispersion and their exchange counterparts,

$$E^{(2)} = E_\mathrm{ind}^{(2)} + E_\mathrm{exch\text{-}ind}^{(2)} + E_\mathrm{disp}^{(2)} + E_\mathrm{exch\text{-}disp}^{(2)}. \tag{1.11}$$

In the standard HF-based SAPT (SAPT-HF) the wavefunctions are obtained from self-consistent field (SCF) calculations for the monomers, hence

$$\begin{cases} \psi_\mathrm{A}^0 = & |(a_i^0\alpha\ a_i^0\beta)_{i\in A}\rangle \\ \psi_\mathrm{B}^0 = & |(b_k^0\alpha\ b_k^0\beta)_{k\in B}\rangle \end{cases}, \tag{1.12}$$

where the unperturbed monomer orbitals satisfy Hartree-Fock (HF) equations, e.g. for monomer A:

$$\hat{f}_\mathrm{A}(\mathbf{r})a_i^0(\mathbf{r}) = \epsilon_{\mathrm{A},i}^0 a_i^0(\mathbf{r}). \tag{1.13}$$

The Fock operator of monomer A reads

$$\hat{f}_\mathrm{A}(\mathbf{r}) = \hat{h}_\mathrm{A}(\mathbf{r}) + \hat{v}_\mathrm{A}^\mathrm{HF}(\mathbf{r}) = \hat{h}_\mathrm{A}(\mathbf{r}) + \hat{\jmath}_\mathrm{A}(\mathbf{r}) + \hat{v}_\mathrm{A}^\mathrm{exch}(\mathbf{r}), \tag{1.14}$$

where the HF potential ($\hat{v}_\mathrm{A}^\mathrm{HF}$) consists of Coulomb ($\hat{\jmath}_\mathrm{A}$) and exchange ($\hat{v}_\mathrm{A}^\mathrm{exch} = -\hat{k}_\mathrm{A}$) operators, respectively [8]. The action of these operators on monomer A's orbitals may be conveniently represented with the help of the one-particle density functions [9]:

$$\hat{\jmath}_\mathrm{A}(\mathbf{r})a_i^0(\mathbf{r}) = \left(\int_{\mathbb{R}^3} \frac{\rho_\mathrm{A}^0(\mathbf{r}')}{|\mathbf{r}-\mathbf{r}'|}\, d^3\mathbf{r}'\right) a_i^0(\mathbf{r}), \tag{1.15}$$

and

$$\hat{v}_\mathrm{A}^\mathrm{exch}(\mathbf{r})a_i^0(\mathbf{r}) = -\frac{1}{2}\int_{\mathbb{R}^3} \frac{\rho_\mathrm{A}^0(\mathbf{r};\mathbf{r}')}{|\mathbf{r}-\mathbf{r}'|} a_i^0(\mathbf{r}')\, d^3\mathbf{r}'. \tag{1.16}$$

The one-particle density function [or one-electron reduced density matrix (1-DM)] reads

$$\rho_{\mathrm{A}}^{0}(\mathbf{r};\mathbf{r}') = N_{\mathrm{A}} \sum_{\sigma_1,\sigma_2,\ldots,\sigma_{N_{\mathrm{A}}}} \int_{\mathbb{R}^3} \ldots \int_{\mathbb{R}^3} \psi_{\mathrm{A}}^{0}\left(\mathbf{r};\sigma_1;(\mathbf{r}_i;\sigma_i)_{i=2}^{N_{\mathrm{A}}}\right) \psi_{\mathrm{A}}^{0*}\left(\mathbf{r}';\sigma_1;(\mathbf{r}_i;\sigma_i)_{i=2}^{N_{\mathrm{A}}}\right) d^3\mathbf{r}_i \ldots d^3\mathbf{r}_{N_{\mathrm{A}}}, \tag{1.17}$$

its diagonal part being the electron density,

$$\rho_{\mathrm{A}}^{0}(\mathbf{r}) = \rho_{\mathrm{A}}^{0}(\mathbf{r};\mathbf{r}). \tag{1.18}$$

For ψ_{A}^{0} in the form of single Slater determinant (1.12) the expression for the density (1.17) simplifies to

$$\rho_{\mathrm{A}}^{0}(\mathbf{r};\mathbf{r}') = 2\sum_{i\in A} a_i^0(\mathbf{r}) a_i^{0*}(\mathbf{r}'). \tag{1.19}$$

The main drawback of the SAPT-HF approach is the neglection of the electronic correlation within monomers, which is inherent to the HF method itself. The problem may be solved through the introduction of the Møller–Plesset (MP) perturbation operators on each monomer,

$$\hat{W}_{\mathrm{A}} = \hat{H}_{\mathrm{A}} - \hat{F}_{\mathrm{A}} = \hat{H}_{\mathrm{A}} - \sum_{i\in A} \hat{f}_{\mathrm{A}}(\mathbf{r}_i). \tag{1.20}$$

The resulting many-body formulation of SAPT, MB-SAPT [10], is formally a triple perturbation theory with the dimer hamiltonian partitioned as

$$\hat{H} = \hat{F}_{\mathrm{A}} + \hat{F}_{\mathrm{B}} + \lambda\hat{V} + \xi_{\mathrm{A}}\hat{W}_{\mathrm{A}} + \xi_{\mathrm{B}}\hat{W}_{\mathrm{B}}. \tag{1.21}$$

The MB-SAPT energies are marked with two numbers, the first being the order of perturbation in $\hat{V}$, the second denoting the sum of perturbation orders in $\hat{W}_{\mathrm{A}}$ and $\hat{W}_{\mathrm{B}}$. Thus, SAPT-HF energies are appended with zero, e.g. $E_{\mathrm{disp}}^{(20)}$, since no intramonomer correlation correction is included. The main drawback of MB-SAPT is its complexity and the need for the inclusion of high-order corrections to obtain reliable energies.

As another cure for the correlation problem, SAPT can be combined with the density functional theory (DFT) method (see Sec. 1.2.4).

1.2.3 Iterative Approaches

The application of perturbation methods to the intermolecular interactions calculations is not straightforward and well-defined since the definition of the order

of perturbation is not unique. Moreover, the expansion of interaction energy components in a parturbational series may not be convergent, as is the case for induction. In consequence, many iterative schemes for computation of interaction energies have been proposed so far. The main advantage of an iterative approach is that its results, provided the calculations have converged, are not affected by higher-order terms as is always the case in perturbation theory where one has to cut the perturbation expansion at some order (usually a second or a third one).

Several iterative decomposition schemes of supermolecular E_{int} have been proposed, e.g. by Kitaura and Morokuma [11], Stone and Alderton [12], Gutowski and Piela [13] or Chałasiński and Szczęśniak [14]. Components of E_{int} have been modeled after perturbational contributions already mentioned in the Sec. 1.2.2. All these schemes include Heitler-London (HL) interaction energy as their starting point — the zeroth iteration:

$$E_{\text{int}}^{\text{HL}} = \frac{\langle \hat{\mathscr{A}}\psi_0 | \hat{H} | \hat{\mathscr{A}}\psi_0 \rangle}{\langle \hat{\mathscr{A}}\psi_0 | \hat{\mathscr{A}}\psi_0 \rangle} - \langle \psi_{\text{A}}^0 | \hat{H}_{\text{A}} | \psi_{\text{A}}^0 \rangle - \langle \psi_{\text{B}}^0 | \hat{H}_{\text{B}} | \psi_{\text{B}}^0 \rangle \,. \tag{1.22}$$

Various division techniques used to obtain the total interaction energy differ in the ΔE term,

$$\Delta E = E_{\text{int}} - E_{\text{int}}^{\text{HL}}. \tag{1.23}$$

Ideally, ΔE should include all the induction, dispersion and exchange effects to infinite order, thus yielding, together with $E_{\text{int}}^{\text{HL}}$, the exact interaction energy of a system. In the Pauli blockade method (to which we will turn our attention later), ΔE is called the deformation energy, E_{def}, and includes all induction and exchange-induction effects up to an infinite order [13].

1.2.4 DFT in Intermolecular Forces

The supermolecular method within DFT has been extensively applied to study interactions, with rather disappointing outcome [15]. It became clear that the standard functionals are not a proper tool within the supermolecular approach. There have been numerous attempts to solve that problematic issue.

The simplest way to obtain reliable results is perhaps the DFT + dispersion (DFT-D) approach in which the supermolecular DFT interaction energy is supplemented with the dispersion correction obtained in a empirical or semi-empirical way [16]. However, the DFT supermolecular interaction energy itself contains non-local contributions, among them the dispersion. Thus, completing such an energy with dispersion correction is neither accurate nor well-justified, unavoidably leading to a so-called *double-counting* problem. Moreover, the use of empirical parameters has the usual drawbacks of such methods: the restriction to a certain class of systems and failure to describe other types of interactions.

Another approach is to design the density functionals (DFs) restoring weak interactions through the fitting to the training set of systems. This way the interaction energy is obtained in one go and does not need to be dispersion-corrected. M05 and M06 family of functionals [17] is a representative example of that approach. These functionals are highly parametrized (several dozens of parameters) and empirical. They prove quite successful, yet the non-local physics of the dispersion is expressed through local or semi-local potentials.

More rigorous approach is taken by the family of DFs explicitly including non-local contributions to exchange-correlation (xc) potentials [18] or based on the exchange dipole moment [19]. Conceptually similar is the idea of using the exact exchange (i.e., HF one) for the long-range part of potential and the local [i.e., Kohn-Sham (KS) one] for its short-range part, smoothly switching between the two with the use of the error function [20]. The range separation approach treats the long-range in and off monomers on equal footing, however, it requires an *arbitrary* parameter switching on the exact exchange at a certain *arbitrary* distance.

DFT-based formulation of SAPT (SAPT-DFT) [21] was a major step in the field. Though not very efficient for big systems (e.g., compared to DFT-D), it is very trustworthy and accurate. In particular, SAPT-DFT yields coupled dispersion energy between the monomers described by the densities from the DFT calculations. Unfortunately, the perturbation theory diverges for the short intersytem distances, mainly due to the lack of strict and consistent treatment of exchange-induction interactions. That restricts SAPT-DFT to non-covalent interactions.

Despite success for small- and medium-sized systems, theoretical modeling of intermolecular forces in large supramolecular structures, crystals, polymers, and nano-materials presents a serious challenge. For *dense matter*, DFT has firmly established its usefulness to account for structure, cohesion and other static properties. To extend DFT's usefulness to the large classes of matter with both high-density fragments with chemical and metallic bonding, and low-density regions, primarily governed by van der Waals forces, a general density functional approach that includes all noncovalent interactions is necessary.

The issues to which solutions are at present of paramount importance are:

- accurate, seamless, and efficient incorporation of long-range electron correlation effects.
- qualitative and quantitative control of all noncovalent interactions that enter the supermolecular DFT interaction energies for different functionals.

The two problems are interrelated as popular DFT schemes are notorious for both neglecting important non-local (dispersion) contributions as well as producing

erroneous artifacts, e.g. double-counting of some of the non-local terms. This is due to the simplified physics of the exchange-correlation potentials, on one side, and to obscure semiempirical parameters used to make up for the resulting deficiencies, on the other. Despite major progress accomplished over the last decade to resolve these issues, they require further research.

Thus, the primary concern of my doctoral work has been to investigate the contents of the supermolecular DFT interaction energies, and aid to alleviate the above two problems. To this end, I have designed a new approach to DFT in terms of mutually interacting monomer densities, which assures that all necessary noncovalent local ingredients are properly accounted for by the so called dispersion-free supermolecular DFT interaction energy, while the non-local terms are confined to the separately evaluated and *a posteriori* added dispersion.

1.3 Many Body Contributions

For dense systems containing large number of molecules (condensed phases, clusters) the many body contributions to $E_{\rm int}$ may be substantial [22–24]. The interaction energy for a system composed of n monomers: $\mathrm{A}_1\mathrm{A}_2\ldots\mathrm{A}_n$ is

$$E_{\rm int} = E_{\mathrm{A}_1\mathrm{A}_2\ldots\mathrm{A}_n} - \sum_{i=1}^{n} E_{\mathrm{A}_n}, \tag{1.24}$$

and it readily reduces to the two-body formula (1.1) for $n = 2$. The many-body expansion of (1.24) reads

$$E_{\rm int} = \Delta E_{\rm int}^{(2,n)} + \Delta E_{\rm int}^{(3,n)} + \ldots + \Delta E_{\rm int}^{(n,n)}, \tag{1.25}$$

the m-body contribution being $(m < n)$

$$\Delta E_{\rm int}^{(m,n)} = \sum_{i_1=1}^{n-m+1} \sum_{i_2=i_1+1}^{n-m+2} \ldots \sum_{i_m=i_{m-1}+1}^{n} \epsilon^{(m,n)}(\mathrm{A}_{i_1}\mathrm{A}_{i_2}\ldots\mathrm{A}_{i_m}), \tag{1.26}$$

where

$$\begin{aligned}\epsilon^{(m,n)}(\mathrm{A}_{i_1}\mathrm{A}_{i_2}\ldots\mathrm{A}_{i_m}) &= E_{\rm int}(\mathrm{A}_{i_1}\mathrm{A}_{i_2}\ldots\mathrm{A}_{i_m}) + \\ &- \left(\sum_{k=1}^{m-1}\sum_{l=k+1}^{m} \epsilon^{(2,m)}(\mathrm{A}_{i_k}\mathrm{A}_{i_l}) + \sum_{k=1}^{m-2}\sum_{l=k+1}^{m-1}\sum_{m=l+1}^{m} \epsilon^{(3,m)}(\mathrm{A}_{i_k}\mathrm{A}_{i_l}\mathrm{A}_{i_m}) + \ldots + \right. \\ &\left. + \sum_{k=1}^{2}\sum_{l=k+1}^{3} \ldots \sum_{q=p+1}^{m} \epsilon^{(m-1,m)}(\mathrm{A}_{i_k}\mathrm{A}_{i_l}\ldots\mathrm{A}_{i_q}) \right)\end{aligned} \tag{1.27}$$

with

$$E_{\rm int}(\mathrm{A}_{i_1}\mathrm{A}_{i_2}\ldots\mathrm{A}_{i_m}) = E_{\mathrm{A}_{i_1}\mathrm{A}_{i_2}\ldots\mathrm{A}_{i_m}} - \sum_{k=1}^{m} E_{\mathrm{A}_{i_k}}. \tag{1.28}$$

The $\Delta E_{\rm int}^{(n,n)}$ term in (1.25) is calculated from that very expression. The sum (1.26) runs over distinctive subsets of m-mers and contains $\binom{n}{m}$ terms.

1.4 Motivation and Goals of the Thesis

Dispersion energy plays a unique role in intermolecular interactions. On one side, it is an omnipresent factor binding atoms, molecules and clusters. Although minute compared to covalent forces, it may be qualitatively decisive if the covalent, electrostatic and induction interactions are absent. On the other hand, reliable modeling of dispersion by quantum mechanical calculations poses a real challenge due to long-range electron correlation effects engaging interacting monomers. It requires both the advanced methods to account for many-electron correlation effects and large highly polarized and diffuse basis sets. Not surprisingly, it has also become the major challenge for DFT which notoriously has problems with the long-range correlation effects.

A widespread and convenient approach to intermolecular interaction calculations is to evaluate the hard dispersion part and the facile non-dispersion part separately. This is the idea behind the vintage SCF-D model introduced by Ahlrichs et al. [25], which was later grafted in DFT in the form of DFT-D methods. It is worthwhile to note that the separation of the two components comes about in a natural way both in SAPT-HF and SAPT-DFT. The SCF-D model has also been generalized for systems with important static-correlation effects described by the CASSCF in the form of CAS-D approximation [26, 27].

The rigorous DFT-D model requires precise separation of dispersion and dispersionless components of the supermolecular interaction energy, the task which has not been previously undertaken (see, however, a recent work of Pernal et al. [28] where a similar goal is pursued through the parameter fitting). To derive such an approach has been the primary motive of this Dissertation.

At the very first phase of my doctoral work, when confronted with the problem of transition metal high-spin polarized dimers, I have used the separation into dispersion and non-dispersion components using the SAPT for the former and the CASSCF supermolecular interaction energy for the latter [27]. The manuscript resulting from that work is enclosed below, and constitutes the first contribution to my doctoral work. That research has made me confident that the original SCF-D approach may be generalized and made accurate by replacing SCF by other definitions of the non-dispersive components, either within the wavefunction framework or on the DFT platform.

More specifically, the major goals pursued in the Thesis are:

- rigorous derivation of the supermolecular DFT interaction energy via the mutual polarization of the monomer densities, implementation in the framework of standard codes, and application to representative non-covalently bound complexes. Such a formulation provides a framework to decompose the interaction energy into components related to monomer densities and properties and to define the DFT analogs of the HL interaction energy and the DFT deformation energy.

- derivation of a novel, dispersionless DFT approach for calculations of intermolecular interactions based on the separation of intra- and intermolecular types of correlation, followed by the implementation and application to representative noncovalently bound complexes.

Interactions of transition metal atoms in high-spin states: Cr_2, Sc–Cr, and Sc–Kr

Łukasz Rajchel[a)]
Department of Chemistry, Oakland University, Rochester, Michigan 48309-4477, USA and Faculty of Chemistry, University of Warsaw, Pasteura 1, 02-093 Warszawa, Poland

Piotr S. Żuchowski[b)]
Faculty of Chemistry, University of Warsaw, Pasteura 1, 02-093 Warszawa, Poland

Jacek Kłos
Department of Chemistry and Biochemistry, University of Maryland, College Park, Maryland 20742-2021, USA

Małgorzata M. Szczęśniak
Department of Chemistry, Oakland University, Rochester, Michigan 48309-4477, USA

Grzegorz Chałasiński
Department of Chemistry, Oakland University, Rochester, Michigan 48309-4477, USA and Faculty of Chemistry, University of Warsaw, Pasteura 1, 02-093 Warszawa, Poland

(Received 30 August 2007; accepted 11 October 2007; published online 26 December 2007)

The high-spin van der Waals states are examined for the following dimers: Cr_2 ($^{13}\Sigma_g^+$), Sc–Cr ($^8\Sigma^+$, $^8\Pi$, $^8\Delta$), and Sc–Kr ($^2\Sigma^+$, $^2\Pi$, $^2\Delta$). These three systems offer a wide range of van der Waals interactions: anomalously strong, intermediate, and typically weak. The single-reference [coupled cluster with single, double, and noniterative triple excitations, RCCSD(T)] method is used in the calculations for all three systems. In addition, a range of configuration-interaction based methods is applied in Cr_2 and Sc–Cr. The three dimers are shown to be bound by the dispersion interaction of varying strength. In a related effort, the dispersion energy and its exchange counterpart are calculated using the newly developed open-shell variant of the symmetry-adapted perturbation theory (SAPT). The restricted open-shell time-dependent Hartree-Fock linear response function is used in the calculations of the dispersion energy in Sc–Cr and Sc–Kr calculations, while the restricted open-shell time-dependent density functional linear response function is used for Cr_2. A hybrid method combining the repulsive restricted open-shell Hartree-Fock (or complete active space self-consistent field) interaction energy with the dispersion and exchange-dispersion terms is tested against the RCCSD(T) results for the three complexes. The Cr_2 ($^{13}\Sigma_g^+$) complex has the well depth of 807.8 cm^{-1} at the equilibrium distance of $6.18a_0$ and the dissociation energy of 776.8 cm^{-1}. The octet-state Sc–Cr is about four times more strongly bound with the order of well depths of $^8\Delta > {}^8\Pi > {}^8\Sigma^+$ and a considerable anisotropy. The enhanced bonding is attributed to the unusually strong dispersion interaction. Sc–Kr ($^2\Sigma^+$, $^2\Pi$, $^2\Delta$) is a typical van der Waals dimer with well depths in the range of 81 cm^{-1} ($^2\Delta$), 84cm^{-1} ($^2\Sigma^+$), and 86 cm^{-1} ($^2\Pi$). The hybrid model based on SAPT leads to results which are in excellent qualitative agreement with RCCSD(T) for all three interactions. © *2007 American Institute of Physics*. [DOI: 10.1063/1.2805390]

I. INTRODUCTION

Interactions involving transition metals (TMs) are interesting for a variety of reasons. Because of the incompletely filled $(n-1)d$ subshell, they are open-shell species which can display a wide diversity of bonding types, from van der Waals, to chemical bonds, to multiple metal-metal bonds.[1,2] While the chemically bound TM dimers have been the subjects of intense investigations (see, e.g., Refs. 3 and 4) the van der Waals states of these species have remained virtually unexplored. These spin-polarized states are of great interest to the cold-matter community. Atoms with partially filled $(n-1)d$ subshell and nonzero orbital angular momentum reveal anisotropic properties. That is, in the interactions with other structureless targets, their electronic states further split into manifolds of adiabatic states. The magnitude of this anisotropy is crucial to the success of the collisional cooling of these atoms in a bath of a buffer gas which is the first step in magnetic trapping experiments.[5] Our recent work has shown that in transition metals this anisotropy is unusually small because of the shielding effect of the outer ns^2 electrons.[6] This suppressed anisotropy offers a chance that atoms with nonzero orbital angular momentum may some day be cooled to achieve quantum degeneracy. The atoms with a half-filled $(n-1)d$ subshell are isotropic in the orbital angular momentum sense, but are "magnetically anisotropic" due to the high magnetic moments which give rise to long-range anisotropic

a)Electronic mail: rajchel@oakland.edu.
b)Electronic mail: pzuch@tiger.chem.uw.edu.pl.

magnetic dipole-dipole interactions.[7] These properties are of intense interest to quantum information processing.

The Zeeman relaxation in cold collisions of Sc and Ti with He buffer gas was investigated by Hancox *et al.*[5] The results indicated that compared to the main-group atoms, the rate of inelastic collisions of these atoms with He is several orders of magnitude smaller.[8] Chromium was buffer-gas cooled and magnetically trapped by Weinstein *et al.*[9] Magnetic trapping selects atoms in low-field seeking states (i.e., states the maximum projection of spin onto the magnetic field axis). Collisions of such atoms may lead to inelastic spin depolarization and trap loss. By contrast, if the atoms are trapped in their high-field seeking states, they can be cooled to quantum degeneracy. This task was recently accomplished for chromium by Griesmaier *et al.*[10] Cr-BEC involves a spin-polarized van der Waals state. Further experiments reported observations of Feshbach resonances,[11] which led to the determination of the C_6 and C_8 coefficients for Cr–Cr pair interactions and to the value of the *s*-wave scattering length for the high-spin $^{13}\Sigma_g^+$ state.

The calculations of intermolecular potentials of transition metal atoms are very challenging for *ab initio* theory because of the multireference character of their wave functions, close proximity of excited states, and many types of correlation. In many instances, the symmetry of ground state is uncertain. Gutsev *et al.*[12,13] studied a number of first-row transition metal dimers by the density functional theory (DFT) based on the unrestricted Kohn-Sham treatment. The aim of these studies was to determine ground states. The Cr_2 interaction potentials for the Σ states with total spin S ranging from 0 to 6 was investigated by Pavlović *et al.*[14] using the complete active space second-order perturbation theory (CASPT2). They combined the short- and intermediate-range *ab initio* CASPT2 potentials with the long-range empirically estimated C_6/R_6 term to generate the potential functions for the elastic cross-section calculations for the $^{13}\Sigma_g^+$ state. They found that the value of the *s*-wave scattering length for this state depends dramatically on the choice of the C_6 coefficient. There is also considerable experimental interest in spin-polarized heterodimers of TM atoms. For example, Cr–Mn was recently confined in a magnetic trap at subkelvin temperature using buffer-gas cooling.[15] The interspecies inelastic rate constant was also measured in this experiment. In order to determine if similar cotrapping is possible for Cr with anisotropic TM atoms, one needs to determine the magnitude of the splitting of adiabatic interaction potentials. Sc–Cr can serve as a convenient model for such a determination in addition to being computationally challenging.

The purpose of the present paper is to calculate adiabatic interaction potentials for the highest-spin states of the Cr–Cr and Sc–Cr interactions by a single-reference coupled-cluster method and a variety of multireference treatments including configuration interaction (MRCI), the averaged quadratic coupled-cluster (AQCC), and the configuration-interaction second-order perturbation theory (CIPT2).[16] In order to determine the appropriate methodology to study these systems, we will also explore the newly developed open-shell variant of the symmetry-adapted perturbation theory (SAPT).[17] The third objective of this work is to understand the properties of Sc–Cr in its van der Waals state. This goal will be accomplished by comparing and contrasting this system with a typical van der Waals complex Sc–Kr.

II. THEORY

A. Electronic properties of Cr_2, Sc–Cr, and Sc–Kr

Ground states of Cr and Sc nominally correspond to the $[Ar]3d^54s^1$ and $[Ar]3d^14s^2$ configurations, respectively, and thus result in ^7S and ^2D ground-state terms. The high-spin states correlating with these asymptotes are for Cr_2 the $^{13}\Sigma_g^+$ state, for Sc–Cr the $^8\Sigma^+$, $^8\Pi$, and $^8\Delta$ states, and for Sc–Kr the $^2\Sigma^+$, $^2\Pi$, and $^2\Delta$ states. All calculations were performed in the C_{2v} (for heteronuclear systems) and D_{2h} (for the chromium dimer) abelian point subgroups of $C_{\infty v}$ and $D_{\infty h}$ groups, respectively.

B. Methods

One of the most accurate methods for the study of high-spin open-shell van der Waals states is an open-shell variant of the coupled-cluster (CC) method, such as the partially spin-adapted restricted coupled cluster method with single, double, and noniterative triple excitations RCCSD(T) (Ref. 18) applied within the framework of the supermolecular method. This approach is limited to the states which can be described in zeroth order by a single configuration. When this is in doubt, the MRCI, or some alternative, should be employed. Unfortunately, the lack of size extensivity in many such approaches makes them difficult to apply within the supermolecular framework. The corrections for size extensivity are only approximate and a correction for basis set superposition error cannot be rigorously applied.[19]

Even if the states are nominally single reference, obtaining meaningful CC interaction potentials is not guaranteed. Transition metal dimers are notorious for intruder-state problems, symmetry-breaking, and CC convergence problems. In such circumstances the open-shell SAPT may provide much needed relief. Such theory was proposed in 1980 by Chałasiński and Szalewicz[20] and implemented within the unrestricted Hartree-Fock formalism with uncoupled Hartree-Fock induction and dispersion energies by Cybulski *et al.*[21] The applications included a number of open-shell complexes including systems with degenerate ground states.[22–24] Later a more advanced treatment of open-shell dispersion energy based on time-dependent HF (TDHF) linear response functions (propagators) was developed[25] (see also Hettema and Wormer[26]) and successfully applied to high-spin open-shell systems such as $^5\Sigma_g^+$ state of He_2 (long range) and to a Π-state complex $O(^3P)$-H_2.[27] Recently, a new and promising treatment for high-spin open-shell has been developed which combines SAPT with restricted open-shell Kohn-Sham description of monomers.[17] This approach, referred to as SAPT(DFT), employs the open-shell TDDFT polarization propagators in the treatment of the induction and dispersion energies within adiabatic local density approximation. It is at present applicable to the interactions of nondegenerate high-spin cases.

In this paper the interaction potentials for the above listed states of Cr_2, Sc–Cr, and Sc–Kr are calculated using

RCCSD(T) with large all-electron basis sets the details of which are described in the respective sections. The role of scalar relativistic Douglas-Kroll-Hess[28,29] effects is explored, as well as the influence of core-valence correlation on the potentials. The following multireference approaches were applied to confirm the RCCSD(T) results. In ($^{13}\Sigma_g^+$) Cr_2 the averaged quadratic coupled cluster[30] (AQCC) and CIPT2 (Ref. 16) were employed. CIPT2 is a relatively new hybrid method in which excitations from the active space are treated by MRCI and the remaining excitations by perturbation theory. It proved quite successful in the study of the formidable $X\ ^1\Sigma_g^+$ state of Cr_2.[16] In ($^8\Sigma^+$, $^8\Pi$, $^8\Delta$) Sc–Cr the internally contracted MRCI (Ref. 31 and 32) was applied. CIPT2 and MRCI employed Davidson's correction to approximate the effect of quadruple excitations, denoted CIPT2+Q and MRCI+Q, respectively. The reference functions for all the multireference calculations were obtained from state-averaged complete active space self consistent field (CASSCF) method which employed the full valence active space (unless stated otherwise).

Another confirmation of the obtained potentials and their interpretation on physical grounds is carried out with the SAPT method. The Sc–Cr and Sc–Kr calculations employ SAPT formulated with respect to restricted HF determinants, whereas those for Cr_2 use SAPT(DFT) formulated with respect to restricted Kohn-Sham (KS) determinants. Of particular importance to the goals of this paper are the dispersion energy and its exchange counterpart. The second-order dispersion energy $E_{\mathrm{disp}}^{(2)}$ for a dimer X–Y is calculated from a modified Polder formula

$$E_{\mathrm{disp}}^{(2)} = -\frac{1}{4\pi} v_{rs}^{pq} v_{r's'}^{p'q'} \int_{-\infty}^{\infty} \Pi_{rr'}^{pp'}(i\omega)\Pi_{ss'}^{qq'}(-i\omega)d\omega, \qquad (1)$$

where $\Pi_{rr'}^{pp'}$ are polarization propagators, v_{rs}^{pq} are two-electron integrals, and ω is a frequency. In the above formula, p, p', r, and r' indices run over the orbitals of mononer X, and the remaining set refers to monomer Y orbitals. Polarization propagators are computed with either TDHF (Refs. 33–35) or time-dependent density functional theory (TDDFT). The second-order exchange-dispersion energies are defined with the uncoupled (UC) dispersion amplitudes (either HF or KS). In the SAPT nomenclature they are the $E_{\mathrm{ex\text{-}disp}}^{(20)}$(HF) and $E_{\mathrm{ex\text{-}disp}}^{(2)}$(UCKS) terms (see Ref. 17), respectively. We will refer to them by one generic name, $E_{\mathrm{ex\text{-}disp}}^{(2)}$. The exchange-dispersion terms were calculated within the S^2 approximation, where S denotes the overlap integral.

In the supermolecular approach the interaction potential V of a X–Y dimer (Y is the S-state atom) in a state Λ is calculated from the formula

$$V_\Lambda^M(R) = E_{\mathrm{X-Y},\Lambda}^M(R) - E_{\mathrm{X},\Lambda}^M(R) - E_{\mathrm{Y},0}^M(R) - \Delta E_{\mathrm{rsc},\Lambda}^M(R), \qquad (2)$$

where M stands for a method and Λ is the projection of total orbital angular momentum on the molecular axis and thus refers to Σ, Π, and Δ states. The last term represents the residual size-consistency correction which vanishes when M is a size-extensive method. This term is used to correct for effects which are not removed by the Davidson's correction in MRCI+Q and CIPT2+Q as well as in the non-size-extensive AQCC method. This term ensures that the interaction potentials V vanish in the limit of large R (assumed to be $R=60a_0$). All the terms in Eq. (2) were calculated in the dimer-centered basis set to apply the counterpoise correction[36] (see also Ref. 37). The SAPT components are included in the hybrid model which describes the interaction potential as the following sum:

$$V_\Lambda(R) = V_\Lambda^{\mathrm{CASSCF}}(R) + E_{\mathrm{disp}}^{(2)}(R;\Lambda) + E_{\mathrm{ex\text{-}disp}}^{(2)}(R;\Lambda), \qquad (3)$$

where $V_\Lambda^{\mathrm{CASSCF}}$ [Eq. (2)] is the supermolecular interaction energy obtained at the CASSCF level of theory and the remaining terms are the Λ-dependent dispersion and exchange-dispersion SAPT components. Depending on the circumstances $V_\Lambda^{\mathrm{CASSCF}}$ may be substituted for $V_\Lambda^{\mathrm{ROHF}}$. This model referred to as CAS+disp represents a generalization of the SCF+disp approximation of Ahlrichs *et al.*[38] CAS+disp is based on an assumption that the CASSCF interaction energy obtained with limited active space includes primarily the nondynamic correlation effects and can be used in metal-metal van der Waals interaction.[39] The inability of CASSCF to account for the dispersion energy results from the fact that valence space calculations optimize monomer components of the supermolecular correlation energy. Dispersion energy is the intermolecular electron correlation effect.

The calculations were performed with the MOLPRO package.[40] The SAPT terms were calculated with codes which became incorporated into SAPT2006.[41]

C. Interaction anisotropy

For the interpretation of the anisotropy of the interaction it is useful to work with the isotropic and anisotropic parts of the interaction potentials.[42,43] For a D-state atom interacting with an S-state one, the interaction potential V_Λ is connected with isotropic (V_0) and anisotropic parts of potential (V_2) according to the formula

$$V_0 = \tfrac{1}{5}(V_\Sigma + 2V_\Pi + 2V_\Delta),$$
$$V_2 = V_\Sigma + V_\Pi - 2V_\Delta, \qquad (4)$$

where V_Σ, V_Π, and V_Δ are interaction potentials. The asymptotic regions of potentials obtained with Eq. (4) are used to find isotropic $C_{6,0}$ and anisotropic $C_{6,2}$ dispersion coefficients by fitting them to a function

$$V_\lambda(R) = -\frac{C_{6,\lambda}}{R^6} - \frac{C_{8,\lambda}}{R^8}. \qquad (5)$$

[The C_8 coefficient in Eq. (5) is used to collect higher-rank terms which otherwise may lead to C_6 dispersion coefficient being overestimated.] These calculations are based on the assumption that the long-range interaction energy is governed by the dispersion interaction.

In order to calculate the dispersion coefficients for the Cr_2 system, we have used the following multipole expansion of two-electron integrals appearing in the Casimir-Polder formula:

TABLE I. Comparison of interaction energies of Cr_2 at different levels of theory (all energies in cm^{-1}).

				E_{int}				
R (a_0)	$E^{(2)}_{disp}$	$E^{(2)}_{ex\text{-}disp}$	ROHF +disp (TDDFT)	RCCSD(T)	RCCSD(T)/ DK	RCCSD(T)/ DK+b	CIPT2+Q/ DK	AQCC/ DK
4.50	−7287.1	2350.2	4311.4	5236.7	4878.1	4807.9	4742.4	5542.6
5.00	−5148.4	1373.4	646.2	1195.6	941.2	893.7	865.7	1503.9
5.25	−4339.8	1082.9	−126.0	273.4	67.6	26.1	11.0	574.6
5.50	−3663.5	867.4	−533.0	−254.1	−416.9	−454.3	−459.6	35.4
5.75				−534.4	−660.9	−695.1	−693.2	−260.0
6.00	−2619.5	573.1	−777.8	−663.6	−760.3	−791.9	−785.1	−406.7
6.25	−2217.9	469.2	−764.2	−703.2	−776.0	−805.7	−795.5	−465.2
6.50	−1879.1	384.7	−713.9	−692.0	−746.1	−774.0	−762.1	−473.7
6.75	−1593.0	315.3	−647.8	−654.1	−693.7	−719.8	−707.5	−455.3
7.00	−1351.2	258.2	−577.7	−603.8	−632.4	−656.4	−645.1	−424.2
7.50	−974.0	172.1	−448.4	−496.2	−510.1	−529.8	−522.4	−352.1
8.00	−704.3	113.6	−345.1	−399.8	−405.5	−421.2	−418.3	−286.1
9.00	−373.1	48.0	−209.0	−256.7	−255.3	−264.8	−267.9	−188.0
9.50	−273.8	30.9	−164.9	−205.4	−202.7	−210.1	−214.3	−152.2
10.00	−202.3	19.9	−130.9	−163.9	−160.8	−166.7	−171.0	−122.8
11.00	−112.9	8.2	−83.2	−103.8	−100.8	−104.8	−107.9	−79.1
12.00	−65.1	3.5	−53.2	−65.5	−63.1	−65.9	−67.7	−50.3

$$v^{pq}_{rs} \propto \sum_{l_X=1}^{\infty}\sum_{l_Y=1}^{\infty}\sum_{M=-l}^{l}(-1)^{l_X-l_Y+M}\begin{pmatrix} l_X & l_Y & l \\ m_X & m_Y & -M \end{pmatrix} \times \frac{\sqrt{2l+1}(Q^{m_X}_{l_X})^k_l (Q^{m_Y}_{l_Y})^m_n}{R^{l+1}}, \tag{6}$$

where $l=l_X+l_Y$ and $(Q^{m_Y}_{l_X})^k_l$ is the matrix element of the 2^{l_X}-pole moment operator of the monomer X (and analogously for the monomer Y). It should be noted that the above methodology can at present be applied only to the interacting S-state atoms.

III. *AB INITIO* RESULTS

A. Cr_2

We begin the discussion from the Cr_2 ($^{13}\Sigma^+_g$) interaction-for which there exist some experimental data.[11] This state is reasonably well represented using the single configuration as evidenced by the fact that the CASSCF and ROHF wave functions are practically the same. The DFT monomer calculations employed the B97-2 functional[44] with the Fermi-Amaldi asymptotic correction[45] which for the open-shell case involves two parameters one for the α-density and one for the β-density. These parameters were equal to 0.248 and 1.768 hartrees, respectively. The hybrid model combined V^{ROHF} with SAPT(DFT) dispersion and exchange-dispersion terms (ROHF+disp). The RCCSD(T) calculations were performed at three different levels of theory. The first included no scalar relativistic Douglas-Kroll-Hess[28,29] (DK) effects and employed the aug-cc-pVQZ (Ref. 46) basis set [denoted RCCSD(T)], so the direct comparison can be carried out with the SAPT(DFT) method for which the inclusion of relativistic effects is not yet implemented. Next, the RCCSD(T) calculations were performed with the inclusion of the Douglass-Kroll-Hess integrals and the aug-cc-pVQZ-DK (Ref. 46) basis set [denoted RCCSD(T)/DK]. The final RCCSD(T) calculation included this basis set augmented with a set of bond functions and DK relativistic correction [RCCSD(T)/DK+b]. The convergence of a CC iterative process in this high-spin system is difficult to achieve with basis sets involving diffuse orbitals because of intruder-state problems. The convergence problem was remedied using a level shift procedure (the shift value of 1 a.u. was sufficient for the CCSD convergence and the maximal value of T_1 diagnostic for all the runs was about 0.02). The CIPT2+Q and AQCC approaches employed a CASSCF reference function and both include the DK effects.

The results shown in Table I list the ROHF+disp values next to RCCSD(T) for a proper comparison. The ROHF +disp interaction energies agree reasonably well with the RCCSD(T) potential except for the discrepancies at short distances, where the RCCSD(T) is more repulsive and in the long range (see $R=12a_0$) where the ROHF+disp is less attractive. In the minimum region, the two potentials agree to within 10%. The similarity of the two potentials indicates that the binding of Cr_2 ($^{13}\Sigma^+_g$) originates from the dispersion interaction combined with its exchange counterpart. The exchange-dispersion energy represents a significant repulsive contribution, which quenches about 20% of the dispersion attraction in the minimum region. The scalar relativistic effects are fairly important for the quantitative description of this potential. The inclusion of the DK effects deepens the minimum of the RCCSD(T) potential by about 10%. The addition of bond functions, to optimize the dispersion interaction, further enhances the well depth by about 4%. This final potential is our most accurate result and the analytical fit is available upon request. The CIPT2+Q results are in very good agreement with the RCCSD(T) results. The AQCC treatment leads to a considerably underestimated potential at all distances.

The minimum characteristics, the long-range C_6 dispersion coefficient, and the dipole polarizability α, values are

TABLE II. Characteristics of the $^{13}\Sigma_g^+$ Cr_2 state.

Method	R_e (a_0)	$\bar{D}_e$ (cm^{-1})	C_6 (a.u.)	α (a.u.)
RCCSD(T)	6.30	704.1		
RCCSD(T)/DK	6.19	777.5	780[a]	82.9
RCCSD(T)/DK+b	6.18	807.8		
CIPT2+Q/DK	6.16	798.4	845	74.2
AQCC/DK	6.43	474.8	540	81.4
ROHF+disp(TDDFT)	6.06	779.1	626	75
Ref. 48			602.0	60.7
Ref. 11			733	
Ref. 50				78.3

[a]Obtained with frozen outer-core electrons (see the text).

shown in Table II. The three treatments, deemed reliable, lead to the well depths in the narrow range of values: 779.1 cm^{-1} (ROHF+disp), 798.4 cm^{-1} (CIPT2+Q/DK) and 807.8 cm^{-1} [RCCSD(T)/DK+b]. The position of the minimum occurs at a slightly shorter distance for the ROHF+disp potential ($R=6.06a_0$) compared to RCCSD(T)/DK+b ($R=6.18a_0$) and CIPT2+Q/DK ($R=6.16a_0$) due to the aforementioned underestimated short-range repulsion. The RCCSD(T)/DK+b potential was employed in the bound-state calculations using discrete variable representation.[47] The calculations predict the ground state of 776.8 cm^{-1}. Our final potential is notably deeper than the CASPT2 potential published by Pavlović *et al.*[14] which has the well depth of 576 cm^{-1}. The C_6 coefficients fitted to the long-range tail of the supermolecular potentials are 780, 645, and 540 a.u. for RCCSD(T)/DK, CIPT2+Q/DK, and AQCC/DK, respectively. It should be mentioned that the RCCSD(T) C_6 could only be fitted upon freezing the outer-core ($3s$ and $3p$) electrons. Otherwise a spurious lower-power R^{-1} term appeared at distances larger than $28a_0$. Our TDDFT C_6 coefficient calculated directly from Eq. (6) amounts to 626 a.u. This is in fairly good agreement with the result of Chu and Dalgarno[48] who employed time-dependent optimized effective potential with self-interaction correction. The experimental value of C_6 can be deduced from the measurements of Feshbach resonances in optically trapped ultracold Cr gas,[10] which are extremely sensitive to the long-range details of the Cr–Cr interaction potential. Two simulations of this experiment provide the values $C_6=733$ (with standard deviation of 70 a.u.)[11] and 770.[49] Our RCCSD(T) result is in very good agreement with these values, whereas the TDDFT result lies below the lower error bar. The higher TDDFT dispersion coefficients C_8 and C_{10} amount to 3.27×10^4 and 1.44×10^6, respectively. The available experimental result for the C_8 coefficient from the work of Werner *et al.*,[11] 7.5×10^4 a.u., is reportedly a weak upper bound for its value.

The calculations of static dipole polarizability of Cr, α, at various levels of theory offer additional clues concerning the performance of DFT and the role of correlation and relativistic effects on this property. Our DFT result for α is 75 a.u. which differs considerably from 60.7 a.u. obtained by Chu and Dalgarno[48] with a different variant of DFT.[48] The value recommended in their work amounts to 78 a.u. (see also Miller[50]) and both CIPT2 and AQCC results are in fairly good agreement. Our most accurate RCCSD(T)/DK treatment yields a slightly larger value of 82.9 a.u. The DK effects contribute about 5% toward lowering its value, consistent with previous findings for other first-row transition metals.[51] The core-valence correlation was found important in atomic properties, such as ionization energies and electron affinities of the $3d$ transition row.[52] To establish its effect on polarizabilities, we removed the outer-core electrons from the correlated space in the RCCSD(T) calculations. The result is a 10% increased α. Based on these observations, some calculations were also performed for Cr_2 with a larger core encompassing the $3s$ and $3p$ electrons. In the minimum region the RCCSD(T)/b calculations lead to a 5% deeper potential. We conclude that in the interaction potential of Cr_2 there is some degree of cancellation between the relativistic effects and the core-valence correlation.

B. Sc–Cr

The reference functions for $^8\Sigma^+$, $^8\Pi$, and $^8\Delta$ states of Sc–Cr were obtained from the state-averaged CASSCF calculations. In the C_{2v} group the Σ^+, Π, and Δ representations correlate with A_1, B_1+B_2, and A_1+A_2, respectively. The state symmetries were distinguished by the calculated values of Λ. The CASSCF calculations employed a valence active space in which the $4s$ orbital of Sc was initially kept doubly occupied. The latter was necessary to prevent root flipping which made the projection on the specific value of Λ impossible. The CASSCF wave functions were used in the MRCI calculations. Proper starting vectors for the ROHF calculations for the three states were obtained by canonicalization of the CASSCF natural orbitals. The ROHF vectors were subsequently used in RCCSD(T) calculations and as the zeroth-order functions in the SAPT method. The RCCSD(T) calculations were performed with averaged atomic natural orbital (ANO) basis sets of Bauschlicher[53] and Partridge[54] with two types of core. The results below were obtained with the *KL* electrons kept in core [denoted RCCSD(T)]. The RCCSD(T) calculations which included the DK effects are denoted RCCSD(T)/DK. The calculations employed a level shift and the T_1 diagnostics did not exceed 0.02. No DK effects were considered in the MRCI calculations. The SAPT treatment employed the TDHF polarization propagator to evaluate state-dependent dispersion and exchange-dispersion energies. In the hybrid model, these terms are combined with CASSCF interaction energy to at least partially account for nondynamic correlation effects (denoted CAS+disp).

The adiabatic potentials for the three octet states of Sc–Cr are displayed in Fig. 1 and the minimum characteristics are listed in Table III. At the CASSCF level of theory [Fig. 1(a)], all the three states are repulsive with the Σ^+ state being considerably more repulsive than Π and Δ. The analogous curves evaluated at the ROHF level of theory are slightly less repulsive, but generally very close to those from CASSCF. At $R=6a_0$ the differences are 63 cm^{-1} for Σ^+, 10 cm^{-1} for Π, and 33 cm^{-1} for Δ. The RCCSD(T) adiabatic curves [Fig. 1(b)] have deep minima (Δ: 3958 cm^{-1}, Π: 3531 cm^{-1}, and Σ^+: 2871 cm^{-1}) occurring at the narrow range of $R=5.7a_0-5.8a_0$. Freezing the outer-core electrons has a small effect (less than 2%) on the well depths, whereas

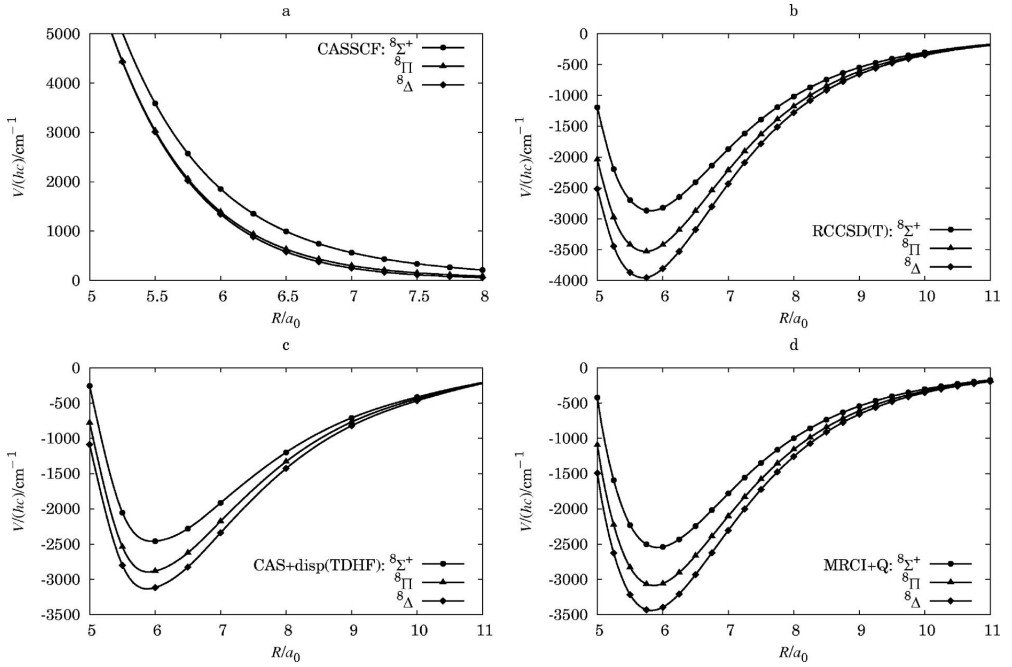

FIG. 1. Interaction potentials for $^8\Sigma^+$, $^8\Pi$, and $^8\Delta$ states of Sc–Cr obtained at the following levels of theory: (a) CASSCF, (b) RCCSD(T), (c) CAS+disp(TDHF), (d) MRCI+Q.

the inclusion of the DK effects leads to further stabilization of about 240–250 cm^{-1} and shortening of R_e by about $0.1a_0$. The hybrid model CAS+disp results in the three potentials which are in qualitative agreement with RCCSD(T), although uniformly shallower [Fig. 1(c)]. Their minima occur at slightly longer distances $R=5.92a_0$. Finally, the relative order of the three states is confirmed by the MRCI results [Fig. 1(d)]. The binding in these states clearly originates from correlation effects, the origins of which are quite interesting. To examine their nature we compare the correlation part of the interaction energy obtained at the RCCSD(T) level of theory, V^{corr}, with the sum of the dispersion and exchange-dispersion terms for the three states. The result for the most attractive state Δ (where the agreement is the least favorable) is shown in Fig. 2. The figure also displays the dispersion energy alone. The agreement between these quantities is excellent and the discrepancies, which occur at short and long distances, respectively, are not unexpected. Specifically, in the short range the present formulation of exchange dispersion (and the S^2 approximation) is expected to deterio-

TABLE III. Minimum characteristics and the dispersion coefficients of the Sc–Cr system.

State	Method	R_e (a_0)	$\bar{D}_e$ (cm^{-1})	$C_{6,0}$ (a.u.)	$C_{6,2}$ (a.u.)
$^8\Sigma^+$	RCCSD(T)	5.81	2871		
	RCCSD(T)/DK	5.71	3118		
	MRCI+Q	5.92	2548		
	CAS+disp(TDHF)	6.01	2459		
$^8\Pi$	RCCSD(T)	5.73	3531		
	RCCSD(T)/DK	5.65	3767		
	MRCI+Q	5.86	3087		
	CAS+disp(TDHF)	5.95	2886		
$^8\Delta$	RCCSD(T)	5.70	3958		
	RCCSD(T)/DK	5.62	4209		
	MRCI+Q	5.83	3442		
	CAS+disp(TDHF)	5.92	3124		
V_0	SAPT			1366	
V_2	SAPT				−48.7

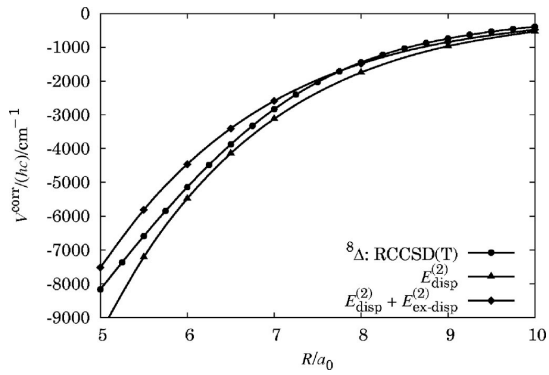

FIG. 2. Comparison of the correlation contribution to the RCCSD(T) interaction energies, V^{corr}, with dispersion and exchange-dispersion energies for $^8\Delta$ state of the Sc–Cr system.

rate. In the long range, where the exchange effects are no longer important, the TDHF and CCSD(T) descriptions of the dispersion energy may show discrepancies (although there are known open-shell cases where the two treatments agree very well; see Ref. 25). One remarkable feature is the sheer magnitude of dispersion energy, which is not seen in van der Waals interactions of main-group elements except for alkali metal and alkaline earth atom dimers. However, in the latter cases it is matched with a very large exchange counterpart.[55,56] It is interesting to examine factors contributing to considerable splittings between potentials. Let us consider the difference between the Σ^+ and Π states at $R=6a_0$ which in CAS+disp amounts to 423 cm^{-1}. CASSCF contributes the largest share to this difference, 465 cm^{-1}. The contribution from the dispersion is -61 cm^{-1}, and the one from the exchange dispersion is 19 cm^{-1}. By comparison, the analogous energy difference in RCCSD(T) is 600 cm^{-1}.

Another interesting aspect is the strengthening of the interaction compared to Cr_2. Substituting Sc for Cr results in a 3.6 (Σ^+)-, 4.3 (Π)-, and 4.9 (Δ)-fold increase in stabilization compared with Cr–Cr. To explain this effect, three factors in order of increasing importance can be identified. First, the V^{CASSCF} curves for the Δ and Π states of Sc–Cr are considerably less repulsive (and slightly less repulsive for Σ^+) than those of Cr_2 for $R>6a_0$. Second, the average C_6 coefficient of the Sc–Sc interaction is 2.3 times larger than that of Cr–Cr.[48] The third is the considerable 50% decrease in the highest occupied molecular orbital–lowest unoccupied molecular orbital gap between Sc–Cr and Cr_2. The latter may be responsible for the violation of combination rules.[57] Our TDHF value of $C_{6,0}=1366$ a.u. for Sc–Cr, which is very close to the Sc–Sc value $C_6=1383$ a.u. of Chu and Dalgarno,[48] seems to indicate such a violation.

Our lowest state, $^8\Delta$, can be compared with the DFT result of Gutsev *et al.*[12] who identified the lowest octet state as $^8\Pi$. Although their assignment is approximate because of unrestricted KS formalism, the other characteristics of this state are in reasonable agreement with our RCCSD(T) findings. The position of the minimum agrees quite well (our value $5.62a_0$ versus $5.51a_0$) and so does the small value of the dipole moment. Unfortunately, they do not report the well-depth value. One interesting insight from the work of Gutsev *et al.*[12] concerns the type of bonding in this state. Their analysis indicates that it involves a single bond between the 4*s* orbitals of Sc and Cr. This may provide an additional explanation for our observed strength of this state.

C. Sc–Kr

By substituting semiclosed Cr atom in Sc–Cr by closed-shell Kr, we can better understand the above results for Sc–Cr by comparing and contrasting it with a typical van der Waals complex Sc–Kr. Such calculations will also allow us to further demonstrate interpretative capabilities of SAPT.

The ROHF wave functions for the $^2\Sigma^+$, $^2\Pi$, and $^2\Delta$ states of Sc–Kr were obtained by the single occupation of Sc $3d_\sigma$, $3d_\pi$, or $3d_\delta$ orbitals, respectively. These functions were used as the starting point for the RCCSD(T) calculations and as the zeroth-order wave functions in SAPT. The SAPT method employed TDHF polarization propagator in the calculation of the dispersion energy. This term, along with its exchange counterpart, was combined with V^{ROHF} to yield the hybrid SAPT model, ROHF+disp(TDHF). The ANO basis set[53,54] was used for Sc and the aug-cc-pVQZ basis set[58] for Kr.

TABLE IV. Minimum characteristics and the dispersion coefficients of the Sc–Kr system.

State	Method	R_e (a_0)	$\bar{D}_e$ (cm^{-1})	$C_{6,0}$ (a.u.)	$C_{6,2}$ (a.u.)
$^2\Sigma^+$	RCCSD(T)	9.536	84.0		
	ROHF+disp(TDHF)	9.37	93.7		
$^8\Pi$	RCCSD(T)	9.463	85.8		
	ROHF+disp(TDHF)	9.35	93.2		
$^2\Delta$	RCCSD(T)	9.646	81.2		
	ROHF+disp(TDHF)	9.52	89.0		
V_0	RCCSD(T)			350	
V_0	SAPT			382	
V_2	RCCSD(T)				−0.62
V_2	SAPT				−5.9

The results for the $^2\Sigma^+$, $^2\Pi$, and $^2\Delta$ states are reported in Table IV and in Figs. 3 and 4. As seen in Table IV the complex is very weakly bound with the well depths of 81–86 cm^{-1} [RCCSD(T)] or 89–94 cm^{-1} (ROHF+disp). The minima of the three potentials occur at large distances, around $9.4a_0-9.6a_0$. The ROHF+disp model agrees very well with RCCSD(T) in describing these characteristics. Both approaches predict the Δ state to be the least stable and Σ^+ and Π to be very close. The minimum region in Sc–Kr is pushed toward longer distances than in Sc–Cr because of much stronger exchange repulsion in the former as evidenced by a comparison of the ROHF potential curves for Sc–Kr in Fig. 3 with the three CASSCF potentials of Sc–Cr in Fig. 1(a). For example, the three sets of curves if compared at the same distance, for example, $R=6.5a_0$, reveal approximately 2.5 larger repulsion in Sc–Kr than in Sc–Cr. The $^2\Sigma^+$ state of Sc–Kr is the most repulsive at short distances just as in Sc–Cr; however, at around $6.8a_0$ a crossing

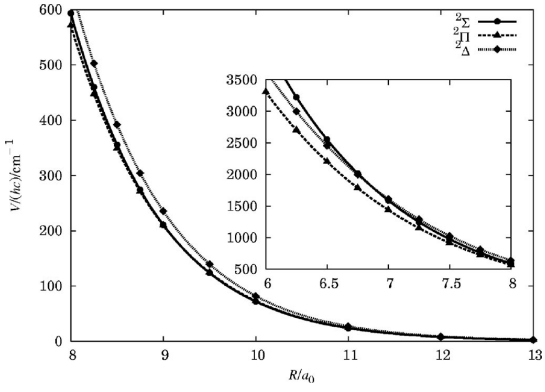

FIG. 3. ROHF interaction energies for the Sc–Kr system (minimum at approximately $9.5a_0$). The outer figure shows the region of minimum, while the inset shows a short range.

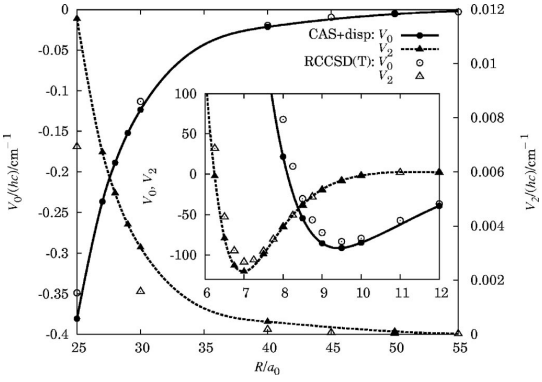

FIG. 4. ROHF+disp and RCCSD(T) isotropic (V_0) and anisotropic (V_2) components of interaction potential for the Sc–Kr system. The outer figure shows the asymptotic region, while the inset shows the minimum region.

occurs and the $^2\Delta$ state becomes the most repulsive. This ordering of the ROHF curves $^2\Delta > {}^2\Pi \approx {}^2\Sigma^+$ at distances of $9.5a_0$ determines the order of minima in the full interaction potentials.

The isotropic V_0 and anisotropic V_2 parts [see Eq. (4)] of the full RCCSD(T) and ROHF+disp potentials are shown in Fig. 4. The ROHF+disp and RCCSD(T) values agree reasonably well in the minimum regions of V_0 and V_2. In the asymptotic region, a similar agreement is seen in V_0 but there are some discrepancies in V_2. Consequently, the dispersion coefficients $C_{6,0}$ (see Table IV) obtained by both methods are very similar, while $C_{6,2}$ differ quantitatively (although both methods predict them to be small). The average $C_{6,0}$ dispersion coefficient of Sc–Kr is 3.6 times smaller than that of Sc–Cr (see Table III), which is consistent with the ratio of dipole polarizabilities of Cr and Kr (4.6). The dispersion coefficients $C_{6,2}$ (see Table IV) of both systems are both negative but differ by one order of magnitude. According to Eq. (4), the negative sign of $C_{6,2}$ indicates that Δ is the lowest state in the asymptotic region. Thus, the order of states in Sc–Kr is different in the minimum and in the asymptotic region. As mentioned above the order in the minimum region is due to the exchange repulsion, whereas that in the long-range results from the dispersion interaction. The source of the long-range anisotropy of dispersion energy in both complexes is the single $3d$ electron of Sc which also gives rise to polarizability anisotropy. It is difficult to rationalize at this point why RCCSD(T) and SAPT lead to significantly different values of $C_{6,2}$. More work along these lines is necessary.

D. Spin-orbit coupling

In the doublet-state Sc–Kr complex the Sc atom is the source of both the orbital **L** and spin **S** angular momenta. This is not the case for the octet state of Sc–Cr which in itself arises from the coupling of the spin momenta of both atoms. The following discussion applies primarily to Sc–Kr but also offers some hints for a treatment of Sc–Cr. The total electronic angular momentum of a spin-orbit coupled state is denoted $\mathbf{J}=\mathbf{L}+\mathbf{S}$ and the basis set is $|J,M_J\rangle$. In this basis set the spin-orbit Hamiltonian $\hat{H}_{\mathrm{SO}}=a\mathbf{L}\cdot\mathbf{S}$ is diagonal. The spin-orbit parameter a for Sc is 67.336 cm^{-1}.[59] Assuming that a is constant with R, the Sc–Kr interaction represents a limiting case where the splitting between the adiabatic potentials is small compared to a. The matrix of $\hat{V}+\hat{H}_{\mathrm{SO}}$ in this basis set is block diagonal with the following diagonal elements:

$$\begin{aligned}
&\left\langle \tfrac{5}{2},\pm\tfrac{5}{2}\middle|\hat{V}\middle|\tfrac{5}{2},\pm\tfrac{5}{2}\right\rangle = V_\Delta + a,\\
&\left\langle \tfrac{5}{2},\pm\tfrac{3}{2}\middle|\hat{V}\middle|\tfrac{5}{2},\pm\tfrac{3}{2}\right\rangle = \tfrac{1}{5}(4V_\Pi + V_\Delta) + a,\\
&\left\langle \tfrac{5}{2},\pm\tfrac{1}{2}\middle|\hat{V}\middle|\tfrac{5}{2},\pm\tfrac{1}{2}\right\rangle = \tfrac{1}{5}(3V_\Sigma + 2V_\Pi) + a,\\
&\left\langle \tfrac{3}{2},\pm\tfrac{3}{2}\middle|\hat{V}\middle|\tfrac{3}{2},\pm\tfrac{3}{2}\right\rangle = \tfrac{1}{5}(V_\Pi + 4V_\Delta) - \tfrac{3}{2}a,\\
&\left\langle \tfrac{3}{2},\pm\tfrac{1}{2}\middle|\hat{V}\middle|\tfrac{3}{2},\pm\tfrac{1}{2}\right\rangle = \tfrac{1}{5}(2V_\Sigma + 3V_\Pi) - \tfrac{3}{2}a,
\end{aligned} \tag{7}$$

and the following nonzero off-diagonal elements:

$$\begin{aligned}
&\left\langle \tfrac{5}{2},-\tfrac{3}{2}\middle|\hat{V}\middle|\tfrac{3}{2},-\tfrac{3}{2}\right\rangle = \tfrac{2}{5}(V_\Pi - V_\Delta),\\
&\left\langle \tfrac{5}{2},-\tfrac{1}{2}\middle|\hat{V}\middle|\tfrac{3}{2},-\tfrac{1}{2}\right\rangle = \tfrac{\sqrt{6}}{5}(V_\Sigma - V_\Pi),\\
&\left\langle \tfrac{5}{2},\tfrac{1}{2}\middle|\hat{V}\middle|\tfrac{3}{2},\tfrac{1}{2}\right\rangle = \tfrac{\sqrt{6}}{5}(V_\Pi - V_\Sigma),\\
&\left\langle \tfrac{3}{2},\tfrac{3}{2}\middle|\hat{V}\middle|\tfrac{5}{2},\tfrac{3}{2}\right\rangle = \tfrac{2}{5}(V_\Delta - V_\Pi).
\end{aligned} \tag{8}$$

The SO adiabats are obtained as the eigenvalues of the above matrix substituting the RCCSD(T) V_Σ, V_Π, and V_Δ potentials. They are subsequently shifted to their respective asymptotes, $J=\frac{5}{2}$ and $J=\frac{3}{2}$, for comparison purposes. The minimum positions in the SO adiabats remain virtually unchanged from their spin-free positions. The interaction energies compared at $R=9.5a_0$ (i.e., in the minimum region) vary between -85.03 cm^{-1} ($\left|\frac{3}{2},\frac{1}{2}\right\rangle$) and -80.62 cm^{-1} ($\left|\frac{5}{2},\frac{5}{2}\right\rangle = V_\Delta$). The energy of the lowest $\left|\frac{3}{2},\frac{1}{2}\right\rangle$ state is very close to that of the lowest spin-free adiabat V_Π (see Table IV). We conclude that this complex should not be affected by the SO coupling as long as the a parameter remains constant with R. The octet Sc–Cr complex presents an opposite case, where the splitting between the adiabatic potentials is one order of magnitude larger than a. However, its treatment is much more complicated (if not intractable) because $\hat{H}_{\mathrm{SO}}$ is expected to couple also the states of lower multiplicity about which nothing is known at this point. If, in the first approximation, one assumes these couplings to be negligible, the ground state Δ will be unaffected by the SO coupling.

IV. SUMMARY AND CONCLUSIONS

We have presented results for two transition metal dimers in their high-spin van der Waals states, ($^{13}\Sigma_g^+$) Cr_2 and ($^8\Sigma^+, {}^8\Pi, {}^8\Delta$) Sc–Cr. To aid the analysis of these interactions, a typical van der Waals complex Sc–Kr involving the $^2\Sigma^+$, $^2\Pi$, $^2\Delta$ manifold has also been studied. The interaction potentials have been calculated by a supermolecular method based on the single-reference RCCSD(T) and on a number of multireference approaches including CIPT2, MRCI, and

AQCC. In addition, we report the open-shell SAPT TDHF dispersion and exchange-dispersion energies for the manifolds of the three states in Sc–Cr and Sc–Kr. In the case of Cr_2 the open-shell SAPT(DFT) was applied in the calculations of the dispersion and exchange-dispersion terms with the TDDFT polarization propagator. The present TM systems pose a very demanding environment for testing these theories. Dispersion and exchange-dispersion energies combined with the supermolecular (purely repulsive) ROHF or CASSCF interaction potentials (CAS+disp, ROHF+disp models, respectively) provide reasonable qualitative results and with substantially less effort than that required to judiciously apply the supermolecular treatments used here. SAPT also proves useful in calculations of properties depending on asymptotic parts of the interaction potentials, such as dispersion coefficients.

The $^{13}\Sigma_g^+$ state of Cr_2 is bound by a midrange van der Waals interaction with the well depth of about 800 cm^{-1}. RCCSD(T), CIPT2, and ROHF+disp are in reasonable agreement with each other. The predictions of the C_6 dispersion coefficient are in reasonable agreement with experiment and previous calculations. Our well depth, however, is much deeper than that of the previously reported CASPT2 potential.[14] SAPT(DFT) reveals a significant role of exchange dispersion in open-shell interactions. This term is seen to more strongly quench the dispersion than in the closed-shell systems of comparable strength.

In Sc–Cr the CASSCF potentials are purely repulsive for the three states and the post-CASSCF correlation effects lead to a relatively strong bonding in all three states. The ordering of well depths from the RCCSD(T) calculations is $^8\Delta$ (about 4000 cm^{-1}), $^8\Pi$ (about 3600 cm^{-1}), and $^8\Sigma^+$ (about 2900 cm^{-1}). Three approaches applied to this system, RCCSD(T), MRCI, and CAS+disp, confirm this ordering although the values differ. The splitting of adiabatic potentials is considerable (400–600 cm^{-1}) and dominated by the differences in the CASSCF repulsion. In view of the strong anisotropy of interactions, the prospects for the sympathetic cooling of a Sc–Cr mixture are unlikely because the relaxation processes will be very fast. It is also expected that the spin-orbit effects will be of secondary importance. The source of the bonding is a very strong dispersion energy.

Sc–Kr is a typical van der Waals complex bound by less than 100 cm^{-1} and with very small splittings among the states. The order of well depths is $^2\Pi \approx {}^2\Sigma^+ > {}^2\Delta$ at the RCCSD(T) and ROHF+disp levels of theory. Both approaches lead to a good agreement for V_0 and V_2.

ACKNOWLEDGMENTS

The authors thank Alexei Buchachenko, Piotr Piecuch, and Bogumił Jeziorski for helpful advice in various aspects of this study. This work was supported by the National Science Foundation under Grant No. CHE-0414241. P.S.Z. wishes to acknowledge the support of the Foundation for the Polish Science. J.K. was supported by NSF grant (CHE-0413743) to Millard H Alexander.

[1] G. Frenking and N. Frohlich, Chem. Rev. (Washington, D.C.) **100**, 717 (2000).
[2] J. F. Harrison, Chem. Rev. (Washington, D.C.) **100**, 679 (2000).
[3] S. R. Langhoff and C. W. Bauschlicher, Annu. Rev. Phys. Chem. **39**, 181 (1988); C. W. Bauschlicher, H. Partridge, S. R. Langhoff, and M. Rosi, J. Chem. Phys. **95**, 1057 (1991).
[4] M. D. Morse, Chem. Rev. (Washington, D.C.) **86**, 1049 (1986).
[5] C. I. Hancox, S. Doret, M. Hummon, R. Krems, and J. Doyle, Phys. Rev. Lett. **94**, 013201 (2005).
[6] J. Kłos, M. F. Rode, J. E. Rode, G. Chałasiński, and M. M. Szcześniak, Eur. Phys. J. D **31**, 429 (2004).
[7] J. Stuhler, A. Griesmaier, T. Koch, M. Fattori, T. Pfau, S. Giovanazzi, P. Pedri, and L. Santos, Phys. Lett. A **95**, 150406 (2005).
[8] R. Krems, J. Kłos, M. Rode, M. M. Szcześniak, G. Chałasiński, and A. Dalgarno, Phys. Rev. Lett. **94**, 013202 (2005).
[9] J. D. Weinstein, R. deCarvalho, J. Kim, D. Patterson, B. Friedrich, and J. M. Doyle, Phys. Rev. A **57**, R3173 (1998).
[10] A. Griesmaier, J. Werner, S. Hensler, J. Stuhler, and T. Pfau, Phys. Rev. Lett. **94**, 160401 (2005).
[11] J. Werner, A. Griesmeier, S. Hensler, J. Stuhler, T. Pfau, A. Simoni, and E. Tiesinga, Phys. Rev. Lett. **94**, 183201 (2005).
[12] G. L. Gutsev, P. Jena, B. K. Rao, and S. N. Khanna, J. Chem. Phys. **114**, 10738 (2001).
[13] G. L. Gutsev, M. D. Mochena, P. Jena, C. W. Bauschlicher, Jr., and H. Partridge, III, J. Chem. Phys. **121**, 6785 (2004).
[14] Z. Pavlović, B. O. Roos, R. Côté, and H. R. Sadeghpour, Phys. Rev. A **69**, 030701 (2004).
[15] S. V. Nguyen, J. S. Helton, K. Maussang, W. Ketterle, and J. M. Doyle, Phys. Rev. A **71**, 025602 (2005).
[16] P. Celani, H. Stoll, H.-J. Werner, and P. J. Knowles, Mol. Phys. **102**, 2369 (2004).
[17] P. S. Żuchowski, R. Podeszwa, R. Moszyński, K. Szalewicz, and B. Jeziorski (unpublished).
[18] P. J. Knowles, C. Hampel, and H.-J. Werner, J. Chem. Phys. **99**, 5219 (1993).
[19] M. Gutowski, F. B. van Duijneveldt, G. Chałasiński and L. Piela, Mol. Phys. **61**, 233 (1987); J. A. Kłos, M. M. Szcześniak and G. Chałasiński, Int. Rev. Phys. Chem. **23**, 541 (2004).
[20] G. Chałasiński and K. Szalewicz, Int. J. Quantum Chem. **18**, 1071 (1980).
[21] S. M. Cybulski, R. Burcl, G. Chałasiński, and M. M. Szcześniak, J. Chem. Phys. **103**, 10116 (1995).
[22] S. M. Cybulski, G. Chałasiński, and M. M. Szcześniak, J. Chem. Phys. **105**, 9525 (1996).
[23] S. M. Cybulski, R. Burcl, M. M. Szcześniak, and G. Chałasiński, J. Chem. Phys. **104**, 7997 (1996).
[24] J. Kłos, G. Chałasiński, M. T. Berry, R. Bukowski, and S. M. Cybulski, J. Chem. Phys. **112**, 2195 (2000).
[25] P. S. Żuchowski, B. Bussery-Honvault, R. Moszyński, and B. Jeziorski, J. Chem. Phys. **119**, 10497 (2003).
[26] H. Hettema and P. E. S. Wormer, J. Chem. Phys. **93**, 3389 (1990).
[27] S. Atahan, J. Kłos, P. S. Żuchowski, and M. H. Alexander, Phys. Chem. Chem. Phys. **8**, 4420 (2006).
[28] M. Douglas and N. M. Kroll, Ann. Phys. (N.Y.) **82**, 89 (1974).
[29] G. Jansen and B. A. Hess, Phys. Rev. A **39**, 6016 (1989).
[30] P. G. Szalay and R. J. Bartlett, J. Chem. Phys. **103**, 3600 (1995).
[31] H.-J. Werner and P. J. Knowles, J. Chem. Phys. **89**, 5803 (1988).
[32] P. J. Knowles and H.-J. Werner, Chem. Phys. Lett. **145**, 514 (1988).
[33] R. Moszyński, B. Jeziorski, and K. Szalewicz, Int. J. Quantum Chem. **45**, 409 (1993).
[34] R. McWeeny, Croat. Chem. Acta **57**, 865 (1984).
[35] M. Jaszuński and R. McWeeny, Mol. Phys. **55**, 1275 (1985).
[36] S. F. Boys and F. Bernardi, Mol. Phys. **19**, 553 (1970).
[37] J. A. Kłos, G. Chałasiński, M. M. Szcześniak, and H.-J. Werner, J. Chem. Phys. **115**, 3085 (2001).
[38] R. Ahlrichs, R. Penco, and G. Scoles, J. Chem. Phys. **19**, 119 (1977).
[39] C. F. Kuntz, C. Hattig, and B. A. Hess, Mol. Phys. **89**, 139 (1996).
[40] H.-J. Werner, P. J. Knowles, R. Lindh, F. R. Manby, M. Schütz, P. Celani, T. Korona, G. Rauhut, R. D. Amos, A. Bernhardsson *et al.*, MOLPRO, version 2006.1, a package of *ab initio* programs (2006), see http://www.molpro.net
[41] R. Bukowski, W. Cencek, P. Jankowski, B. Jeziorski, M. Jeziorska, S. A. Kucharski, V. F. Lotrich, A. J. Misquitta, R. Moszyński, K. Patkowski *et al.*, SAPT2006, an *ab initio* program for many-body symmetry-adapted perturbation theory calculations of intermolecular interaction energies (2006), see http://www.physics.udel.edu/~szalewic/SAPT/SAPT.html

[42] V. Aquilanti and G. Grossi, J. Chem. Phys. **73**, 1165 (1980).
[43] R. Krems and A. Dalgarno, *Fundamental World of Quantum Chemistry* (Kluwer, Dordrecht, 2004), Vol. 3, pp. 273–294.
[44] P. J. Wilson, T. J. Bradley, and D. J. Tozer, J. Chem. Phys. **115**, 9233 (2001).
[45] D. J. Tozer and N. C. Handy, J. Chem. Phys. **109**, 10180 (1998).
[46] N. B. Balabanov and K. Peterson, J. Chem. Phys. **123**, 064107 (2005).
[47] D. T. Colbert and W. H. Miller, J. Chem. Phys. **96**, 1982 (1992).
[48] X. Chu and A. Dalgarno, J. Chem. Phys. **121**, 4083 (2004).
[49] Z. Pavlović, R. V. Krems, R. Côté, and H. R. Sadeghpour, Phys. Rev. A **71**, 061402 (2005).
[50] T. M. Miller, *CRC Handbook of Chemistry and Physics*, 79th ed. (CRC, Boca Raton, FL, 1998), pp. 160–174.
[51] J. A. Kłos, J. Chem. Phys. **123**, 024308 (2005).
[52] N. B. Balabanov and K. Peterson, J. Chem. Phys. **125**, 074110 (2006).
[53] C. W. Bauschlicher, Jr., Theor. Chim. Acta **92**, 183 (1995).
[54] H. Partridge, J. Chem. Phys. **90**, 1043 (1989).
[55] W. T. Zemke and W. C. Stwalley, J. Chem. Phys. **111**, 4956 (1999).
[56] B. Bussery-Honvault, J.-M. Launay, and R. Moszyński, Phys. Rev. A **68**, 032718 (2003).
[57] G. Maitland, M. Rigby, B. Smith, and W. Wakeham, *Intermolecular Forces: Their Origin and Determination* (Clarendon, Oxford, 1987).
[58] D. E. Woon and T. H. Dunning, Jr., J. Chem. Phys. **98**, 1358 (1993).
[59] *NIST handbook of basic atomic spectroscopic data*, see http://www.physics.nist.gov/PhysRefData/Handbook.

Chapter 2

Bifunctional Approach to the Interaction Energy in the DFT

Whereabouts

In this Chapter we derive the coupled KS equations for the interacting monomers. We present an alternative way of performing KS iterations, in the sense that we have a coupled set of equations to solve, instead of one, as in the original KS method [29]. However, that apparent complication allows us to separate the resulting interaction energy into the HL and deformation terms and serves as a starting point on our road to dispersionless DFT interaction energy.

2.1 KS Description of Monomers

We start with the KS isolated monomers, i.e. with the monomer orbitals satisfying the KS equations, e.g. for the monomer A

$$\hat{f}_{\mathrm{A}}^{\mathrm{KS}}(\mathbf{r})a_i^0(\mathbf{r}) = \epsilon_{\mathrm{A},i}^0 a_i^0(\mathbf{r}). \tag{2.1}$$

The KS operator of monomer A is

$$\hat{f}_{\mathrm{A}}^{\mathrm{KS}}(\mathbf{r}) = \hat{h}_{\mathrm{A}}(\mathbf{r}) + \hat{\jmath}(\mathbf{r}) + v_{\mathrm{A}}^{\mathrm{xc}}(\mathbf{r}), \tag{2.2}$$

where the xc potential is a variational derivative of the xc energy functional with respect to the density:

$$v_{\mathrm{A}}^{\mathrm{xc}}(\mathbf{r}) = \frac{\delta E_{\mathrm{xc}}[\rho_{\mathrm{A}}^0]}{\delta \rho_{\mathrm{A}}^0(\mathbf{r})}. \tag{2.3}$$

The nuclear and Coulomb potentials together constitute the electrostatic potential,

$$\hat{v}_{\mathrm{A}}^{\mathrm{elst}}(\mathbf{r}) = v_{\mathrm{A}}^{\mathrm{ne}}(\mathbf{r}) + \hat{\jmath}(\mathbf{r}), \tag{2.4}$$

so (2.2) can be rewritten as

$$\hat{f}_{\mathrm{A}}^{\mathrm{KS}}(\mathbf{r}) = -\frac{1}{2}\Delta_{\mathbf{r}} + \hat{v}_{\mathrm{A}}^{\mathrm{elst}}(\mathbf{r}) + v_{\mathrm{A}}^{\mathrm{xc}}(\mathbf{r}). \tag{2.5}$$

The density expression (1.18) for the single Slater determinant wavefunction takes particularly simple form:

$$\rho_{\mathrm{A}}^{0}(\mathbf{r}) = 2\sum_{i\in A} |a_i^0(\mathbf{r})|^2. \tag{2.6}$$

Having solved Eq. (2.1) and its equivalent for monomer B, we get KS orbitals, $\{a_i^0\}_{i\in A}$ and $\{b_k^0\}_{k\in B}$, for isolated monomers A and B.

2.2 Interaction Energy from Interacting Monomer Densities

At this point our goal is to restore DFT supermolecular interaction energy,

$$E_{\mathrm{int}}^{\mathrm{DFT}} = E_{\mathrm{AB}}^{\mathrm{DFT}} - E_{\mathrm{A}}^{\mathrm{DFT}} - E_{\mathrm{B}}^{\mathrm{DFT}}, \tag{2.7}$$

starting with the monomers satisfying KS equations (2.1). In the KS approach, the non-interacting reference system of the AB dimer is a single Slater determinant built of mutually orthonormal orbitals:

$$\psi_{\mathrm{AB}} = |x_1\alpha x_1\beta \ldots x_{\mathscr{M}}\alpha x_{\mathscr{M}}\beta\rangle\,. \tag{2.8}$$

From the monomer KS functions we construct the normalized and antisymmetric function

$$\psi_{\mathrm{AB}}^{0} = \mathscr{N}\hat{\mathscr{A}}\psi_{\mathrm{A}}^{0}\psi_{\mathrm{B}}^{0} \tag{2.9}$$

and perform the symmetric orthogonalization of monomers' orbitals. That leads to a new function,

$$\tilde{\psi}_{\mathrm{AB}}^{0} = \hat{\mathscr{A}}\tilde{\psi}_{\mathrm{A}}^{0}\tilde{\psi}_{\mathrm{B}}^{0}, \tag{2.10}$$

which, owing the orthonormality of monomers' orbitals, is normalized to unity. The density of a system is invariant with respect to the unitary transformations of Slater determinant, so the densities resulting from functions (2.9) and (2.10)

are equal. Moreover, the system density is simply a sum of monomer densities provided that all orbitals are mutually orthonormal:

$$\begin{aligned}
&\rho^0_{\mathrm{AB}}(\mathbf{r}) = \tilde{\rho}^0_{\mathrm{AB}}(\mathbf{r}) = \\
&= \sum_{\sigma_1,\sigma_2,\ldots,\sigma_N} \int_{\mathbb{R}^3} \ldots \int_{\mathbb{R}^3} \left| \tilde{\psi}^0_{\mathrm{AB}} \left(\mathbf{r}; \sigma_1; (\mathbf{r}_i; \sigma_i)_{i=2}^N \right) \right|^2 d^3\mathbf{r}_2 \ldots d^3\mathbf{r}_N = \\
&= \tilde{\rho}^0_{\mathrm{A}}(\mathbf{r}) + \tilde{\rho}^0_{\mathrm{B}}(\mathbf{r}).
\end{aligned} \tag{2.11}$$

It should be stressed, however, that $\rho^0_{\mathrm{AB}} \neq \rho^0_{\mathrm{A}} + \rho^0_{\mathrm{B}}$.

In KS theory, the energy of a system referred to the KS function built of $\{x_p\}_{p=1}^{\mathscr{M}}$ orbitals is a functional of density which in general reads

$$\begin{aligned}
&E[\rho] = \\
&= T[\rho] + V^{\mathrm{ne}}[\rho] + V^{\mathrm{ee}}[\rho] + V^{\mathrm{nn}} = \\
&= T^{\mathrm{s}}[\rho] + V^{\mathrm{ne}}[\rho] + J[\rho] + T[\rho] - T^{\mathrm{s}}[\rho] + V^{\mathrm{ee}}[\rho] - J[\rho] + V^{\mathrm{nn}} = \\
&= T^{\mathrm{s}}[\rho] + V^{\mathrm{ne}}[\rho] + J[\rho] + E^{\mathrm{xc}}[\rho] + V^{\mathrm{nn}} = \\
&= -\frac{1}{2} \int_{\mathbb{R}^3} [\Delta_{\mathbf{r}} \rho(\mathbf{r}; \mathbf{r}')]_{\mathbf{r}'=\mathbf{r}} \, d^3\mathbf{r} + \int_{\mathbb{R}^3} v^{\mathrm{ne}}(\mathbf{r}) \rho(\mathbf{r}) \, d^3\mathbf{r} + \\
&\quad + \frac{1}{2} \int_{\mathbb{R}^3} \int_{\mathbb{R}^3} \frac{\rho(\mathbf{r}_1)\rho(\mathbf{r}_2)}{r_{12}} \, d^3\mathbf{r}_1 d^3\mathbf{r}_2 + E^{\mathrm{xc}}[\rho] + V^{\mathrm{nn}},
\end{aligned} \tag{2.12}$$

so the xc energy $E^{\mathrm{xc}}[\rho]$ includes the amount of kinetic energy not included in the HF-like expression in (2.12), $T[\rho] - T^{\mathrm{s}}[\rho]$, and the non-classical electron-electron interaction, $V^{\mathrm{ee}}[\rho] - J[\rho]$. $T^{\mathrm{s}}[\rho]$ is referred to as the non-interacting kinetic energy. V^{nn} is the nuclear-nuclear repulsion term and it is simply a constant for a given geometry.

At this point we turn on the interaction between the monomers and assume the KS function in the form analogous to (2.10):

$$\tilde{\psi}_{\mathrm{AB}} = \hat{\mathscr{A}} \tilde{\psi}_{\mathrm{A}} \tilde{\psi}_{\mathrm{B}}. \tag{2.13}$$

The monomer functions in (2.13) are constructed from mutually orthogonal orbitals. This assures that the densities fulfill the additivity condition (2.11). The total energy of AB dimer is

$$\begin{aligned}
E_{\mathrm{AB}}[\rho_{\mathrm{AB}}] &= E_{\mathrm{AB}}[\tilde{\rho}_{\mathrm{AB}}] = E_{\mathrm{AB}}[\tilde{\rho}_{\mathrm{A}} + \tilde{\rho}_{\mathrm{B}}] = \\
&= T^{\mathrm{s}}[\tilde{\rho}_{\mathrm{A}} + \tilde{\rho}_{\mathrm{B}}] + V^{\mathrm{ne}}_{\mathrm{AB}}[\tilde{\rho}_{\mathrm{A}} + \tilde{\rho}_{\mathrm{B}}] + J[\tilde{\rho}_{\mathrm{A}} + \tilde{\rho}_{\mathrm{B}}] + \\
&+ E^{\mathrm{xc}}[\tilde{\rho}_{\mathrm{A}} + \tilde{\rho}_{\mathrm{B}}] + V^{\mathrm{nn}}_{\mathrm{AB}}.
\end{aligned} \tag{2.14}$$

Now we rewrite the functional (2.14) digging out the monomer contributions to the dimer energy through the careful inspection of the terms in (2.14). It is clear from (2.12) that the non-interacting kinetic energy functional is linear,

$$T^{\mathrm{s}}[\tilde{\rho}_{\mathrm{A}} + \tilde{\rho}_{\mathrm{B}}] = T^{\mathrm{s}}[\tilde{\rho}_{\mathrm{A}}] + T^{\mathrm{s}}[\tilde{\rho}_{\mathrm{B}}], \tag{2.15}$$

the nuclear-electron attraction separates as

$$\begin{aligned} V_{\mathrm{AB}}^{\mathrm{ne}}[\tilde{\rho}_{\mathrm{A}}+\tilde{\rho}_{\mathrm{B}}] &= \int_{\mathbb{R}^3}\Big(v_{\mathrm{A}}^{\mathrm{ne}}(\mathbf{r})+v_{\mathrm{B}}^{\mathrm{ne}}(\mathbf{r})\Big)\Big(\tilde{\rho}_{\mathrm{A}}(\mathbf{r})+\tilde{\rho}_{\mathrm{B}}(\mathbf{r})\Big)\,d^3\mathbf{r} = \\ &= V_{\mathrm{A}}^{\mathrm{ne}}[\tilde{\rho}_{\mathrm{A}}]+V_{\mathrm{B}}^{\mathrm{ne}}[\tilde{\rho}_{\mathrm{B}}]+ \\ &+ \int_{\mathbb{R}^3} v_{\mathrm{B}}^{\mathrm{ne}}(\mathbf{r})\tilde{\rho}_{\mathrm{A}}(\mathbf{r})\,d^3\mathbf{r}+\int_{\mathbb{R}^3} v_{\mathrm{A}}^{\mathrm{ne}}(\mathbf{r})\tilde{\rho}_{\mathrm{B}}(\mathbf{r})\,d^3\mathbf{r}, \end{aligned} \tag{2.16}$$

and the Coulomb term decomposes according to

$$\begin{aligned} &J[\tilde{\rho}_{\mathrm{A}}+\tilde{\rho}_{\mathrm{B}}] = \\ &= \frac{1}{2}\int_{\mathbb{R}^3}\int_{\mathbb{R}^3}\frac{\Big(\tilde{\rho}_{\mathrm{A}}(\mathbf{r}_1)+\tilde{\rho}_{\mathrm{B}}(\mathbf{r}_1)\Big)\Big(\tilde{\rho}_{\mathrm{A}}(\mathbf{r}_2)+\tilde{\rho}_{\mathrm{B}}(\mathbf{r}_2)\Big)}{r_{12}}\,d^3\mathbf{r}_1 d^3\mathbf{r}_2 = \\ &= J[\tilde{\rho}_{\mathrm{A}}]+J[\tilde{\rho}_{\mathrm{B}}]+\int_{\mathbb{R}^3}\int_{\mathbb{R}^3}\frac{\tilde{\rho}_{\mathrm{A}}(\mathbf{r}_1)\tilde{\rho}_{\mathrm{B}}(\mathbf{r}_2)}{r_{12}}\,d^3\mathbf{r}_1 d^3\mathbf{r}_2. \end{aligned} \tag{2.17}$$

However, the general explicit analytical form of the xc functional is unknown and its actual form depends on the applied approximation. Thus, we introduce the xc energy non-additivity:

$$E^{\mathrm{xc}}[\tilde{\rho}_{\mathrm{A}}+\tilde{\rho}_{\mathrm{B}}] = E^{\mathrm{xc}}[\tilde{\rho}_{\mathrm{A}}]+E^{\mathrm{xc}}[\tilde{\rho}_{\mathrm{B}}]+\Delta E_{\mathrm{xc}}[\tilde{\rho}_{\mathrm{A}}+\tilde{\rho}_{\mathrm{B}}] \tag{2.18}$$

which can be calculated directly from (2.18).

Although the expression (2.14) is a functional of a single density, we now make use of (2.11) and treat the system energy as a bifunctional depending on both monomer densities: $E_{\mathrm{AB}}[\tilde{\rho}_{\mathrm{A}}+\tilde{\rho}_{\mathrm{B}}] = E_{\mathrm{AB}}[\tilde{\rho}_{\mathrm{A}};\tilde{\rho}_{\mathrm{B}}]$, and $\Delta E_{\mathrm{xc}}[\tilde{\rho}_{\mathrm{A}}+\tilde{\rho}_{\mathrm{B}}] = \Delta E_{\mathrm{xc}}[\tilde{\rho}_{\mathrm{A}};\tilde{\rho}_{\mathrm{B}}]$. Thus, in our quest for the ground-state dimer energy, we will minimize with respect to $\tilde{\rho}_{\mathrm{A}}$ and $\tilde{\rho}_{\mathrm{B}}$ the bifunctional

$$\begin{aligned} E_{\mathrm{AB}}[\tilde{\rho}_{\mathrm{A}};\tilde{\rho}_{\mathrm{B}}] &= T^{\mathrm{s}}[\tilde{\rho}_{\mathrm{A}}]+V_{\mathrm{A}}^{\mathrm{ne}}[\tilde{\rho}_{\mathrm{A}}]+J[\tilde{\rho}_{\mathrm{A}}]+E^{\mathrm{xc}}[\tilde{\rho}_{\mathrm{A}}]+V_{\mathrm{A}}^{\mathrm{nn}}+ \\ &+ T^{\mathrm{s}}[\tilde{\rho}_{\mathrm{B}}]+V_{\mathrm{B}}^{\mathrm{ne}}[\tilde{\rho}_{\mathrm{B}}]+J[\tilde{\rho}_{\mathrm{B}}]+E^{\mathrm{xc}}[\tilde{\rho}_{\mathrm{B}}]+V_{\mathrm{B}}^{\mathrm{nn}}+ \\ &+ \tilde{E}_{\mathrm{int}}[\tilde{\rho}_{\mathrm{A}};\tilde{\rho}_{\mathrm{B}}] = \\ &= E_{\mathrm{A}}[\tilde{\rho}_{\mathrm{A}}]+E_{\mathrm{B}}[\tilde{\rho}_{\mathrm{B}}]+\tilde{E}_{\mathrm{int}}[\tilde{\rho}_{\mathrm{A}};\tilde{\rho}_{\mathrm{B}}], \end{aligned} \tag{2.19}$$

where

$$\begin{aligned} &\tilde{E}_{\mathrm{int}}[\tilde{\rho}_{\mathrm{A}};\tilde{\rho}_{\mathrm{B}}] = \int_{\mathbb{R}^3} v_{\mathrm{B}}^{\mathrm{ne}}(\mathbf{r})\tilde{\rho}_{\mathrm{A}}(\mathbf{r})\,d^3\mathbf{r}+\int_{\mathbb{R}^3} v_{\mathrm{A}}^{\mathrm{ne}}(\mathbf{r})\tilde{\rho}_{\mathrm{B}}(\mathbf{r})\,d^3\mathbf{r}+ \\ &+\int_{\mathbb{R}^3}\int_{\mathbb{R}^3}\frac{\tilde{\rho}_{\mathrm{A}}(\mathbf{r}_1)\tilde{\rho}_{\mathrm{B}}(\mathbf{r}_2)}{r_{12}}\,d^3\mathbf{r}_1 d^3\mathbf{r}_2+V_{\mathrm{int}}^{\mathrm{nn}}+\Delta E_{\mathrm{xc}}[\tilde{\rho}_{\mathrm{A}};\tilde{\rho}_{\mathrm{B}}] = \\ &= E_{\mathrm{elst}}[\tilde{\rho}_{\mathrm{A}};\tilde{\rho}_{\mathrm{B}}]+\Delta E_{\mathrm{xc}}[\tilde{\rho}_{\mathrm{A}};\tilde{\rho}_{\mathrm{B}}], \end{aligned} \tag{2.20}$$

constrained with densities integration conditions, i.e.

$$\mathscr{L}[\tilde{\rho}_{\mathrm{A}};\tilde{\rho}_{\mathrm{B}}] = E_{\mathrm{AB}}[\tilde{\rho}_{\mathrm{A}};\tilde{\rho}_{\mathrm{B}}]+ \\ + \mu_{\mathrm{A}}\left(N_{\mathrm{A}} - \int_{\mathbb{R}^3}\tilde{\rho}_{\mathrm{A}}(\mathbf{r})\,d^3\mathbf{r}\right) + \mu_{\mathrm{B}}\left(N_{\mathrm{B}} - \int_{\mathbb{R}^3}\tilde{\rho}_{\mathrm{B}}(\mathbf{r})\,d^3\mathbf{r}\right). \tag{2.21}$$

The intermonomer nuclear-nuclear repulsion energy is

$$V_{\mathrm{int}}^{\mathrm{nn}} = \sum_{\alpha\in\mathcal{A}}\sum_{\beta\in\mathcal{B}}\frac{Z_\alpha Z_\beta}{R_{\alpha\beta}}. \tag{2.22}$$

However, for the density additivity condition (2.11) to hold, all orbitals must be kept mutually orthogonal which also ensures that the intersystem Pauli exclusion principle is fulfilled. To achieve that we perform the variational optimization in the two steps, using the PB method of Gutowski and Piela [13]: firstly, the bifunctional extremal search itself is performed without the imposition of the intermonomer orthogonality constraint and finally, the penalty operator is added in the resulting iterative scheme. The penalty operator for monomer A reads

$$\hat{\tilde{R}}_{\mathrm{A}} = \sum_{i\in A}|\tilde{a}_i\rangle\langle\tilde{a}_i|, \tag{2.23}$$

and it is obvious that its action on monomer B's orbitals annihilates them once the orbitals are mutually orthogonal. Now we turn to the former step: to find a bifunctional minimum, we need to calculate the variational derivative of (2.21) with respect to $\tilde{\rho}_{\mathrm{A}}$. However, since the non-interacting kinetic energy is a functional of one-matrix, we have to minimize (2.19) over one-matrix $\tilde{\rho}_{\mathrm{A}}(\mathbf{r};\mathbf{r}')$ instead of density $\tilde{\rho}_{\mathrm{A}}(\mathbf{r})$. For that purpose the Dirac delta function proves very useful. The kinetic energy functional may be written as

$$\begin{aligned} T^{\mathrm{s}}[\rho] &= -\frac{1}{2}\int_{\mathbb{R}^3}\left[\Delta_{\mathbf{r}}\rho(\mathbf{r};\mathbf{r}')\right]_{\mathbf{r}'=\mathbf{r}}\,d^3\mathbf{r} = \\ &= -\frac{1}{2}\int_{\mathbb{R}^3}\delta(\mathbf{r}-\mathbf{r}')\Delta_{\mathbf{r}}\rho(\mathbf{r};\mathbf{r}')\,d^3\mathbf{r}d^3\mathbf{r}', \end{aligned} \tag{2.24}$$

and one easily finds

$$\frac{\delta T^{\mathrm{s}}[\rho]}{\delta\rho(\mathbf{r};\mathbf{r}')} = -\frac{1}{2}\Delta_{\mathbf{r}}\delta(\mathbf{r}-\mathbf{r}').$$

We also note that for the functionals depending on the density only, e.g. $J[\rho]$, we can relate the functional derivatives with respect to one-matrix and density as follows:

$$\frac{\delta J[\rho]}{\delta\rho(\mathbf{r};\mathbf{r}')} = \frac{\delta J[\rho]}{\delta\rho(\mathbf{r})}\delta(\mathbf{r}-\mathbf{r}'), \tag{2.25}$$

which results from (1.18). The functional derivative of (2.21) thus reads

$$\frac{\delta \mathscr{L}_{\mathrm{AB}}[\tilde{\rho}_{\mathrm{A}};\tilde{\rho}_{\mathrm{B}}]}{\delta \tilde{\rho}_{\mathrm{A}}(\mathbf{r};\mathbf{r}')} = \\ = \left(-\frac{1}{2}\Delta_{\mathbf{r}} + v_{\mathrm{A}}^{\mathrm{ne}}(\mathbf{r}) + \tilde{\jmath}_{\mathrm{A}}(\mathbf{r}) + \tilde{v}_{\mathrm{A}}^{\mathrm{xc}}(\mathbf{r}) + v_{\mathrm{B}}^{\mathrm{ne}}(\mathbf{r}) + \tilde{\jmath}_{\mathrm{B}}(\mathbf{r}) + \Delta\tilde{v}_{\mathrm{A}}^{\mathrm{xc}}(\mathbf{r}) + \mu_{\mathrm{A}}\right)\delta(\mathbf{r}-\mathbf{r}') \tag{2.26}$$

with the non-additivity xc potential being

$$\begin{aligned} \Delta\tilde{v}_{\mathrm{A}}^{\mathrm{xc}}(\mathbf{r}) &= \frac{\delta \Delta E_{\mathrm{xc}}[\tilde{\rho}_{\mathrm{A}};\tilde{\rho}_{\mathrm{B}}]}{\delta\tilde{\rho}_{\mathrm{A}}(\mathbf{r})} = \\ &= \frac{\delta E_{\mathrm{xc}}[\tilde{\rho}_{\mathrm{A}}+\tilde{\rho}_{\mathrm{B}}]}{\delta\tilde{\rho}_{\mathrm{A}}(\mathbf{r})} - \frac{\delta E_{\mathrm{xc}}[\tilde{\rho}_{\mathrm{A}}]}{\delta\tilde{\rho}_{\mathrm{A}}(\mathbf{r})} = \\ &= \frac{\delta E_{\mathrm{xc}}[\tilde{\rho}_{\mathrm{AB}}]}{\delta\tilde{\rho}_{\mathrm{AB}}(\mathbf{r})} - \tilde{v}_{\mathrm{A}}^{\mathrm{xc}}(\mathbf{r}) = \\ &= \tilde{v}_{\mathrm{AB}}^{\mathrm{xc}}(\mathbf{r}) - \tilde{v}_{\mathrm{A}}^{\mathrm{xc}}(\mathbf{r}). \end{aligned} \tag{2.27}$$

The Euler equation for the bifunctional (2.21) is

$$\mu_{\mathrm{A}} = \left(-\frac{1}{2}\Delta_{\mathbf{r}} + v_{\mathrm{A}}^{\mathrm{eff}}(\mathbf{r})\right)\delta(\mathbf{r}-\mathbf{r}') \tag{2.28}$$

with

$$v_{\mathrm{A}}^{\mathrm{eff}}(\mathbf{r}) = \tilde{v}_{\mathrm{A}}^{\mathrm{elst}}(\mathbf{r}) + \tilde{v}_{\mathrm{A}}^{\mathrm{xc}}(\mathbf{r}) + \tilde{v}_{\mathrm{B}}^{\mathrm{elst}}(\mathbf{r}) + \Delta\tilde{v}_{\mathrm{A}}^{\mathrm{xc}}(\mathbf{r}). \tag{2.29}$$

The minimization of (2.19) with respect to $\tilde{\rho}_{\mathrm{B}}$ proceeds in an analogous way.

Finally, the orbitals minimizing the functional (2.19) satisfy

$$\boxed{\begin{cases} \left(\hat{\tilde{f}}_{\mathrm{A}}^{\mathrm{KS}}(\mathbf{r}) + \Delta\tilde{v}_{\mathrm{A}}^{\mathrm{xc}}(\mathbf{r}) + \hat{\tilde{v}}_{\mathrm{B}}^{\mathrm{elst}}(\mathbf{r})\right)\tilde{a}_i(\mathbf{r}) = \epsilon_{\mathrm{A},i}\tilde{a}_i(\mathbf{r}) \\ \left(\hat{\tilde{f}}_{\mathrm{B}}^{\mathrm{KS}}(\mathbf{r}) + \Delta\tilde{v}_{\mathrm{B}}^{\mathrm{xc}}(\mathbf{r}) + \hat{\tilde{v}}_{\mathrm{A}}^{\mathrm{elst}}(\mathbf{r})\right)\tilde{b}_k(\mathbf{r}) = \epsilon_{\mathrm{B},k}\tilde{b}_k(\mathbf{r}) \end{cases}} \tag{2.30}$$

together with the intra- and intermonomer orthogonality conditions:

$$\boxed{\forall_{i,j\in A,k,l\in B} : \langle\tilde{a}_i\,|\,\tilde{a}_j\rangle = \delta_{ij} \wedge \left\langle\tilde{b}_k\,\middle|\,\tilde{b}_l\right\rangle = \delta_{kl} \wedge \left\langle\tilde{a}_i\,\middle|\,\tilde{b}_k\right\rangle = 0}. \tag{2.31}$$

In the latter step of the PB procedure, we formulate the iterative process of solving Eqs. (2.30) with the aid of the penalty operator:

$$\begin{cases} \left(\hat{\tilde{f}}_{\mathrm{A}}^{\mathrm{KS}[n-1]} + \Delta\tilde{v}_{\mathrm{A}}^{\mathrm{xc}[n-1]} + \hat{\tilde{v}}_{\mathrm{B}}^{\mathrm{elst}[n-1]} + \eta\hat{\tilde{R}}_{\mathrm{B}}^{[n-1]}\right)a_i^{[n]} = \epsilon_{\mathrm{A},i}^{[n]}a_i^{[n]} \\ \left(\hat{\tilde{f}}_{\mathrm{B}}^{\mathrm{KS}[n-1]} + \Delta\tilde{v}_{\mathrm{B}}^{\mathrm{xc}[n-1]} + \hat{\tilde{v}}_{\mathrm{A}}^{\mathrm{elst}[n-1]} + \eta\hat{\tilde{R}}_{\mathrm{A}}^{[n-1]}\right)b_k^{[n]} = \epsilon_{\mathrm{B},k}^{[n]}b_k^{[n]} \end{cases}, \tag{2.32}$$

where the numbers in brackets denote iteration numbers. However, the penalty operator does not suffice to impose conditions (2.31) so the orbitals obtained in (2.32) are orthogonalized after each iteration, yielding

$$\tilde{\Omega}^{[n]} = \left\{ \left\{ \tilde{a}_i^{[n]} \right\}_{i \in A} ; \left\{ \tilde{b}_k^{[n]} \right\}_{k \in B} \right\} \tag{2.33}$$

set.

The interaction energy at the nth iteration is obtained upon the insertion of the orthogonalized densities calculated with orbitals (2.33) into (2.19) and subtracting the unperturbed monomer energies:

$$\begin{aligned} E_{\text{int}}^{\text{PB}[n]} &= E_{\text{AB}} \left[\tilde{\rho}_{\text{A}}^{[n]}; \tilde{\rho}_{\text{B}}^{[n]} \right] - E_{\text{A}} \left[\rho_{\text{A}}^{0} \right] - E_{\text{B}} \left[\rho_{\text{B}}^{0} \right] = \\ &= \Delta \tilde{E}_{\text{A}}^{[n]} + \Delta \tilde{E}_{\text{B}}^{[n]} + E_{\text{elst}} \left[\tilde{\rho}_{\text{A}}^{[n]}; \tilde{\rho}_{\text{B}}^{[n]} \right] + \Delta E_{\text{xc}} \left[\tilde{\rho}_{\text{A}}^{[n]}; \tilde{\rho}_{\text{B}}^{[n]} \right], \end{aligned} \tag{2.34}$$

where the A monomer deformation is

$$\Delta \tilde{E}_{\text{A}} = E_{\text{A}} \left[\tilde{\rho}_{\text{A}}^{[n]} \right] - E_{\text{A}} \left[\rho_{\text{A}}^{0} \right], \tag{2.35}$$

and analogously for monomer B. Upon self-consistency, the energy (2.34) equals the supermolecular DFT interaction energy (2.7).

Since the iterative process (2.32) starts with the unperturbed orbitals calculated with (2.1), the zeroth-iteration interaction energy may be viewed as an analogue of the well-known HF-based HL interaction energy. More specifically, the DFT-based HL interaction energy is

$$E_{\text{int}}^{\text{HL}} = E_{\text{int}}^{\text{PB}[0]} = E_{\text{AB}} \left[\tilde{\rho}_{\text{A}}^{0}; \tilde{\rho}_{\text{B}}^{0} \right] - E \left[\rho_{\text{A}}^{0} \right] - E \left[\rho_{\text{B}}^{0} \right], \tag{2.36}$$

and such a definition is the same as that proposed by Cybulski and Seversen [30].

It is worthwhile to note that he expressions (2.34) together with (2.7) yield an exact non-relativistic interaction energy once an exact xc functional is applied.

2.3 Related Publication

The following publication [31] contains results for the bifunctional approach.

Chemical Physics Letters 486 (2010) 160–165

Contents lists available at ScienceDirect

Chemical Physics Letters

journal homepage: www.elsevier.com/locate/cplett

Derivation of the supermolecular interaction energy from the monomer densities in the density functional theory

Łukasz Rajchel [a,b], Piotr S. Żuchowski [c], Małgorzata M. Szczęśniak [a], Grzegorz Chałasiński [b,*]

[a] Department of Chemistry, Oakland University, Rochester, MI 48309-4477, USA
[b] Faculty of Chemistry, University of Warsaw, 02-093 Warszawa, Pasteura 1, Poland
[c] Department of Chemistry, Durham University, South Road, Durham DH1 3LE, United Kingdom

ARTICLE INFO

Article history:
Received 7 November 2009
In final form 29 December 2009
Available online 25 January 2010

ABSTRACT

The density functional theory (DFT) interaction energy of a dimer is rigorously derived from the monomer densities. To this end, the supermolecular energy bifunctional is formulated in terms of mutually orthogonal sets of orbitals of the constituent monomers. The orthogonality condition is preserved in the solution of the Kohn–Sham equations through the Pauli blockade method. Numerical implementation of the method provides interaction energies which agree with those obtained from standard supermolecular calculations within less than 0.1% error for three example functionals: Slater–Dirac, PBE0 and B3LYP, and for two model van der Waals dimers: Ne_2 and $(C_2H_4)_2$, and two model H-bond complexes: $(HF)_2$ and $(NH_3)_2$.

1. Introduction

Deriving the dimer interaction energy via mutual polarization of constituent monomers is important both from the fundamental perspective and from a practical point of view. In particular, it may aid the understanding how the non-covalent systems are described in the density functional theory which is one of the most problematic issues of the electronic structure theory. The major problem of DFT as applied to the van der Waals systems is a wrong description of dispersion forces [1–3]. Surprisingly enough, little has been done to better understand the performance of supermolecular interaction energy in the framework of DFT. For the Hartree–Fock (HF) interaction energy, such an approach has been pioneered by Morokuma [4] in the 1970s, and a decade later, inspired by the work of Sadlej [5], rigorously derived by Gutowski and Piela [6] (see also Ref. [7]). The perturbation approach within the symmetry-adapted perturbatin theory (SAPT) formalism was also extensively exploited in this context [8,9]. In the age of DFT, it is highly desirable to develop such an approach also for the density functional formalism. Approximate DFT treatments have already been advanced by Cortona and coworkers [10,11]; see also recent energy decomposition schemes proposed in Refs. [12–14], and Refs. therein, as well as the density functional formulation of SAPT [15,16].

The goal of this work is to derive rigorously the supermolecular density functional theory (DFT) interaction energy via the mutual polarization of the monomer densities. To this end the supermolecular (dimer) energy functional is expressed in terms of mutually orthogonalized sets of the Kohn–Sham (KS) orbitals of the constituent monomers. The coupled KS equations are next solved iteratively, by using the Pauli blockade (PB) technique of Gutowski and Piela [6]. The correctness of the derivation is demonstrated by comparing the interaction energy calculated from the equations developed here and the supermolecular interaction energies. The DFT approximation to the Heitler–London interaction energy, based on the decomposition of the interaction energy introduced in this Letter, is also discussed.

2. Theory

In this Letter we consider the interaction between two closed-shell systems, however, the generalization for high-spin open-shell systems and clusters is straightforward. The supermolecular interaction energy in terms of DFT can be defined as the difference between the total energies of the dimer AB and the individual monomers A and B, separated to infinity:

$$E_{\mathrm{int}}^{\mathrm{DFT}} = E_{\mathrm{AB}}^{\mathrm{DFT}} - E_{\mathrm{A}}^{\mathrm{DFT}} - E_{\mathrm{B}}^{\mathrm{DFT}}. \quad (1)$$

It was demonstrated by Gutowski and Piela [6] that the HF supermolecular interaction energy may be exactly recovered by solving the HF equations for monomers in the presence of the external perturbation, consisting of the electrostatic potential and the non-local exchange potential generated by the second monomer. They have also proposed a convenient computational scheme for the PB method in terms of mutually orthogonalized A

* Corresponding author. Fax: +48 22 8222309.
E-mail addresses: lrajchel@tiger.chem.uw.edu.pl (Ł. Rajchel), chalbie@tiger.chem.uw.edu.pl (G. Chałasiński).

0009-2614/$ - see front matter © 2009 Elsevier B.V. All rights reserved.
doi:10.1016/j.cplett.2009.12.083

and B orbitals with the penalty operator forcing the orthogonality of monomers' occupied orbitals. In this section we derive an analogous formalism in terms of appropriately modified KS equations and monomer densities.

We begin with KS equations for the isolated monomers which yield the starting orbitals $\{a_i^0\}_{i\in A}$ and $\{b_k^0\}_{k\in B}$. The orbitals of monomer A are the solutions of the following eigen equation:

$$\hat{f}_{\mathrm{A}}^{\mathrm{KS},0}(\mathbf{r})a_i^0(\mathbf{r}) = \epsilon_{\mathrm{A},i}^0 a_i^0(\mathbf{r}), \tag{2}$$

and the analogous equations hold for the monomer B. The KS operator of Eq. (2) is written as

$$\hat{f}_{\mathrm{A}}^{\mathrm{KS},0}(\mathbf{r}) = -\frac{1}{2}\Delta_{\mathbf{r}} + v_{\mathrm{A}}^{\mathrm{ne}}(\mathbf{r}) + \hat{\jmath}_{\mathrm{A}}(\mathbf{r}) + v_{\mathrm{A}}^{\mathrm{xc}}(\mathbf{r}), \tag{3}$$

where the monomer A nuclear potential is

$$v_{\mathrm{A}}^{\mathrm{ne}}(\mathbf{r}) = -\sum_{\alpha=1}^{\mathcal{N}_{\mathrm{A}}}\frac{Z_\alpha}{|\mathbf{r}-\mathbf{R}_\alpha|} \tag{4}$$

with $\mathcal{N}_{\mathrm{A}}$ being the number of monomer A nuclei, each described by its position $\mathbf{R}_\alpha$ and charge Z_α. Its coulombic potential reads

$$\hat{\jmath}_{\mathrm{A}}(\mathbf{r}) = \int_{\mathbb{R}^3}\frac{\rho_{\mathrm{A}}^0(\mathbf{r}')}{|\mathbf{r}-\mathbf{r}'|}d^3\mathbf{r}'. \tag{5}$$

The total energy of monomer A can be written as

$$E_{\mathrm{A}}[\rho_{\mathrm{A}}^0] = T^{\mathrm{s}}[\rho_{\mathrm{A}}^0] + V_{\mathrm{A}}^{\mathrm{ne}}[\rho_{\mathrm{A}}^0] + J[\rho_{\mathrm{A}}^0] + E^{\mathrm{xc}}[\rho_{\mathrm{A}}^0] + V_{\mathrm{A}}^{\mathrm{nn}}. \tag{6}$$

The functional (6) comprises the non-interacting kinetic energy:

$$T^{\mathrm{s}}[\rho_{\mathrm{A}}^0] = 2\sum_{i\in A}\left\langle a_i^0\middle|-\frac{1}{2}\Delta_{\mathbf{r}}\middle|a_i^0\right\rangle, \tag{7}$$

with A being the set of the indices of occupied orbitals of the monomer A, nuclear–electron attraction energy:

$$V_{\mathrm{A}}^{\mathrm{ne}}[\rho_{\mathrm{A}}^0] = \int_{\mathbb{R}^3} v_{\mathrm{A}}^{\mathrm{ne}}(\mathbf{r})\rho_{\mathrm{A}}^0(\mathbf{r})d^3\mathbf{r}, \tag{8}$$

coulombic energy

$$J[\rho_{\mathrm{A}}^0] = \frac{1}{2}\int_{\mathbb{R}^3}\int_{\mathbb{R}^3}\frac{\rho_{\mathrm{A}}^0(\mathbf{r}_1)\rho_{\mathrm{A}}^0(\mathbf{r}_2)}{r_{12}}d^3\mathbf{r}_1\,d^3\mathbf{r}_2, \tag{9}$$

exchange-correlation (xc) energy

$$E^{\mathrm{xc}}[\rho_{\mathrm{A}}^0] = \int_{\mathbb{R}^3} F^{\mathrm{xc}}\left(\rho_{\mathrm{A}}^0(\mathbf{r}); \{\nabla_{\mathbf{r}}\rho_{\mathrm{A}}^0(\mathbf{r}); \ldots\}\right)d^3\mathbf{r}, \tag{10}$$

which is evaluated through the numerical integration of the F^{xc} integrand on a grid of points around monomer A, and the nuclear–nuclear repulsion term

$$V_{\mathrm{A}}^{\mathrm{nn}} = \sum_{\alpha=1}^{\mathcal{N}_{\mathrm{A}}-1}\sum_{\beta=\alpha+1}^{\mathcal{N}_{\mathrm{A}}}\frac{Z_\alpha Z_\beta}{R_{\alpha\beta}}, \tag{11}$$

which is constant for a fixed geometry. The density of monomer A is

$$\rho_{\mathrm{A}}^0(\mathbf{r}) = 2\sum_{i\in A}\left|a_i^0(\mathbf{r})\right|^2. \tag{12}$$

Similar expressions can be written for monomer B.

The original, isolated-monomer orbital sets $\{a_i^0\}_{i\in A}$ and $\{b_k^0\}_{k\in B}$ are not mutually orthogonal. To proceed, it is also important to introduce the set of orthonormalized orbitals which are obtained by using Löwdin symmetric orthonormalization [17]. The quantities expressed in the orthonormalized orbitals are henceforth marked with tilde. One should remember that the orthonormalization leaves the total density of the dimer unchanged. However, it does change the monomer densities into the densities deformed by the presence of the interacting partner.

In the PB method the zeroth-order wavefunction of the dimer is the wavefunction of the system in the absence of molecular interaction. It is constructed from the antisymmetrized product of the orthogonalized occupied orbitals of the monomers A and B. In case of KS equations for dimer the KS determinant can be constructed in the same manner as:

$$\psi_{\mathrm{AB}}^0 = \hat{\mathscr{A}}\tilde{\psi}_{\mathrm{A}}^0\tilde{\psi}_{\mathrm{B}}^0, \tag{13}$$

where $\tilde{\psi}_{\mathrm{A}}^0$ and $\tilde{\psi}_{\mathrm{B}}^0$ are KS determinants of monomers A and B, respectively. Since the determinants are constructed from orthonormalized orbitals, the ψ_{AB}^0 is normalized.

It can be easily shown that the zeroth-order density of the system can be simply written as a sum of monomer densities expressed in terms of orthonormalized orbitals,

$$\rho_{\mathrm{AB}}^0 = \tilde{\rho}_{\mathrm{AB}}^0 = \tilde{\rho}_{\mathrm{A}}^0 + \tilde{\rho}_{\mathrm{B}}^0. \tag{14}$$

Note that (14) does not hold for the densities obtained from non-orthonormal orbitals of the dimer, i.e. $\rho_{\mathrm{AB}}^0 \neq \rho_{\mathrm{A}}^0 + \rho_{\mathrm{B}}^0$.

If the interaction between monomers is switched on we assume that the KS determinant of the dimer can be written as the antisymmetrized product of two determinants for both the monomers:

$$\tilde{\psi}_{\mathrm{AB}} = \hat{\mathscr{A}}\tilde{\psi}_{\mathrm{A}}\tilde{\psi}_{\mathrm{B}}, \tag{15}$$

and hence the dimer density fulfills the additivity condition (14). Owing to (14) and using (6), the energy functional for the system corresponding to (15) is

$$\begin{aligned}E_{\mathrm{AB}}[\rho_{\mathrm{AB}}] = E_{\mathrm{AB}}[\tilde{\rho}_{\mathrm{AB}}] &= E_{\mathrm{AB}}[\tilde{\rho}_{\mathrm{A}} + \tilde{\rho}_{\mathrm{B}}] = T^{\mathrm{s}}[\tilde{\rho}_{\mathrm{A}} + \tilde{\rho}_{\mathrm{B}}] \\ &+ V_{\mathrm{AB}}^{\mathrm{ne}}[\tilde{\rho}_{\mathrm{A}} + \tilde{\rho}_{\mathrm{B}}] + J[\tilde{\rho}_{\mathrm{A}} + \tilde{\rho}_{\mathrm{B}}] + E^{\mathrm{xc}}[\tilde{\rho}_{\mathrm{A}} + \tilde{\rho}_{\mathrm{B}}] + V_{\mathrm{AB}}^{\mathrm{nn}}.\end{aligned} \tag{16}$$

Now we rewrite the functional (16) extracting the monomer contributions to the dimer energy through a careful inspection of the terms in (16). It is clear from (7) that the non-interacting kinetic energy functional is linear,

$$T^{\mathrm{s}}[\tilde{\rho}_{\mathrm{A}} + \tilde{\rho}_{\mathrm{B}}] = T^{\mathrm{s}}[\tilde{\rho}_{\mathrm{A}}] + T^{\mathrm{s}}[\tilde{\rho}_{\mathrm{B}}], \tag{17}$$

the nuclear–electron attraction may be separated as

$$\begin{aligned}V_{\mathrm{AB}}^{\mathrm{ne}}[\tilde{\rho}_{\mathrm{A}} + \tilde{\rho}_{\mathrm{B}}] &= \int_{\mathbb{R}^3}\left(v_{\mathrm{A}}^{\mathrm{ne}}(\mathbf{r}) + v_{\mathrm{B}}^{\mathrm{ne}}(\mathbf{r})\right)\left(\tilde{\rho}_{\mathrm{A}}(\mathbf{r}) + \tilde{\rho}_{\mathrm{B}}(\mathbf{r})\right)d^3\mathbf{r} \\ &= V_{\mathrm{A}}^{\mathrm{ne}}[\tilde{\rho}_{\mathrm{A}}] + V_{\mathrm{B}}^{\mathrm{ne}}[\tilde{\rho}_{\mathrm{B}}] \\ &+ \int_{\mathbb{R}^3} v_{\mathrm{B}}^{\mathrm{ne}}(\mathbf{r})\tilde{\rho}_{\mathrm{A}}(\mathbf{r})d^3\mathbf{r} + \int_{\mathbb{R}^3} v_{\mathrm{A}}^{\mathrm{ne}}(\mathbf{r})\tilde{\rho}_{\mathrm{B}}(\mathbf{r})d^3\mathbf{r},\end{aligned} \tag{18}$$

and the coulombic term may be decomposed according to

$$\begin{aligned}J[\tilde{\rho}_{\mathrm{A}} + \tilde{\rho}_{\mathrm{B}}] &= \frac{1}{2}\int_{\mathbb{R}^3}\int_{\mathbb{R}^3}\left(\tilde{\rho}_{\mathrm{A}}(\mathbf{r}_1) + \tilde{\rho}_{\mathrm{B}}(\mathbf{r}_1)\right)\left(\tilde{\rho}_{\mathrm{A}}(\mathbf{r}_2) + \tilde{\rho}_{\mathrm{B}}(\mathbf{r}_2)\right) \\ &\times r_{12}^{-1}d^3\mathbf{r}_1 d^3\mathbf{r}_2 \\ &= J[\tilde{\rho}_{\mathrm{A}}] + J[\tilde{\rho}_{\mathrm{B}}] + \int_{\mathbb{R}^3}\int_{\mathbb{R}^3}\frac{\tilde{\rho}_{\mathrm{A}}(\mathbf{r}_1)\tilde{\rho}_{\mathrm{B}}(\mathbf{r}_2)}{r_{12}}d^3\mathbf{r}_1 d^3\mathbf{r}_2.\end{aligned} \tag{19}$$

However, the explicit analytical form of the xc functional is unknown and its approximations depend on the functional used. Thus, we introduce the xc energy non-additivity, ΔE_{xc}:

$$\Delta E_{\mathrm{xc}}[\tilde{\rho}_{\mathrm{A}} + \tilde{\rho}_{\mathrm{B}}] = E^{\mathrm{xc}}[\tilde{\rho}_{\mathrm{A}} + \tilde{\rho}_{\mathrm{B}}] - E^{\mathrm{xc}}[\tilde{\rho}_{\mathrm{A}}] - E^{\mathrm{xc}}[\tilde{\rho}_{\mathrm{B}}]. \tag{20}$$

It is worthwhile to note that the present formulation neither separates nor approximates any of the kinetic non-additivity terms appearing in the method of Wesotowski and Warshel [11]. These terms are implicitly and exactly included in the term (20) and thus are automatically accounted for in a consistent manner for any functional. Although the expression (16) is a functional of a single density, we now make use of (14) and treat the system energy as a bifunctional depending on both monomer densities:

$$E_{\mathrm{AB}}[\tilde{\rho}_{\mathrm{A}} + \tilde{\rho}_{\mathrm{B}}] \equiv E_{\mathrm{AB}}[\tilde{\rho}_{\mathrm{A}}; \tilde{\rho}_{\mathrm{B}}]. \tag{21}$$

Thus, in our search for the ground-state dimer energy, we will minimize, with respect to $\tilde{\rho}_A$ and $\tilde{\rho}_B$, the bifunctional of the form:

$$\begin{aligned}
&E_{AB}[\tilde{\rho}_A;\tilde{\rho}_B]\\
&\quad= T^s[\tilde{\rho}_A]+V_A^{ne}[\tilde{\rho}_A]+J[\tilde{\rho}_A]+E^{xc}[\tilde{\rho}_A]+V_A^{nn}\\
&\qquad+T^s[\tilde{\rho}_B]+V_B^{ne}[\tilde{\rho}_B]+J[\tilde{\rho}_B]+E^{xc}[\tilde{\rho}_B]+V_B^{nn}\\
&\qquad+\widetilde{E}_{int}[\tilde{\rho}_A;\tilde{\rho}_B]\\
&\quad= E_A[\tilde{\rho}_A]+E_B[\tilde{\rho}_B]+\widetilde{E}_{int}[\tilde{\rho}_A;\tilde{\rho}_B],
\end{aligned}\tag{22}$$

where

$$\begin{aligned}
&\widetilde{E}_{int}[\tilde{\rho}_A;\tilde{\rho}_B]\\
&\quad=\int_{\mathbb{R}^3} v_B^{ne}(\mathbf{r})\tilde{\rho}_A(\mathbf{r})d^3\mathbf{r}+\int_{\mathbb{R}^3} v_A^{ne}(\mathbf{r})\tilde{\rho}_B(\mathbf{r})d^3\mathbf{r}\\
&\qquad+\int_{\mathbb{R}^3}\int_{\mathbb{R}^3}\frac{\tilde{\rho}_A(\mathbf{r}_1)\tilde{\rho}_B(\mathbf{r}_2)}{r_{12}}d^3\mathbf{r}_1d^3\mathbf{r}_2+V_{int}^{nn}\\
&\qquad+\Delta E_{xc}[\tilde{\rho}_A;\tilde{\rho}_B]\\
&\quad= E_{elst}[\tilde{\rho}_A;\tilde{\rho}_B]+\Delta E_{xc}[\tilde{\rho}_A;\tilde{\rho}_B].
\end{aligned}\tag{23}$$

In the above equation, V_{int}^{nn} is intermonomer nuclear–nuclear repulsion energy. However, for the density additivity condition (14) to hold, all orbitals must be kept mutually orthogonal, and the orthogonality also ensures that the intersystem Pauli exclusion principle is fulfilled. To this end, we perform the variational optimization in two steps, using the Pauli blockade (PB) method of Gutowski and Piela [6]: first, the bifunctional extremal search is performed without the imposition of the intermonomer orthogonality constraint, and secondly, the penalty operator is added in the resulting iterative scheme. The penalty operator for monomer A reads

$$\hat{\tilde{R}}_A=\sum_{i\in A}|\tilde{a}_i\rangle\langle\tilde{a}_i|,\tag{24}$$

and it is obvious that its action on monomer B's orbitals annihilates them once the orbitals are orthogonal. Now we turn to the first step: to find a bifunctional minimum, we calculate the variational derivative of (22) with respect to $\tilde{\rho}_A$:

$$\begin{aligned}
&\frac{\delta E_{AB}[\tilde{\rho}_A;\tilde{\rho}_B]}{\delta\tilde{\rho}_A(\mathbf{r})}\\
&\quad=-\frac{1}{2}\Delta_{\mathbf{r}}+v_A^{ne}(\mathbf{r})+\hat{\tilde{J}}_A(\mathbf{r})+\tilde{v}_A^{xc}(\mathbf{r})\\
&\qquad+v_B^{ne}(\mathbf{r})+\hat{\tilde{J}}_B(\mathbf{r})+\Delta\tilde{v}_A^{xc}(\mathbf{r})\\
&\quad=\hat{\tilde{f}}_A^{KS}(\mathbf{r})+\Delta\tilde{v}_A^{xc}(\mathbf{r})+\hat{\tilde{v}}_B^{elst}(\mathbf{r}),
\end{aligned}\tag{25}$$

where the electrostatic potential is

$$\hat{\tilde{v}}_B^{elst}(\mathbf{r})=v_B^{ne}(\mathbf{r})+\hat{\tilde{J}}_B(\mathbf{r}),\tag{26}$$

and the non-additivity xc operator reads

$$\begin{aligned}
\Delta\tilde{v}_A^{xc}(\mathbf{r})&=\frac{\delta\Delta E^{xc}[\tilde{\rho}_A;\tilde{\rho}_B]}{\delta\tilde{\rho}_A(\mathbf{r})}=\frac{\delta E^{xc}[\tilde{\rho}_A+\tilde{\rho}_B]}{\delta\tilde{\rho}_A(\mathbf{r})}-\frac{\delta E^{xc}[\tilde{\rho}_A]}{\delta\tilde{\rho}_A(\mathbf{r})}\\
&=\frac{\delta E^{xc}[\rho_{AB}]}{\delta\rho_{AB}(\mathbf{r})}-\tilde{v}_A^{xc}(\mathbf{r})=v_{AB}^{xc}(\mathbf{r})-\tilde{v}_A^{xc}(\mathbf{r}).
\end{aligned}\tag{27}$$

Hence, the Euler equation for the bifunctional (22) is

$$\mu_A=-\frac{1}{2}\Delta_{\mathbf{r}}+\hat{v}_A^{eff}(\mathbf{r})\tag{28}$$

with

$$\hat{v}_A^{eff}(\mathbf{r})=\hat{\tilde{v}}_A^{elst}(\mathbf{r})+\tilde{v}_A^{xc}(\mathbf{r})+\hat{\tilde{v}}_B^{elst}(\mathbf{r})+\tilde{v}_A^{xc}(\mathbf{r})+\Delta\tilde{v}_A^{xc}(\mathbf{r}),\tag{29}$$

and μ_A being the Lagrange multiplier for the constraint:

$$N_A-\int_{\mathbb{R}^3}\tilde{\rho}_A(\mathbf{r})d^3\mathbf{r}=0.\tag{30}$$

The minimization of (22) with respect to $\tilde{\rho}_B$ proceeds in an analogous way. Finally, the orbitals minimizing the functional (22) are determined to satisfy

$$\begin{cases}\left(\hat{\tilde{f}}_A^{KS}(\mathbf{r})+\Delta\tilde{v}_A^{xc}(\mathbf{r})+\hat{\tilde{v}}_B^{elst}(\mathbf{r})\right)\tilde{a}_i(\mathbf{r})=\epsilon_{A,i}\tilde{a}_i(\mathbf{r})\\ \left(\hat{\tilde{f}}_B^{KS}(\mathbf{r})+\Delta\tilde{v}_B^{xc}(\mathbf{r})+\hat{\tilde{v}}_A^{elst}(\mathbf{r})\right)\tilde{b}_k(\mathbf{r})=\epsilon_{B,k}\tilde{b}_k(\mathbf{r}).\end{cases}\tag{31}$$

In the second step of the PB procedure, the iterative process of solving Eq. (31) with the aid of the penalty operator is formulated. For monomer A the nth iterative step reads

$$\left(\hat{\tilde{f}}_A^{KS[n-1]}+\Delta\tilde{v}_A^{xc[n-1]}+\hat{\tilde{v}}_B^{elst[n-1]}+\eta\hat{\tilde{R}}_B^{[n-1]}\right)a_i^{[n]}=\epsilon_{A,i}^{[n]}a_i^{[n]},\tag{32}$$

and its equivalent for monomer B is obtained through the interchange of the A and B subscripts in (32). $\eta>0$ is a parameter not affecting the final solutions. The orbitals obtained in (32) are orthogonalized, yielding an orthonormal $\left\{\{\tilde{a}_i^{[n]}\}_{i\in A};\{\tilde{b}_k^{[n]}\}_{k\in B}\right\}$ set. The interaction energy at the nth iteration is obtained upon the insertion of the densities calculated with these orbitals into (22) and subtracting the unperturbed monomer energies:

$$\begin{aligned}
E_{int}^{PB[n]}&=E_{AB}\left[\tilde{\rho}_A^{[n]};\tilde{\rho}_B^{[n]}\right]-E_A\left[\rho_A^0\right]-E_B\left[\rho_B^0\right]\\
&=\Delta\widetilde{E}_A^{[n]}+\Delta\widetilde{E}_B^{[n]}+E_{elst}\left[\tilde{\rho}_A^{[n]};\tilde{\rho}_B^{[n]}\right]+\Delta E_{xc}\left[\tilde{\rho}_A^{[n]};\tilde{\rho}_B^{[n]}\right].
\end{aligned}\tag{33}$$

In the above equation, the A monomer deformation is

$$\Delta\widetilde{E}_A=E_A\left[\tilde{\rho}_A^{[n]}\right]-E_A\left[\rho_A^0\right],\tag{34}$$

and analogously for monomer B. Upon reaching self-consistency, the energy (33) is equal to the supermolecular DFT interaction energy of (1). The computational cost of our approach is essentially the same as that of the standard KS calculations.

Since the iterative process (32) starts with the KS orbitals of the isolated monomers, the zero-iteration interaction energy may be viewed as an analog of the well-known HF-based Heitler–London interaction energy. Specifically, we define the DFT-based HL interaction energy as

$$E_{int}^{HL}=E_{int}^{PB[0]}=E_{AB}\left[\tilde{\rho}_A^0;\tilde{\rho}_B^0\right]-E_A\left[\rho_A^0\right]-E_B\left[\rho_B^0\right].\tag{35}$$

This definition is equivalent to that proposed by Cybulski and Seversen [12]. The difference between the self-consistent interaction energy and the HL interaction energy,

$$E_{def}^{PB}=E_{int}^{PB}-E_{int}^{HL},\tag{36}$$

is referred to as the deformation energy.

It should be stressed here that both E_{int}^{HL} and E_{def}^{PB}, as defined by the above equations, are uniquely defined, and are independent of the orthogonalization procedure, and may be interpreted in terms of SAPT. The E_{int}^{HL} is the HL energy arising between the unperturbed, non-orthogonal monomers. At the HF level of theory, it includes the intermolecular electrostatic and exchange energies. In the DFT case, depending on a particular functional, it may also contain some obscure residual inter-monomer electron correlation terms that are related to the dispersion effect. This is because the interaction operator is, in general, the exchange-correlation operator rather than the exact-exchange one only, and the correlation is basically of a local type.

The E_{def}^{PB} term represents the deformation effect with respect to the non-orthogonal isolated monomers. First, it includes both the induction effects and the CT effects that are related to the induction and exchange-induction energies as defined by SAPT except that it is obtained iteratively through the infinite order rather than perturbatively through the finite order. Second, if an exact ex-

change-correlation operator were used the dispersion energy would be included in $E_{\mathrm{def}}^{\mathrm{PB}}$. As for now, the majority of existing functionals fail to account for dispersion and at the same time they are not entirely dispersion-free. Consequently, for such functionals, $E_{\mathrm{def}}^{\mathrm{PB}}$ contains some residual dispersion terms as well.

3. Numerical results

3.1. Computational details

The method described in Section 2 has been coded within the MOLPRO program suite [18]. Numerical calculations were carried out for three different functionals: Slater–Dirac [19] (henceforth termed DIRAC), PBE0 [20], and B3LYP [21,22], and for model systems: two van der Waals complexes (Ne_2 and the ethylene dimer), and two hydrogen-bonded dimers [$(HF)_2$ and $(NH_3)_2$]. For comparison, we also present the results for the standard Hartree–Fock method (HF). The distance between Ne atoms in Ne_2 was set to $6a_0$. The geometries for $(NH_3)_2$ and $(C_2H_4)_2$ were taken from Ref. [23] and from Ref. [24] for $(HF)_2$. The numerical procedure depends on the following parameters: energy threshold, i.e. the minimum difference in interaction energies from successive iterations for which the iterations are continued, the grid threshold, i.e. the accuracy with which the Slater–Dirac functional can be integrated using the grid as compared to its analytical integral, and η parameter of Eq. (32). $\eta = 10^5$ was used for all calculations. However, we stress once more that η does not affect the final solutions, only the convergence.

In Table 1 we present the numerical values of the components of Eq. (33) together with the DFT-based HL interaction energy (35), the deformation (36), and the relative difference between the interaction energies obtained in a bifunctional and supermolecular approaches,

$$\delta E_{\mathrm{int}} = \frac{E_{\mathrm{int}}^{\mathrm{PB}} - E_{\mathrm{int}}^{\mathrm{DFT}}}{E_{\mathrm{int}}^{\mathrm{DFT}}} \cdot 100\%. \tag{37}$$

In Fig. 1 we present the dependence of the relative difference (37) on the grid threshold. The energy threshold was set to 10^{-9} mH and it was kept at that value for all values of the grid threshold reported in Fig. 1. The calculations employed aug-cc-pVQZ basis set for neon dimer and aug-cc-pVTZ for the other systems [25–27]. Dimer-centred basis set (DCBS) has been used throughout the calculations and the supermolecular interaction energies were counterpoise (CP)-corrected for the basis set superposition error (BSSE).

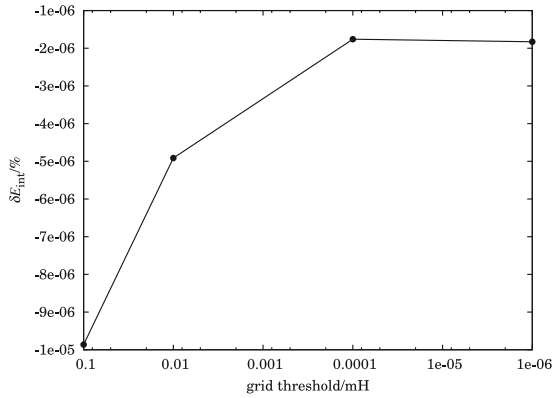

Fig. 1. Dependence of δE_{int} on grid threshold for the Ne_2 dimer at $R = 6\ a_0$ for PBE0 functional in aug-cc-pVQZ basis set.

3.2. Discussion

From the results of Table 1 it is clear that the bifunctional approach converges to the same values of the interaction energies as the conventional KS procedure, within excellent accuracy of below 0.003% for the H-bonded dimers, and 0.05% for the van der Waals dimers.

In general, as long as our procedure is convergent, it must converge to the same result as the standard KS approach. This is because no extra constraints are imposed on the functional, and the finally optimized total density must be the same in both cases. However, the details of the convergence depend on several factors:

- the particular functional,
- the system under consideration,
- the initial orthogonalization of monomer orbitals, and
- the orthogonality forcing technique in the iteration process.

The functional and system convergence dependence is evident in Table 1. The dependence on mutual orthogonalization scheme and the manner it is forced in the iteration process have not been studied so far as only one approach has been adopted – they will be studied in the future in the context of actual applications. For instance, convergence problems may appear for complexes which

Table 1
Interaction energies and their contributions for the bifunctional approach and its comparison with the DFT supermolecular energies. All values in mH. The numbers in parentheses denote powers of 10.

System	Functional	$\Delta\bar{E}_{\mathrm{A}}$	$\Delta\bar{E}_{\mathrm{B}}$	E_{elst}	ΔE_{xc}	$E_{\mathrm{int}}^{\mathrm{HL}}$	$E_{\mathrm{def}}^{\mathrm{PB}}$	$E_{\mathrm{int}}^{\mathrm{PB}}$	δE_{int} (%)
Ne_2 ($R = 6\ a_0$)	DIRAC	0.658	0.658	−0.953	−0.625	−0.262	−0.0249	−0.287	−5.54(−5)
	PBE0	0.416	0.416	−0.587	−0.343	−0.098	−0.00862	−0.107	−3.74(−6)
	B3LYP	0.463	0.463	−0.664	−0.155	0.108	−0.00905	0.0993	2.8(−6)
	HF	0.238	0.238	−0.325	−0.0872	0.064	−0.00148	0.0626	0.00014
$(C_2H_4)_2$	DIRAC	6.04	6.04	−6.71	−7.15	−1.77	−1.21	−2.98	−0.00285
	PBE0	4.58	4.58	−5.11	−3.98	0.0664	−0.702	−0.636	−0.0412
	B3LYP	4.86	4.86	−5.37	−2.82	1.54	−0.708	0.834	0.047
	HF	4.4	4.4	−4.96	−2.14	1.7	−0.374	1.32	0.000301
$(HF)_2$	DIRAC	16.3	19.3	−28.7	−10.7	−3.68	−6.28	−9.96	−0.00402
	PBE0	13.3	15.9	−24.7	−6.91	−2.31	−4.98	−7.28	−0.00026
	B3LYP	14.2	17	−25.9	−7	−1.69	−5.08	−6.77	−0.00223
	HF	11	13.1	−22.2	−4.17	−2.19	−3.61	−5.8	−2.12(−5)
$(NH_3)_2$	DIRAC	11.8	11.8	−18.9	−8.78	−4.04	−2.89	−6.93	−0.00268
	PBE0	9.4	9.4	−15.7	−5.49	−2.36	−2.06	−4.41	−0.000912
	B3LYP	9.97	9.97	−16.4	−4.9	−1.31	−2.11	−3.43	−0.000516
	HF	8.69	8.69	−14.9	−3.3	−0.813	−1.42	−2.23	−2.16(−6)

undergo major redistribution of electron densities between monomers, such as in donor–acceptor interactions and also for those which are poorly described by a single determinant due to static correlation effects.

The total interaction energy is composed of the HL energy and the PB deformation energy. As pointed out in the previous section, both $E_{\mathrm{int}}^{\mathrm{HL}}$ and $E_{\mathrm{def}}^{\mathrm{PB}}$ are uniquely defined, and are independent of the orthogonalization procedure. However, this is not the case for the first four terms of Eq. (33) in Table 1. They describe the monomer deformation effects due to orthogonalization (cols. 3 and 4), and electrostatic and exchange-correlation effects, arising between the monomers described with orthogonalized occupied orbitals (cols. 5 and 6). Therefore, they are not uniquely defined, and are strongly dependent on the orthogonalization scheme – they are not useful to interpret the interaction.

The total interaction energies listed in Table 1 are qualitatively correct only for polar molecules; for atoms and non-polar species they are erroneous due to the well-known fact that the functionals: DIRAC, PBE0, B3LYP do not reproduce the dispersion component. The $E_{\mathrm{int}}^{\mathrm{HL}}$ and $E_{\mathrm{def}}^{\mathrm{PB}}$ components may be compared to similar terms at the HF level of theory (the last entry for every dimer). Assuming that the functionals reproduce only the local correlation terms, but fail to recover dispersion contributions, the DFT $E_{\mathrm{int}}^{\mathrm{HL}}$ results should differ from the HF ones by a relatively small intramonomer correlation effect. This is apparently not the case for DIRAC, for van der Waals complexes: Ne_2 and $(C_2H_4)_2$. Also PBE0 shows attraction, albeit small, for Ne_2, and seems to be not repulsive enough for $(C_2H_4)_2$. Such a behavior indicates that some residual dispersion terms are present. As to the B3LYP functional, it seems to be the most dispersion-free, since its values of $E_{\mathrm{int}}^{\mathrm{HL}}$ are the closest to the HF values. These results are in agreement with the observations that the amount of dispersion in a functional correlates to the steepness of the exchange enhancement factor: it becomes steeper when moving from DIRAC to B3LYP, and, consequently, the amount of dispersion included in these functionals is reduced (see Refs. [28–31]) Finally, for hydrogen-bonded complexes, all methods give qualitatively correct $E_{\mathrm{int}}^{\mathrm{HL}}$, only PBE0 and B3LYP are closer to the HF result than DIRAC.

The above discussion suggests a useful application of the formalism presented in this Letter. For approximate functionals the partitioning of the interaction energy into the $E_{\mathrm{int}}^{\mathrm{HL}}$ and $E_{\mathrm{def}}^{\mathrm{PB}}$ components may serve as a diagnostic of the functional's adequacy in the intermolecular interaction energy problems. Indeed, one can determine, what components and how efficiently are recovered by a tested functional.

4. Summary and outlook

In this Letter we provided a rigorous derivation of the supermolecular DFT interaction energy in terms of mutual monomer polarization via the Pauli blockade method. Numerical calculations for four model systems and three example functionals of different types have proved that the formalism leads to interaction energies rapidly converging to the supermolecular interaction energies. The accuracy achieved is better than 0.1% and appears to be limited only by the size of the grid. The accuracy is qualitatively similar for all three DFT functionals under investigation. Our formalism appears thus to be a viable and useful alternative of solving the KS equations in terms of separated-monomer orbitals rather than supermolecular orbitals. This fact has several important practical implications.

On the one hand, the presented formalism offers possibilities of using different functionals to describe the monomers and to describe the interaction. We have recently exploited this feature to design a novel DFT+dispersion approach [32]. On the other, it would be of interest to combine our approach for the DFT that is capable to reproduce the dispersion energy, e.g. of range-separated family of functionals [1].

The bifunctional formulation provides a platform for deriving a choice of DFT treatments which use different functionals (or even theories) for different subsystems. The results may thus be of interest for those who use subsystem formulation in the context of embedding potentials [10,33–35].

Our formalism may also be useful when interpreting different interaction energy decomposition schemes that have recently been proposed within the DFT approach [12–14,36].

Acknowledgments

Financial support from NSF (Grant No. CHE-0719260) is gratefully acknowledged. We acknowledge computational resources purchased through NSF MRI program (Grant No.CHE-0722689). We are grateful to Bogumił Jeziorski and Maciej Gutowski for helpful discussion.

References

[1] J.G. Ángyán, I.C. Gerber, A. Savin, J. Toulouse, Phys. Rev. A 72 (2005) 012510, doi:10.1103/PhysRevA.72.012510.
[2] M. Dion, H. Rydberg, E. Schröder, D.C. Langreth, B.I. Lundqvist, Phys. Rev. Lett. 92 (2004) 246401, doi:10.1103/PhysRevLett.92.246401.
[3] J.F. Dobson, J. Wang, B.P. Dinte, K. McLennan, H.M. Le, Int. J. Quant. Chem. 101 (2005) 579, doi:10.1002/qua.20314.
[4] K. Morokuma, J. Chem. Phys. 55 (1971) 1236, doi:10.1063/1.1676210.
[5] A.J. Sadlej, Mol. Phys. 39 (1980) 1249, doi:10.1080/00268978000101031.
[6] M. Gutowski, L. Piela, Mol. Phys. 64 (1988) 337, doi:10.1080/00268978800100263.
[7] K.A. Olszewski, M. Gutowski, L. Piela, J. Phys. Chem. 94 (1990) 5710, doi:10.1021/j100378a020.
[8] B. Jeziorski, R. Moszyński, K. Szalewicz, Chem. Rev. 94 (1994) 1887, doi:10.1021/cr00031a008.
[9] M. Jeziorska, B. Jeziorski, J. Čížek, Int. J. Quant. Chem. 32 (1987) 149, doi:10.1002/qua.560320202.
[10] P. Cortona, Phys. Rev. B 44 (1991) 8454, doi:10.1103/PhysRevB.44.8454.
[11] T.A. Wesołowski, A. Warshel, J. Phys. Chem. 97 (1993) 8050, doi:10.1021/j100132a040.
[12] S.M. Cybulski, C.E. Seversen, J. Chem. Phys. 119 (2003) 12704, doi:10.1063/1.1635351.
[13] P. Reinhardt, J.-P. Piquemal, A. Savin, J. Chem. Theory Comput. 4 (2008) 2020, doi:10.1021/ct800242n.
[14] P. Su, H. Li, J. Chem. Phys. 131 (2009) 014102, doi:10.1063/1.3159673.
[15] A.J. Misquitta, B. Jeziorski, K. Szalewicz, Phys. Rev. Lett. 91 (2003) 033201, doi:10.1103/PhysRevLett.91.033201.
[16] A. Heßelmann, G. Jansen, Chem. Phys. Lett. 367 (2003) 778, doi:10.1016/S0009-261(02)01796-7.
[17] P.-O. Löwdin, J. Chem. Phys. 18 (1950) 365, doi:10.1063/1.1747632.
[18] H.-J. Werner, P.J. Knowles, R. Lindh, F.R. Manby, M. Schütz, et al., Molpro, Version 2008.1, A Package of Ab Initio Programs, see http://www.molpro.net (note that the PBE0 functional in this version of Molpro uses PW91C for the correlation part, while other codes use PBEC).
[19] J.C. Slater, Phys. Rev. 81 (1951) 385, doi:10.1103/PhysRev.81.385.
[20] C. Adamo, V. Barone, J. Chem. Phys. 110 (1999) 6158, doi:10.1063/1.478522.
[21] A. Becke, J. Chem. Phys. 98 (1993) 5648, doi:10.1063/1.464913.
[22] P.J. Stephens, F.J. Devlin, C.F. Chabalowski, M.J. Frisch, J. Phys. Chem. 98 (1994) 11623, doi:10.1021/j100096a001.
[23] P. Jurečka, J. Černý, P. Hobza, Phys. Chem. Chem. Phys. 8 (2006) 1985, doi:10.1039/b600027d.
[24] A. Halkier, W. Klopper, T. Helgaker, P. Jørgensen, P.R. Taylor, J. Chem. Phys. 111 (1999) 9157, doi:10.1063/1.479830.
[25] Basis Sets were Obtained from the Basis Set Exchange Database, Version 1.2.2, as Developed and Distributed by the Environmental and Molecular Sciences Laboratory Which is Part of the Pacific Northwest Laboratory, P.O. Box 999, Richland, WA 99352 and funded by the US Department of Energy.
[26] D. Feller, J. Comp. Chem. 17 (1996) 1571. doi:10.1002/(SICI)1096-987X(199610)17:13<1571::AID-JCC9>3.0.CO;2-P.
[27] K.L. Schuchardt, B. Didier, T. Elsethagen, L. Sun, V. Gurumoorthi, J. Chase, J. Liand, T.L. Windus, J. Chem. Inf. Model. 47 (2007) 1045, doi:10.1021/ci600510j.
[28] D.J. Lacks, R.G. Gordon, Phys. Rev. A 47 (1993) 4681, doi:10.1103/PhysRevA.47.4681.
[29] Y. Zhang, W. Pan, W. Yang, J. Chem. Phys. 107 (1997) 7921, doi:10.1063/1.475105.
[30] T.A. Wesołowski, O. Parisel, Y. Ellinger, J. Weber, J. Phys. Chem. A 101 (1997) 7818, doi:10.1021/jp970586k.
[31] G. Menconi, D.J. Tozer, Mol. Phys. 103 (2005) 2397, doi:10.1080/00268970500129938.

[32] Ł. Rajchel, P.S. Żuchowski, M.M. Szcześniak, G. Chałasiński, arXiv:0907.5286v2.
[33] R. Kevorkyants, M. Dulak, T.A. Wesołowski, J. Chem. Phys. 124 (2006) 024104, doi:10.1063/1.2150820.
[34] E.V. Stefanovich, T.N. Truong, J. Chem. Phys. 104 (1996) 2946, doi:10.1063/1.471115.
[35] T. Klüner, N. Govind, Y.A. Wang, E.A. Carter, Phys. Rev. Lett. 86 (2001) 5954, doi:10.1103/PhysRevLett.86.5954.
[36] G. Frenking, K. Wichmann, N. Fröhlich, C. Loschen, M. Lein, J. Frunzke, V.M. Rayón, Coord. Chem. Rev. 238–239 (2003) 55, doi:10.1016/S0010-854(02)00285-0.

Chapter 3

HF-Based Picture of Intermolecular Forces

Whereabouts

In this Chapter we turn back to the wavefunction-based theory. The bifunctional formalism of Chapter 2 smoothly transitions into the Pauli blockade method in the HF theory if the xc potential is replaced with the HF exchange. First, we make a short digression on the general variations of the dimer. Second, we present the open-shell and many body extensions to the original Pauli blockade approach. Both approaches, DFT- (presented in Chapter 2) and HF-based (presented in this Chapter) are smoothly linked together in Chapter 4 leading to the dispersion-free DFT interaction energy.

3.1 Variational Approach to the Dimer Energy

The approach introduced in Sec. 2.2 can be applied to wavefunction-based theories. For the reference, in the present Section we briefly sketch the exchangeless approach to the interactions.

Let us consider a dimer AB whose constituent monomers' wavefunctions fulfill eigenequations (1.7) and the total hamiltonian of the system is separated according to (1.2). The wavefunction of a system is assumed as a simple Hartree product of the monomer functions perturbed by the interaction,

$$\psi_{\mathrm{AB}} = \psi_{\mathrm{A}}\psi_{\mathrm{B}}. \tag{3.1}$$

Our goal is to minimize the dimer energy, which is the expectation value of the total hamiltonian (1.2) with the function (3.1) by varying the monomer func-

tions ψ_A and ψ_B. The energy may be written as a bifunctional depending on monomer functions:

$$E[\psi_\mathrm{A};\psi_\mathrm{B}] = \frac{\langle\psi_\mathrm{A}\psi_\mathrm{B}|\hat{H}|\psi_\mathrm{A}\psi_\mathrm{B}\rangle}{\langle\psi_\mathrm{A}\psi_\mathrm{B}\,|\,\psi_\mathrm{A}\psi_\mathrm{B}\rangle}. \tag{3.2}$$

To facilitate derivations, we assume the normalization of the monomer functions,

$$\langle\psi_\mathrm{A}|\psi_\mathrm{A}\rangle = \langle\psi_\mathrm{B}|\psi_\mathrm{B}\rangle = 1. \tag{3.3}$$

Using (1.2), (3.2) and (3.3), we obtain

$$E[\psi_\mathrm{A};\psi_\mathrm{B}] = \langle\psi_\mathrm{A}|\hat{H}_\mathrm{A}|\psi_\mathrm{A}\rangle + \langle\psi_\mathrm{B}|\hat{H}_\mathrm{B}|\psi_\mathrm{B}\rangle + \langle\psi_\mathrm{A}\psi_\mathrm{B}|\hat{V}|\psi_\mathrm{A}\psi_\mathrm{B}\rangle\,. \tag{3.4}$$

To find the energy extremals we first calculate the variational derivatives of the functional (3.4) constrained with normalization conditions:

$$\mathscr{L}[\psi_\mathrm{A};\psi_\mathrm{B}] = E[\psi_\mathrm{A};\psi_\mathrm{B}] - \mu_\mathrm{A}\left(\langle\psi_\mathrm{A}|\psi_\mathrm{A}\rangle - 1\right) - \mu_\mathrm{B}\left(\langle\psi_\mathrm{B}|\psi_\mathrm{B}\rangle - 1\right) \tag{3.5}$$

with respect to the monomer functions and equate them to zero. Assuming the monomer functions to be real, for monomer A we get

$$\frac{\delta\mathscr{L}[\psi_\mathrm{A};\psi_\mathrm{B}]}{\delta\psi_\mathrm{A}(\{\mathbf{r}_i;\sigma_i\}_{i\in A})} = 2\left(\hat{H}_\mathrm{A} + \langle\psi_\mathrm{B}|\hat{V}|\psi_\mathrm{B}\rangle_B - \mu_\mathrm{A}\right)\psi_\mathrm{A} = 0, \tag{3.6}$$

where the B subscript means that the integration is performed only over monomer B's coordinates. From (1.5) readily follows the eigenequation for the perturbed function of monomer A (we put $\mu_\mathrm{A} = \mathscr{E}_\mathrm{A}$):

$$\left(\hat{H}_\mathrm{A} + \sum_{i\in A} v_\mathrm{B}^\mathrm{ne}(\mathbf{r}_i) + \sum_{i\in A}\int_{\mathbb{R}^3}\frac{\rho_\mathrm{B}(\mathbf{r})}{|\mathbf{r}-\mathbf{r}_i|}\,d^3\mathbf{r} - \sum_{\alpha\in\mathcal{A}} Z_\alpha\int_{\mathbb{R}^3}\frac{\rho_\mathrm{B}(\mathbf{r})}{|\mathbf{r}-\mathbf{R}_\alpha|}\,d^3\mathbf{r}\right)\psi_\mathrm{A} = \mathscr{E}_\mathrm{A}\psi_\mathrm{A} \tag{3.7}$$

where monomer B's nuclear potential is

$$v_\mathrm{B}^\mathrm{ne}(\mathbf{r}) = -\sum_{\beta\in\mathcal{B}}\frac{Z_\beta}{|\mathbf{r}-\mathbf{R}_\beta|} \tag{3.8}$$

and its density is calculated according to (1.17) and (1.18). The equation for monomer A is obtained through the interchange of A and B subscripts in (3.7). Eq. (3.7) has a clear physical interpretation: monomer A is distorted in the electrostatic field of the monomer B. Thus the interaction energy,

$$E_\mathrm{int} = E[\psi_\mathrm{A};\psi_\mathrm{B}] - E_\mathrm{A}^0 - E_\mathrm{B}^0, \tag{3.9}$$

should include electrostatic and induction effects in an exchangeless manner. The application of such a formalism has been realized for the HF functions by Sadlej [32] and is known as the Hartree-Hartree-Fock (HHF) method.

3.2 Exchange Effects in the HF Interaction Energy

3.2.1 Pauli Blockade Method

The HHF method does not include any exchange so it fails to describe short-range interactions. The HF-based formalism including the exchange effects has been introduced by Gutowski and Piela [13]. The same formalism can be derived from the bifunctional approach presented in Sec. 2.2. The original Pauli-blockade HF method derivation follows the total system partitioning (1.2) and assumes the dimer function in as the antisymmetrized product of the monomer HF functions built of orthogonalized orbitals:

$$\psi_{\mathrm{AB}}^{\mathrm{PB}} = \hat{\mathscr{A}}\tilde{\psi}_{\mathrm{A}}\tilde{\psi}_{\mathrm{B}}. \tag{3.10}$$

The variation of the energy calculated with (3.10) with respect to monomer orbitals leads to the following conditions for the optimum orbitals:

$$\begin{cases} \hat{\tilde{f}}_{\mathrm{A}}(\mathbf{r};\lambda)\tilde{a}_i(\mathbf{r};\lambda) = \epsilon_{\mathrm{A},i}(\lambda)\tilde{a}_i(\mathbf{r};\lambda) \\ \hat{\tilde{f}}_{\mathrm{B}}(\mathbf{r};\lambda)\tilde{b}_k(\mathbf{r};\lambda) = \epsilon_{\mathrm{B},k}(\lambda)\tilde{b}_k(\mathbf{r};\lambda) \end{cases}, \tag{3.11}$$

where the perturbed Fock operators of (3.11) include exchange contributions that are absent in the HHF approach, i.e. the exchange potential from a partner. λ is the perturbation parameter of (1.2). The perturbed Fock operator of monomer A is

$$\hat{\tilde{f}}_{\mathrm{A}}(\mathbf{r};\lambda) = \hat{h}_{\mathrm{A}}(\mathbf{r}) + \hat{v}_{\mathrm{A}}^{\mathrm{HF}}(\mathbf{r};\lambda) + \lambda\left(\hat{v}_{\mathrm{B}}^{\mathrm{elst}}(\mathbf{r};\lambda) + \hat{v}_{\mathrm{B}}^{\mathrm{exch}}(\mathbf{r};\lambda)\right). \tag{3.12}$$

Coupled equations (3.11) can be solved iteratively, using the penalty operator (2.23) to enforce orthogonality. For $\lambda = 1$ the iterative scheme is

$$\begin{cases} \left(\hat{\tilde{f}}_{\mathrm{A}}^{[n-1]} + \hat{v}_{\mathrm{B}}^{\mathrm{elst}[n-1]} + \hat{v}_{\mathrm{B}}^{\mathrm{exch}[n-1]} + \eta\hat{\tilde{R}}_{\mathrm{B}}^{[n-1]}\right) a_i^{[n]} = \epsilon_{\mathrm{A},i}^{[n]} a_i^{[n]} \\ \left(\hat{\tilde{f}}_{\mathrm{B}}^{[n-1]} + \hat{v}_{\mathrm{A}}^{\mathrm{elst}[n-1]} + \hat{v}_{\mathrm{A}}^{\mathrm{exch}[n-1]} + \eta\hat{\tilde{R}}_{\mathrm{A}}^{[n-1]}\right) b_k^{[n]} = \epsilon_{\mathrm{B},k}^{[n]} b_k^{[n]} \end{cases} \tag{3.13}$$

and the interaction energy is

$$E_{\mathrm{int}}^{\mathrm{PB}[n]} = \tilde{E}_{\mathrm{int}}^{\mathrm{PB}[n]} + \Delta\tilde{E}_{\mathrm{A}}^{[n]} + \Delta\tilde{E}_{\mathrm{B}}^{[n]}. \tag{3.14}$$

The explicit expression for $\tilde{E}_{\mathrm{int}}^{\mathrm{PB}[n]}$ is readily found applying standard Slater-Condon rules as the dimer function is built of orthonormal orbitals. As usual in the HF scheme, it can be partitioned into electrostatic and exchange terms,

$$\tilde{E}_{\mathrm{int}}^{\mathrm{PB}[n]} = \tilde{E}_{\mathrm{elst}}^{[n]} + \tilde{E}_{\mathrm{exch}}^{[n]} \tag{3.15}$$

with

$$\tilde{E}^{[n]}_{\text{elst}} = \int_{\mathbb{R}^3} v^{\text{ne}}_{\text{A}}(\mathbf{r})\tilde{\rho}^{[n]}_{\text{B}}(\mathbf{r})\, d^3\mathbf{r} + \int_{\mathbb{R}^3} v^{\text{ne}}_{\text{B}}(\mathbf{r})\tilde{\rho}^{[n]}_{\text{A}}(\mathbf{r})\, d^3\mathbf{r} + 4\sum_{i\in A}\sum_{k\in B}\left\langle \tilde{a}^{[n]}_i\tilde{b}^{[n]}_k \,\middle|\, \tilde{a}^{[n]}_i\tilde{b}^{[n]}_k \right\rangle + V^{\text{nn}}_{\text{int}}, \tag{3.16}$$

and

$$\tilde{E}^{[n]}_{\text{exch}} = -2\sum_{i\in A}\sum_{k\in B}\left\langle \tilde{a}^{[n]}_i\tilde{b}^{[n]}_k \,\middle|\, \tilde{b}^{[n]}_k\tilde{a}^{[n]}_i \right\rangle. \tag{3.17}$$

The deformation terms of Eq. (3.14) are

$$\Delta\tilde{E}^{[n]}_{\text{A}} = \tilde{E}^{[n]}_{\text{A}} - E^{0}_{\text{A}} \tag{3.18}$$

and similarly for monomer B. $E^0_{\text{A}} = E^{\text{HF}}_{\text{A}}$ is the isolated monomer A's HF energy. The mean value of $\hat{H}$ with the zero-order PB function, $\psi^{\text{PB}[0]}_{\text{AB}}$, is simply the dimer HL energy:

$$E^{\text{HL}}_{\text{int}} = E^{\text{PB}[0]}_{\text{int}}. \tag{3.19}$$

To summarize, the total PB interaction energy [e.g. obtained by converging the iterative Eqs. (3.13)] is

$$E^{\text{PB}}_{\text{int}} = \Delta\tilde{E}_{\text{A}} + \Delta\tilde{E}_{\text{B}} + \tilde{E}_{\text{elst}} + \tilde{E}_{\text{exch}}, \tag{3.20}$$

where we have dropped iteration number indices to emphasize that (3.20) represents the converged solution to PB equations. The energy (3.20) equals supermolecular HF interaction energy,

$$E^{\text{HF}}_{\text{int}} = E^{\text{HF}}_{\text{AB}} - E^{\text{HF}}_{\text{A}} - E^{\text{HF}}_{\text{B}}. \tag{3.21}$$

3.2.2 Relation Between PB-HF and SAPT-HF

Being equal to $E^{\text{HF}}_{\text{int}}$, the PB interaction energy satisfies

$$E^{\text{PB}}_{\text{int}} = E^{(10)}_{\text{elst}} + E^{(10)}_{\text{exch}} + E^{(20)}_{\text{ind,resp}} + E^{(20)}_{\text{exch-ind,resp}} + \delta_{\text{HF}}, \tag{3.22}$$

where the δ_{HF} term collects all higher-order induction and exchange terms absent in the SAPT-HF through the second order. Both $E^{(20)}_{\text{ind,resp}}$ and $E^{(20)}_{\text{exch-ind,resp}}$ energies are obtained within coupled HF (CHF) formalism [3, 32]. It is clear that the PB interaction energy misses any intramonomer correlation as well as a dispersion component which is a result of intermonomer correlation.

In the PB-HF method HL interaction energy is calculated according to Eq. (3.19), which is the equivalent of Eq. (1.22). The difference between HL and the first-order SAPT energy of Eq. (1.10) is decomposed into the sum of Murrell (Δ^{M})

and Landshoff deltas (Δ^{L}) [33–35] and can be further partitioned into monomer contributions:

$$\Delta = E_{\mathrm{int}}^{\mathrm{HL}} - E^{(1)} = \Delta^{\mathrm{M}} + \Delta^{\mathrm{L}} = \Delta_{\mathrm{A}}^{\mathrm{M}} + \Delta_{\mathrm{B}}^{\mathrm{M}} + \Delta_{\mathrm{A}}^{\mathrm{L}} + \Delta_{\mathrm{B}}^{\mathrm{M}} = \Delta_{\mathrm{A}} + \Delta_{\mathrm{B}}, \tag{3.23}$$

where

$$\Delta_{\mathrm{A}} = \frac{\langle \psi_{\mathrm{A}}^0 \psi_{\mathrm{B}}^0 | \hat{\mathscr{A}} \hat{H}_{\mathrm{A}} | \psi_{\mathrm{A}}^0 \psi_{\mathrm{B}}^0 \rangle}{\langle \psi_{\mathrm{A}}^0 \psi_{\mathrm{B}}^0 | \hat{\mathscr{A}} | \psi_{\mathrm{A}}^0 \psi_{\mathrm{B}}^0 \rangle} - E_{\mathrm{A}}^0. \tag{3.24}$$

The deltas can be calculated using interaction density matrices formalism introduced by Jeziorski et al. [34] The Murrell delta in terms of unperturbed molecular orbitals of monomer A (a_i^0) or both monomers (x_p^0) is

$$\Delta_{\mathrm{A}}^{\mathrm{M}} = \sum_{i,j \in A} \sum_{p,q \in AB} U_{pi} U_{qj} \left\langle a_i^0 a_j^0 \,\middle|\, x_p^0 x_q^0 \right\rangle, \tag{3.25}$$

where the matrix $\mathbb{U}$ is defined as

$$\mathbb{U} = -(\mathbb{T} - \mathbb{I}_{\mathscr{M}})\mathbb{T}^{-1}. \tag{3.26}$$

$\mathbb{T}$ is the molecular orbital overlap matrix,

$$T_{pq} = \left\langle x_p^0 \,\middle|\, x_q^0 \right\rangle, \tag{3.27}$$

and $\mathbb{I}_{\mathscr{M}}$ is $\mathscr{M} \times \mathscr{M}$ identity matrix. The expression for the Landshoff delta reads

$$\begin{aligned} \Delta_{\mathrm{A}}^{\mathrm{L}} &= \sum_{i \in A} \sum_{p \in AB} U_{pi} \left(\langle a_i^0 | \hat{h}_{\mathrm{A}} | x_p^0 \rangle + \sum_{j=1}^{M_{\mathrm{A}}} \left(2 \left\langle a_i^0 a_j^0 \,\middle|\, x_p^0 a_j^0 \right\rangle - \left\langle a_i^0 a_j^0 \,\middle|\, a_j^0 x_p^0 \right\rangle \right) \right) = \\ &= \sum_{i \in A} \sum_{p \in AB} U_{pi} \langle a_i^0 | \hat{f}_{\mathrm{A}}^0 | x_p^0 \rangle . \end{aligned} \tag{3.28}$$

It vanishes for the dimer-centred basis set (DCBS). [35]

3.2.3 Extension to Open Shell Systems

Eqs. (3.13) can be easily extended to open-shell cases within unrestricted HF (UHF) formalism. The UHF-based PB (PB-UHF) iterations are given by

$$\begin{cases} \left(\hat{\tilde{f}}_{\mathrm{A}\sigma}^{[n-1]} + \hat{\tilde{v}}_{\mathrm{B}}^{\mathrm{elst}[n-1]} + \hat{\tilde{v}}_{\mathrm{B}\sigma}^{\mathrm{exch}[n-1]} + \eta \hat{\tilde{R}}_{\mathrm{B}\sigma}^{[n-1]} \right) a_{\sigma,i}^{[n]} = \epsilon_{\mathrm{A}\sigma,i}^{[n]} a_{\sigma,i}^{[n]} \\ \left(\hat{\tilde{f}}_{\mathrm{B}\sigma}^{[n-1]} + \hat{\tilde{v}}_{\mathrm{A}}^{\mathrm{elst}[n-1]} + \hat{\tilde{v}}_{\mathrm{A}\sigma}^{\mathrm{exch}[n-1]} + \eta \hat{\tilde{R}}_{\mathrm{A}\sigma}^{[n-1]} \right) b_{\sigma,k}^{[n]} = \epsilon_{\mathrm{B}\sigma,k}^{[n]} b_{\sigma,k}^{[n]} \end{cases}, \tag{3.29}$$

where $\sigma \in \{\alpha; \beta\}$. The Fock operator for a σ-electron of monomer A is given by

$$\hat{\tilde{f}}_{\mathrm{A}\sigma}(\mathbf{r}) = \hat{h}_{\mathrm{A}}(\mathbf{r}) + \hat{\tilde{j}}_{\mathrm{A}}(\mathbf{r}) + \hat{\tilde{v}}_{\mathrm{A}\sigma}^{\mathrm{exch}}(\mathbf{r}) \tag{3.30}$$

and physically it describes the σ-electron of monomer A in the Coulomb field of its all other electrons, yet feeling only the exchange potential ($\hat{\tilde{v}}_{\mathrm{A}\sigma}^{\mathrm{exch}}$) of electrons with the same spin (σ).

3.2.4 Three-Body Open-Shell Pauli Blockade Method

The extension of PB method to three-body open-shell systems is straightforward. Analogously as in the two-body case, the PB procedure for ABC trimer starts with the orthogonalization of isolated monomer orbitals which yields the two sets for α and β electrons:

$$\left\{ \left\{ \tilde{a}^0_{\sigma,i} \right\}_{i\in A} ; \left\{ \tilde{b}^0_{\sigma,k} \right\}_{k\in B} ; \left\{ \tilde{c}^0_{\sigma,m} \right\}_{m\in B} \right\}, \ \sigma \in \{\alpha;\beta\}. \tag{3.31}$$

The orbitals of the interacting trimer satisfy six equations analogous to (3.29), e.g. for α electrons of monomer A they are eigenfunctions of the monomer A's Fock operator perturbed by the electrostatic and exchange potentials from the two other monomers,

$$\hat{\tilde{f}}_{\mathrm{A}\alpha} + \sum_{\mathrm{X}\in\{\mathrm{B};\mathrm{C}\}} \left(\hat{\tilde{v}}^{\mathrm{elst}}_{\mathrm{X}} + \hat{\tilde{v}}^{\mathrm{exch}}_{\mathrm{X}\alpha} \right). \tag{3.32}$$

The orbitals are orthogonal between monomers. From (1.25) we obtain the general formula for the three-body contribution to the interaction energy,

$$\begin{aligned} \Delta E^{(3,3)}_{\mathrm{int}} &= E_{\mathrm{int}} - \Delta E^{(2,3)}_{\mathrm{int}} = \\ &= E_{\mathrm{int}} - \Big(E_{\mathrm{int}}(\mathrm{AB}) + E_{\mathrm{int}}(\mathrm{BC}) + E_{\mathrm{int}}(\mathrm{AC}) \Big), \end{aligned} \tag{3.33}$$

where

$$E_{\mathrm{int}} = E_{\mathrm{ABC}} - \sum_{\mathrm{X}\in\{\mathrm{A};\mathrm{B};\mathrm{C}\}} E_{\mathrm{X}} \tag{3.34}$$

is the total interaction energy of the trimer.

3.3 Results

The elements of the open-shell formalism and codes described in this Chapter have already been used in the work on metal trimers [36], to calculate the HL three-body contributions in spin-polarized alkaline earth-metal complexes — they were calculated with the UHF monomer wavefunctions. The reader is referred to that Paper for more details, here we briefly present the results that have not been published elsewhere.

Table 3.1 presents the components of PB interaction energy (3.20) for the Cr_2 system. The chromium dimer is not stable at the HF level (it is bound by the dispersion, see Ref. 27). Note that the deformation, electrostatic and exchange energies refer to the interaction between monomers described with orthogonalized orbitals and not the real system. However, asymptotically they approach the respective SAPT first-order energies as the overlap between monomers' orbitals

becomes negligible. The physically meaningful terms are HL and deformation terms. In the case of Cr_2, the repulsive HL term outweighs the attraction from mutual relaxation (deformation) thus making the dimer unstable at HF-based Pauli blockade (PB) theory, which is of course in accordance with HF theory.

In Table 3.2 are shown the three-body contributions to the HL, deformation and total PB interaction energies for the Na_3 system. Note that the three-body HL effect for the Na_3 is of attractive nature and it outweighs the three-body repulsive deformation term, so the total three-body energy is negative. Despite that, the Na_3 trimer remains unstable at the HF level for all distances.

Table 3.1: Components of the PB interaction energy for the $X^{13}\Sigma_g^+$ state of Cr_2 in aug-cc-pVTZ basis set with respect to the internuclear distance.

R/a_0	$E_{\text{int}}^{\text{HL}}$	$\Delta\tilde{E}_{\text{A,B}}$	$\tilde{E}_{\text{elst}}$	$\tilde{E}_{\text{exch}}$	$E_{\text{int}}^{\text{PB}}$
6	14.8	53.8	−69.8	−31.6	6.19
7	6.63	25.8	−33.4	−15.6	2.51
8	2.96	12	−15.5	−7.36	1.2
9	1.28	5.46	−7.01	−3.33	0.569
10	0.525	2.4	−3.08	−1.47	0.255

Table 3.2: Three-body contributions to the PB energy components for the X^4A_1' state of Na_3 in equilateral triangle geometry in VQZ basis set with respect to the triangle side length (the numbers in parentheses denote powers of ten).

R/Å	$E_{\text{int}}^{\text{HL}}$	E_{def}	$E_{\text{int}}^{\text{PB}}$	$E_{\text{int}}^{\text{HL(3,3)}}$	$E_{\text{def}}^{(3,3)}$	$E_{\text{int}}^{\text{PB(3,3)}}$
2	2.54(+5)	−4.57(+4)	2.08(+5)	−2.81(+5)	2.94(+4)	−2.52(+5)
3	6.03(+4)	−2.71(+4)	3.32(+4)	−7.29(+4)	1.73(+4)	−5.57(+4)
4	1.58(+4)	−9.4(+3)	6.4(+3)	−2.01(+4)	8.34(+3)	−1.17(+4)
5	4.2(+3)	−2.51(+3)	1.69(+3)	−5.2(+3)	2.54(+3)	−2.66(+3)
6	1.02(+3)	−579	444	−1.19(+3)	597	−597
7	219	−118	101	−242	120	−122
8	41	−21.6	19.4	−43.5	21.8	−21.7
9	6.79	−3.58	3.22	−7.03	3.58	−3.45
10	1.01	−0.557	0.451	−1.03	0.558	−0.469

Chapter 4

Dispersion-Free Approximation

Whereabouts

This is a pivotal Chapter of the Thesis, collecting the knowledge of Chapters 2 and 3. Its aim is to present the procedure the obtain the dispersion-free DFT interaction energy. In short, the idea is to use local xc potential within monomers, but the non-local HF-like exchange between them. In such a way we eliminate the intermonomer electron correlation which manifests as dispersion. As the results show, the idea works satisfactorily, yielding the first rigorous dispersion-less DFT interaction energy.

4.1 Correlation Issue

We have already mentioned that the HF method lacks any type of correlation. Such a disadvantage concerns energies calculated with this method, including $E_{\text{int}}^{\text{HF}}$. But in order to obtain reliable interaction energies, both types of correlation, i.e. intra- and itermonomer one, have to be properly accounted for. The intramonomer correlation may affect the interaction energies quite severely as attested by the rigorous many-body SAPT (MB-SAPT) calculations [10].

The goal pursued in the following sections is to present a DFT-based formalism that accounts for the intramonomer correlation yet leaves out the intermonomer correlation to a large degree, thus obtaining the approximation of dispersion-free interaction energy.

4.2 Elimination of Dispersion

At this stage we propose a way to eliminate the dispersion energy between subsystems using the bifunctional approach similar to that already developed in Sec. 2.2. The very idea is to describe the interacting monomers with full xc potentials letting only the exact exchange potential operate between them. Mathematically, this means that the ΔE_{xc} term in (2.19) is replaced with the exact exchange interaction. The exchange energy in terms of 1-DMs for the closed-shell system reads (cf. McWeeny [9])

$$E_{\mathrm{exch}}[\tilde{\rho}_{\mathrm{A}};\tilde{\rho}_{\mathrm{B}}] = -\frac{1}{2}\int_{\mathbb{R}^3}\int_{\mathbb{R}^3}\frac{\tilde{\rho}_{\mathrm{A}}(\mathbf{r}_1;\mathbf{r}_2)\tilde{\rho}_{\mathrm{B}}(\mathbf{r}_2;\mathbf{r}_1)}{r_{12}}\,d^3\mathbf{r}_1 d^3\mathbf{r}_2. \tag{4.1}$$

The 1-DM is calculated with (1.19). Hence, the bifunctional incorporating the exact exchange takes the form

$$\mathscr{E}_{\mathrm{AB}}[\tilde{\rho}_{\mathrm{A}};\tilde{\rho}_{\mathrm{B}}] = E_{\mathrm{A}}[\tilde{\rho}_{\mathrm{A}}] + E_{\mathrm{B}}[\tilde{\rho}_{\mathrm{B}}] + E_{\mathrm{elst}}[\tilde{\rho}_{\mathrm{A}};\tilde{\rho}_{\mathrm{B}}] + E_{\mathrm{exch}}[\tilde{\rho}_{\mathrm{A}};\tilde{\rho}_{\mathrm{B}}]. \tag{4.2}$$

Now, in full analogy to Sec. 2.2, we perform the variational search of the minimum of (4.2) with respect to $\tilde{\rho}_{\mathrm{A}}$ and $\tilde{\rho}_{\mathrm{B}}$. The orbitals minimizing (1.19) are readily found to satisfy

$$\boxed{\begin{cases}\left(\hat{\tilde{f}}_{\mathrm{A}}^{\mathrm{KS}} + \hat{\tilde{v}}_{\mathrm{B}}^{\mathrm{elst}} + \hat{\tilde{v}}_{\mathrm{B}}^{\mathrm{exch}}\right)\tilde{a}_i = \epsilon_{\mathrm{A},i}\tilde{a}_i \\ \left(\hat{\tilde{f}}_{\mathrm{B}}^{\mathrm{KS}} + \hat{\tilde{v}}_{\mathrm{A}}^{\mathrm{elst}} + \hat{\tilde{v}}_{\mathrm{A}}^{\mathrm{exch}}\right)\tilde{b}_k = \epsilon_{\mathrm{B},k}\tilde{b}_k\end{cases}}, \tag{4.3}$$

so the iterative scheme for monomer A reads

$$\left(\hat{\tilde{f}}_{\mathrm{A}}^{\mathrm{KS}[n-1]} + \hat{\tilde{v}}_{\mathrm{B}}^{\mathrm{elst}[n-1]} + \hat{\tilde{v}}_{\mathrm{B}}^{\mathrm{exch}[n-1]} + \eta\hat{\tilde{R}}_{\mathrm{B}}^{[n-1]}\right)a_i^{[n]} = \epsilon_{\mathrm{A},i}^{[n]}a_i^{[n]} \tag{4.4}$$

with the interaction energy at the nth iteration being

$$\begin{aligned}\mathscr{E}_{\mathrm{int}}^{\mathrm{PB}[n]} &= \mathscr{E}_{\mathrm{AB}}\left[\tilde{\rho}_{\mathrm{A}}^{[n]};\tilde{\rho}_{\mathrm{B}}^{[n]}\right] - E_{\mathrm{A}}\left[\rho_{\mathrm{A}}^{0}\right] - E_{\mathrm{B}}\left[\rho_{\mathrm{B}}^{0}\right] = \\ &= \Delta\tilde{E}_{\mathrm{A}}^{[n]} + \Delta\tilde{E}_{\mathrm{B}}^{[n]} + E_{\mathrm{elst}}\left[\tilde{\rho}_{\mathrm{A}}^{[n]};\tilde{\rho}_{\mathrm{B}}^{[n]}\right] + E_{\mathrm{exch}}\left[\tilde{\rho}_{\mathrm{A}}^{[n]};\tilde{\rho}_{\mathrm{B}}^{[n]}\right].\end{aligned} \tag{4.5}$$

The deformation energies are calculated according to (2.35) and the electrostatic term is given by (2.20). Energy at the zeroth iteration is then

$$\mathscr{E}_{\mathrm{int}}^{\mathrm{HL}} = \mathscr{E}_{\mathrm{AB}}\left[\tilde{\rho}_{\mathrm{A}}^{0};\tilde{\rho}_{\mathrm{B}}^{0}\right] - E\left[\rho_{\mathrm{A}}^{0}\right] - E\left[\rho_{\mathrm{B}}^{0}\right]. \tag{4.6}$$

Hereinafter, the energy (4.6) will be referred to as dispersion-free HL interaction energy.

It is well known that the xc potential has wrong asymptotic behaviour [37], which may significantly influence the properties that are heavily dependent on

virtual KS orbitals and long-range interaction energies. Therefore, we have applied the AC scheme of Grüning et al. [38], but found the results fairly insensitive to the correction, see Ref. [39], included in Sec. 4.4.

$\mathscr{E}_{\text{int}}^{\text{PB}}$ represents the final PB energy, calculated with (4.5) using self-consistent orbitals satisfying (4.3). It results from the mutual electric polarization of DFT monomers, and, owing to Pauli blockade procedure, it contains exchange contributions. It is related to the induction terms of the SAPT formalism, with two important advantages over the latter: PB sums all electric polarization terms to infinity and accounts for accompanying exchange effects in a consistent manner within the DFT formalism.

4.3 Total Interaction Energy

The total interaction energy, termed PB plus dispersion (PBD), is obtained by adding to $\mathscr{E}_{\text{int}}^{\text{PB}}$ the dispersion component obtained at the DFT level of theory, either from SAPT or by other accurate techniques [16, 40–42]:

$$E_{\text{int}}^{\text{PBD}} = \mathscr{E}_{\text{int}}^{\text{PB}} + E_{\text{disp}}. \tag{4.7}$$

In this work we have used the second-order coupled KS (CKS) dispersion combined with the exchange-dispersion term from SAPT-DFT [21]:

$$E_{\text{disp}} = E_{\text{disp}}^{(2)} + E_{\text{exch-disp}}^{(2)}. \tag{4.8}$$

For the sake of comparison, we have also calculated DFT-based SAPT (SAPT-DFT) interaction energies,

$$E_{\text{int}}^{\text{SAPT}\delta} = E^{(1)} + E^{(2)} + \delta_{\text{HF}}, \tag{4.9}$$

where the δ_{HF} term provides rough approximation of higher than second-order induction-with-exchange terms which are necessary to correct otherwise divergent perturbation expansion. It is calculated using HF supermolecular interaction energy and the SAPT-HF terms from (3.22).

The results for noble-gas diatomics, hydrogen-bonded and other molecular systems are presented in Refs. [43] and [39]. In the Fig. 4.1 the geometries together with appropriate references for some of these systems are presented.

4.4 Related Publications

Ref. [43] concisely presents the dispersion-free approximation and shows the results of the approach for several diatomic and hydrogen-bonded systems. Ref. [39] presents the dispersion-free approach in more detail and also contains further applications of the method.

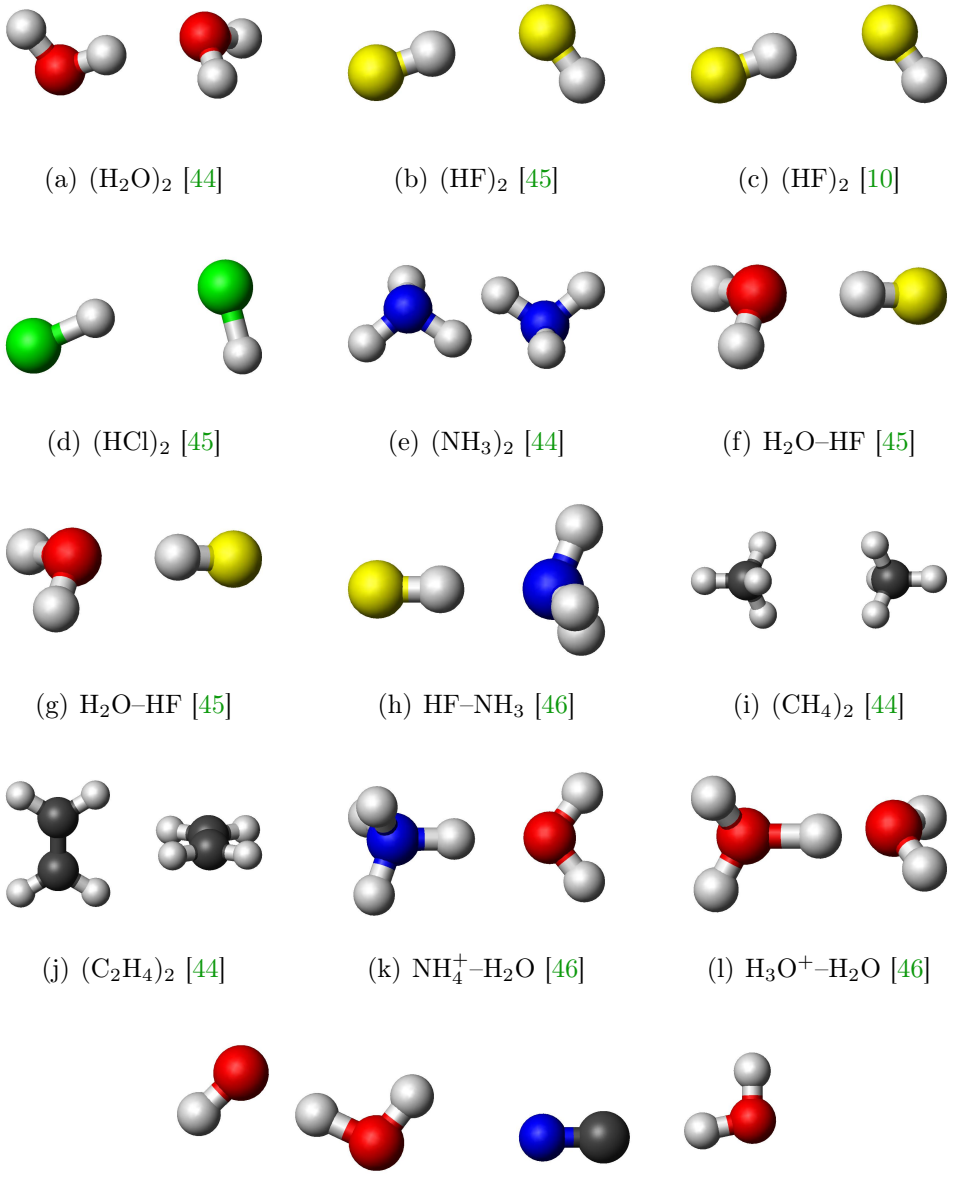

(a) $(H_2O)_2$ [44] (b) $(HF)_2$ [45] (c) $(HF)_2$ [10]

(d) $(HCl)_2$ [45] (e) $(NH_3)_2$ [44] (f) H_2O–HF [45]

(g) H_2O–HF [45] (h) HF–NH_3 [46] (i) $(CH_4)_2$ [44]

(j) $(C_2H_4)_2$ [44] (k) NH_4^+–H_2O [46] (l) H_3O^+–H_2O [46]

(m) OH^-–H_2O [46] (n) CN^-–H_2O [46]

Figure 4.1: Geometries of the systems presented in Refs. [43] and [39].

Density Functional Theory Approach to Noncovalent Interactions via Monomer Polarization and Pauli Blockade

Łukasz Rajchel,[1,2,*] Piotr S. Żuchowski,[3] Małgorzata M. Szczęśniak,[1] and Grzegorz Chałasiński[2,†]
[1]*Department of Chemistry, Oakland University, Rochester, Michigan 48309-4477, USA*
[2]*Faculty of Chemistry, University of Warsaw, 02-093 Warszawa, Pasteura 1, Poland*
[3]*Department of Chemistry, Durham University, South Road, Durham DH1 3LE, United Kingdom*
(Received 31 July 2009; published 21 April 2010)

We propose a ''DFT + dispersion'' treatment which avoids double counting of dispersion terms by deriving the dispersion-free density functional theory (DFT) interaction energy and combining it with DFT-based dispersion. The formalism involves self-consistent polarization of DFT monomers restrained by the exclusion principle via the Pauli-blockade technique. Any exchange-correlation potential can be used within monomers, but only the exchange operates between them. The applications to rare-gas dimers, ion–rare-gas interactions, and hydrogen bonds demonstrate that the interaction energies agree with benchmark values.

DOI: 10.1103/PhysRevLett.104.163001 PACS numbers: 31.15.E−, 34.20.Gj

The applicability of the density functional theory (DFT) to calculations of intermolecular potentials of van der Waals complexes depends upon a seamless inclusion of the dispersion energy, a long-range correlation effect, in the DFT treatment. This goal has been pursued vigorously along many lines [1–7] with varying success. One promising avenue consists of using an *a posteriori* dispersion correction added to supermolecular DFT calculations of interaction energy, in the spirit of Ref. [8]. For this strategy to succeed two elements are necessary: an adequate description of dispersion energy between DFT monomers and a sensible dispersion-free description of supermolecular interaction energy within DFT.

A highly accurate and computationally efficient formulation of dispersion energy is now available from the time-dependent DFT as proposed by Misquitta *et al.* [9] and Heßelmann and Jansen [10], referred to as coupled Kohn-Sham (CKS) dispersion. The second element of this strategy, however, has not been available up to now. In contrast to the Hartree-Fock (HF) interaction energy which is well defined and contains physically interpretable effects, the analogous DFT interaction energy has neither of these characteristics. Depending on a particular functional it may include a variety of obscure terms. In particular, for all current generalized gradient approximation formalisms no dispersion contribution is accounted for at large intermolecular separations R and only some part appears at intermediate and small R. As a consequence, approximate exchange-correlation (XC) functionals often exhibit an artifactual behavior in the long range as well as in the van der Waals minimum region. A rigorous DFT + dispersion approach should be based on a DFT interaction energy that *a priori* avoids these residual dispersion terms but allows for accurate mutual exchange and polarization effects—an analog of the HF interaction energy at the DFT level of theory [8]. Such a DFT interaction energy could then be combined with a dispersion component obtained either from CKS [9,10] or other formalisms [2,11–13].

To this end we adapt the formalism of Pauli-blockade Hartree-Fock (PB HF) [14] combined with the bifunctional subsystem formulation of DFT of Rajchel *et al.* [15] Specifically, the energy of the complex is evaluated from the classic Heitler-London formula which takes the antisymmetrized product of participating monomer wave functions while the monomers are described with the KS orbitals from DFT calculations. In the second step, one iteratively evaluates the interaction energy between two DFT monomers, described by KS determinants, in a manner analogous to the HF method. That is, the monomers are polarized in each other's fields until self-consistency under the constraint of the Pauli exclusion principle between monomers. Within the monomers any exchange-correlation DFT potential may be employed, whereas between monomers the exact exchange potential is used to avoid the dispersion contribution. In the third step, the dispersion component is *a posteriori* added. In such a way the erratic behavior of approximate XC functionals is eliminated and all physically important effects are included without the problem of the dispersion double counting. Note that the concept of the separated monomers resembles the idea of the ''range-separation'' approach in DFT methodology [16].

In the present Letter we present an outline of the application of the PB scheme to the calculation of the interaction energy of DFT monomers. The method has been coded within the MOLPRO package [17]. More details on derivation and implementation will be published elsewhere. The procedure starts with KS solutions for the isolated monomers A and B. The solution is obtained in a self-consistent

way involving coupled equations for both subsystems. The equation for monomer A reads

$$(\hat{\tilde{f}}_A^{\mathrm{KS}[n]} + \hat{\tilde{v}}_B^{\mathrm{elst}[n]} + \hat{\tilde{v}}_B^{\mathrm{exch}[n]} + \eta\hat{\tilde{R}}_B^{[n]})a_i^{[n+1]} = \epsilon_{A,i}^{[n+1]}a_i^{[n+1]}, \tag{1}$$

and its monomer B counterpart is simply generated through the exchange of A and B indices. In Eq. (1), $[n]$ superscripts denote iteration numbers,

$$\hat{\tilde{f}}_A^{\mathrm{KS}}(\mathbf{r}) = \hat{h}_A(\mathbf{r}) + \int \frac{\tilde{\rho}_A(\mathbf{r}')}{|\mathbf{r}-\mathbf{r}'|}d\mathbf{r}' + \tilde{v}_A^{\mathrm{XC}}(\mathbf{r}) \tag{2}$$

is the standard KS operator (e.g., see Ref. [18]) built from the monomer A orbitals (a_i), the two following terms are electrostatic and exchange HF potentials, and the last term is the so-called penalty operator enforcing the proper mutual orthogonality between A and B monomer orbitals so that the intersystem Pauli exclusion principle is fulfilled. $\eta > 0$ is a parameter that does not affect the final solution, though it affects the convergence. Monomer A density in terms of KS orbitals is

$$\rho_A(\mathbf{r}) = 2\sum_{i\in A}|a_i(\mathbf{r})|^2. \tag{3}$$

The XC potential in (2) may be easily asymptotically corrected (we used the correction of Grüning *et al.* [19] and the results proved to be fairly insensitive to this correction). The orbitals are symmetrically orthogonalized after each iteration, yielding $\{\tilde{a}_i^{[n+1]}\}_{i\in A}$, $\{\tilde{b}_k^{[n+1]}\}_{k\in B}$ set. The tilde sign (e.g., $\tilde{E}_{\mathrm{int}}^{\mathrm{PB}}$) denotes quantities calculated with such orbitals. The interaction energy at each iteration is decomposed into several terms:

$$E_{\mathrm{int}}^{\mathrm{PB}} = \Delta\tilde{E}_A + \Delta\tilde{E}_B + \tilde{E}_{\mathrm{elst}} + \tilde{E}_{\mathrm{exch}}. \tag{4}$$

$\Delta\tilde{E}_X = E_X[\tilde{\rho}_X] - E_X[\rho_X^0]$ terms are a result of the imposition of the intersystem Pauli exclusion principle and contain repulsion energy. The expressions for electrostatic and exchange energies are very simple due to the orthogonality of orbitals:

$$\tilde{E}_{\mathrm{elst}} = \int v_A^{\mathrm{ne}}(\mathbf{r})\tilde{\rho}_B(\mathbf{r})d\mathbf{r} + \int v_B^{\mathrm{ne}}(\mathbf{r})\tilde{\rho}_A(\mathbf{r})d\mathbf{r} + 4\sum_{i\in A}\sum_{k\in B}\langle\tilde{a}_i\tilde{b}_k|\tilde{a}_i\tilde{b}_k\rangle + V_{AB}^{\mathrm{nn}}, \tag{5}$$

and

$$\tilde{E}_{\mathrm{exch}} = -2\sum_{i\in A}\sum_{k\in B}\langle\tilde{a}_i\tilde{b}_k|\tilde{b}_k\tilde{a}_i\rangle, \tag{6}$$

where v_A^{ne} is the potential due to monomer A nuclei and V_{AB}^{nn} the intermonomer nuclear-nuclear repulsion term. The zero-iteration energy (4) is the DFT analog of the well-known Heitler-London (HL) interaction energy: $E_{\mathrm{int}}^{\mathrm{PB}[0]} \equiv \mathscr{E}_{\mathrm{int}}^{\mathrm{HL}}$ (cf. also Cybulski and Seversen [20]). The Heitler-London energy contains the well-defined electrostatic and exchange interaction contributions, in this case between unperturbed isolated DFT monomers. It is closely related to the first-order energy in the symmetry-adapted perturbation theory based on DFT [SAPT(DFT)]. Coupling between the subsystems via Eq. (1) leads to the system energy lowering, and is referred to as deformation energy:

$$\mathscr{E}_{\mathrm{def}}^{\mathrm{PB}} = \mathscr{E}_{\mathrm{int}}^{\mathrm{PB}} - \mathscr{E}_{\mathrm{int}}^{\mathrm{HL}}. \tag{7}$$

$\mathscr{E}_{\mathrm{int}}^{\mathrm{PB}}$ represents the final PB energy, calculated with (4) using self-consistent orbitals satisfying (1). It results from the mutual electric polarization of DFT monomers, and, owing to the Pauli-blockade procedure, it contains exchange contributions. It is related to the induction terms of the SAPT formalism with two important advantages over the latter: PB gathers all electric polarization terms to infinity and accounts for accompanying exchange effects in a consistent manner within the DFT formalism.

In the original HF-based formulation, the PB procedure simply restores the supermolecular HF interaction energy, and obviously neglects any kind of electron correlation. For the DFT analog, both monomers are described with the full KS operator, but are coupled using HF Coulomb and exchange operators [$\hat{\tilde{v}}_B^{\mathrm{elst}}$ and $\hat{\tilde{v}}_B^{\mathrm{exch}}$ in Eq. (1), respectively] built from KS orbitals. Such an approach accounts for intramonomer local electron correlation, leaving out the intermonomer nonlocal contributions. Then $\mathscr{E}_{\mathrm{int}}^{\mathrm{PB}}$ represents the "nondispersion" part of the interaction energy that includes the electrostatic, exchange, and induction components. For rare-gas dimers it is purely repulsive. In Fig. 1 $\mathscr{E}_{\mathrm{int}}^{\mathrm{PB}}$ is compared with the supermolecular counterpoise corrected DFT interaction energy for Ar_2. Calculations employed three DFT functionals of the generalized gradient approximation Perdew-Burke-Ernzerhof (PBE) hierarchy, which systematically improve on the description of monomers: PBEX [21] (exchange only), PBEREV [22] (local exchange plus correlation), and PBE0 [23] (a hybrid of local and exact exchange plus correlation). All calculations used augmented correlation-consistent polarized triple-zeta (aug-cc-pVTZ) basis sets. As seen in Fig. 1 $\mathscr{E}_{\mathrm{int}}^{\mathrm{PB}}$ is indeed purely repulsive for Ar_2. By contrast, the supermolecular DFT interaction energies reveal minima of an unknown origin.

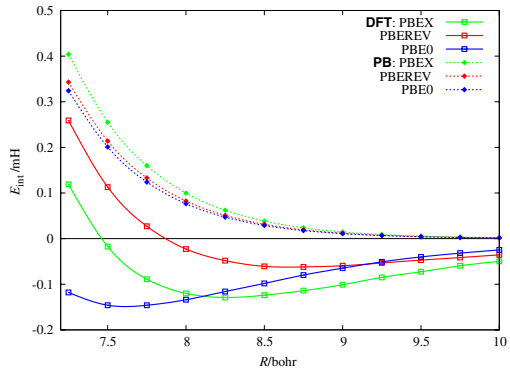

FIG. 1 (color online). Comparison of PB and supermolecular DFT interaction energies for Ar_2.

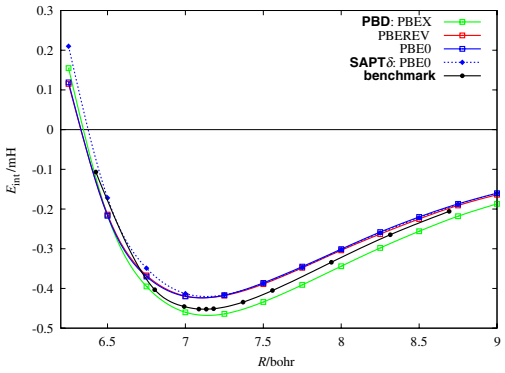

FIG. 2 (color online). Comparison of PBD and SAPTδ interaction energies for Ar_2.

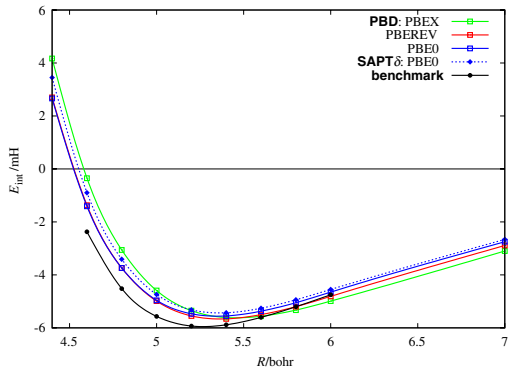

FIG. 3 (color online). Comparison of PBD and SAPTδ interaction energies for $ArNa^+$.

The total interaction energy, termed PBD for Pauli-blockade plus dispersion, is obtained in the spirit of Ref. [8]:

$$E_{\mathrm{int}}^{\mathrm{PBD}} = \mathscr{E}_{\mathrm{int}}^{\mathrm{PB}} + E_{\mathrm{disp}}. \tag{8}$$

In this work E_{disp} is the second-order CKS dispersion component combined with the exchange-dispersion term from SAPT(DFT) [9,24,25].

$E_{\mathrm{int}}^{\mathrm{PBD}}$ can now be compared with SAPT(DFT) theory. SAPT(DFT) interaction energy

$$E_{\mathrm{int}}^{\mathrm{SAPT}\delta} = E^{(1)} + E^{(2)} + \delta_{\mathrm{HF}} \tag{9}$$

includes first-order (electrostatic and exchange) and second-order (induction, dispersion, and their exchange counterparts) contributions derived from KS orbitals. δ_{HF} denotes approximate correction for higher-order induction effects derived at the HF level of theory [26]. The SAPT (DFT) terms were calculated using the MOLPRO program [17].

To test the efficiency of the PBD approach, we performed calculations for several diatomic systems composed of closed-shell atoms and ions: Ar_2, $ArNa^+$, and $ArCl^-$. Again, the same set of PBE functionals has been used with the same aug-cc-pVTZ basis set. The comparison of energies calculated with Eqs. (8) and (9) is presented in Figs. 2–4.

The results are compared with high-level *ab initio* data from Ref. [27] (Ar_2), [28] ($ArNa^+$), and [29] ($ArCl^-$). One can see a remarkably good agreement of PBD and benchmark data, similar to that of SAPTδ, for Ar_2 and $ArNa^+$. The agreement for $ArCl^-$ is somewhat worse; however, for this system the benchmark calculation may be up to 10% too shallow.

Another test of the proposed approach was performed for hydrogen-bonded and other molecular complexes. The results for a representative set of these complexes are shown in Table I.

The PBD interaction energies are compared with SAPTδ and with benchmark values. PBD and SAPTδ share the same values of dispersion energy. The benchmarks correspond to basis set saturated coupled-cluster with single, double and perturbative triple excitations [CCSD(T)] results. The comparison indicates that PBD leads to very reasonable interaction energies for hydrogen-bonded systems. As mentioned above, the two components $\mathscr{E}_{\mathrm{int}}^{\mathrm{HL}}$ and $\mathscr{E}_{\mathrm{int}}^{\mathrm{PB}}$ have a clear physical interpretation of electrostatic-plus-exchange interaction of two unperturbed monomers and mutual monomer polarization contribution restrained by exchange, respectively. It should also be noted that whereas SAPTδ provides results of equally high quality, it is dependent upon inclusion of δ_{HF} which is substantial.

Calculations of $\mathscr{E}_{\mathrm{int}}^{\mathrm{PB}}$ scale with the system size N (where N is the number of basis functions) as the standard KS calculations, i.e., as N^3.

In summary, we presented a new treatment of interaction energy between two DFT monomers which is exactly dispersion-free. This interaction energy is combined with

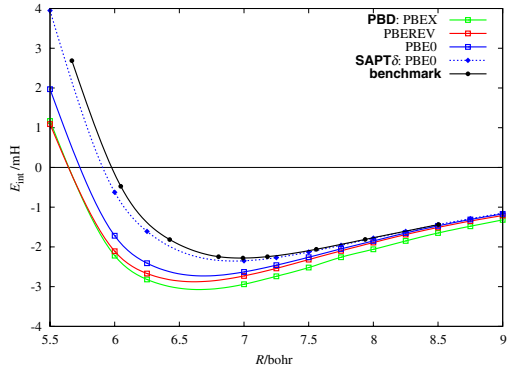

FIG. 4 (color online). Comparison of PBD and SAPTδ interaction energies for $ArCl^-$.

TABLE I. Comparison of interaction energies and their components from PBD calculations with SAPT(DFT) and benchmark values (in mH). Equilibrium geometries are from indicated references. PBE0 functionals with aug-cc-pVTZ basis set are used for monomers [augmented correlation-consistent polarized double-zeta (aug-cc-pVDZ) for CO_2 dimer].

System	$\mathscr{E}_{\rm int}^{\rm HL}$[a]	$\mathscr{E}_{\rm int}^{\rm PB}$[b]	$E_{\rm int}^{\rm PBD}$[c]	$\delta_{\rm HF}$[d]	$E_{\rm int}^{{\rm SAPT}\delta}$	Benchmark
$(H_2O)_2$	−1.02	−4.94	−8.56	−1.45	−8.12	−9.00 [30]
$(HF)_2$	−0.69	−4.78	−7.59	−1.19	−6.48	−7.22 [31]
$(HCl)_2$	1.65	−0.55	−3.48	−0.98	−3.16	−3.10 [31]
$(NH_3)_2$	−0.48	−2.03	−5.34	−0.52	−4.78	−5.05 [30]
H_2O–HF	−1.15	−10.17	−14.85	−3.02	−13.21	−13.55 [31]
$(CH_4)_2$	0.70	0.63	−0.85	−0.04	−0.95	−0.81 [30]
$(CO_2)_2$	0.85	0.50	−1.74	−0.07	−2.11	−1.80[e] [32]

[a]Electrostatic + exchange.
[b]Electrostatic + exchange + mutual polarization.
[c]Electrostatic + exchange + mutual polarization + dispersion.
[d]Higher-order induction.
[e]CCSD(T) result for the global minimum from [32].

existing treatments of dispersion to yield the first theoretically sound DFT + dispersion approach.

Financial support from NSF (Grant No. CHE-0719260) and the Polish Funds for Sciences (Grant No. N204/108335) is gratefully acknowledged. The computational resources were purchased through NSF MRI program (Grant No. CHE-0722689). We are grateful to Bogumił Jeziorski and Maciej Gutowski for helpful discussion.

*lrajchel@tiger.chem.uw.edu.pl
†chalbie@tiger.chem.uw.edu.pl

[1] B. I. Lundqvist, Y. Andersson, H. Shao, S. Chan, and D. C. Langreth, Int. J. Quantum Chem. **56**, 247 (1995).
[2] S. Grimme, J. Comput. Chem. **25**, 1463 (2004).
[3] X. Xu and W. A. Goddard III, Proc. Natl. Acad. Sci. U.S.A. **101**, 2673 (2004).
[4] O. A. von Lilienfeld, I. Tavernelli, U. Rothlisberger, and D. Sebastiani, Phys. Rev. Lett. **93**, 153004 (2004).
[5] D. G. Truhlar and Y. Zhao, J. Chem. Phys. **125**, 194101 (2006).
[6] J. Toulouse, I. C. Gerber, G. Jansen, A. Savin, and J. G. Ángyán, Phys. Rev. Lett. **102**, 096404 (2009).
[7] B. G. Janesko, T. M. Henderson, and G. E. Scuseria, J. Chem. Phys. **130**, 081105 (2009).
[8] R. Ahlrichs, R. Penco, and G. Scoles, Chem. Phys. **19**, 119 (1977); X. Wu, M. C. Vargas, S. Nayak, V. Lotrich, and G. Scoles, J. Chem. Phys. **115**, 8748 (2001).
[9] A. J. Misquitta, B. Jeziorski, and K. Szalewicz, Phys. Rev. Lett. **91**, 033201 (2003).
[10] A. Heßelmann and G. Jansen, Chem. Phys. Lett. **367**, 778 (2003).
[11] A. D. Becke and E. R. Johnson, J. Chem. Phys. **127**, 124108 (2007).
[12] M. Dion, H. Rydberg, E. Schröder, D. C. Langreth, and B. I. Lundqvist, Phys. Rev. Lett. **92**, 246401 (2004).
[13] G. J. Williams and A. J. Stone, J. Chem. Phys. **119**, 4620 (2003); A. J. Misquitta and A. J. Stone, Mol. Phys. **106**, 1631 (2008).
[14] M. Gutowski and L. Piela, Mol. Phys. **64**, 337 (1988).
[15] Ł. Rajchel, P. S. Żuchowski, M. M. Szczęśniak, and G. Chałasiński, Chem. Phys. Lett. **486**, 160 (2010).
[16] J. G. Ángyán, I. C. Gerber, A. Savin, and J. Toulouse, Phys. Rev. A **72**, 012510 (2005).
[17] H.-J. Werner, P. J. Knowles, R. Lindh, F. R. Manby, M. Schütz *et al.*, MOLPRO, version 2009.2, http://www.molpro.net
[18] W. Koch and M. C. Holthausen, *A Chemists Guide to Density Functional Theory* (Wiley-VCH Verlag GmbH, Weinheim, 2001).
[19] M. Grüning, O. V. Gritsenko, S. J. A. van Gisbergen, and E. J. Baerends, J. Chem. Phys. **114**, 652 (2001).
[20] S. M. Cybulski and C. E. Seversen, J. Chem. Phys. **122**, 014117 (2005).
[21] J. P. Perdew, K. Burke, and M. Ernzerhof, Phys. Rev. Lett. **77**, 3865 (1996).
[22] Y. Zhang and W. Yang, Phys. Rev. Lett. **80**, 890 (1998).
[23] C. Adamo and V. Barone, J. Chem. Phys. **110**, 6158 (1999).
[24] A. J. Misquitta and K. Szalewicz, Chem. Phys. Lett. **357**, 301 (2002).
[25] G. Jansen and A. Heßelmann, J. Phys. Chem. A **105**, 11 156 (2001).
[26] A. J. Misquitta, R. Podeszwa, B. Jeziorski, and K. Szalewicz, J. Chem. Phys. **123**, 214103 (2005).
[27] K. Patkowski, G. Murdachaew, C.-M. Fou, and K. Szalewicz, Mol. Phys. **103**, 2031 (2005).
[28] G. R. Ahmadi, J. Almlöf, and I. Røeggen, Chem. Phys. **199**, 33 (1995).
[29] A. A. Buchachenko, R. Krems, M. M. Szczęśniak, Y.-D. Xiao, L. A. Viehland, and G. Chałasiński, J. Chem. Phys. **114**, 9919 (2001).
[30] P. Jurečka, J. Šponer, J. Černý, and P. Hobza, Phys. Chem. Chem. Phys. **8**, 1985 (2006).
[31] A. Halkier, W. Klopper, T. Helgaker, P. Jørgensen, and P. R. Taylor, J. Chem. Phys. **111**, 9157 (1999).
[32] R. Bukowski, J. Sadlej, B. Jeziorski, P. Jankowski, K. Szalewicz, S. A. Kucharski, H. L. Williams, and B. M. Rice, J. Chem. Phys. **110**, 3785 (1999).

A density functional theory approach to noncovalent interactions *via* interacting monomer densities

Łukasz Rajchel,*[ab] Piotr S. Żuchowski,[c] Michał Hapka,[b] Marcin Modrzejewski,[b] Małgorzata M. Szczęśniak[d] and Grzegorz Chałasiński[b]

Received 19th May 2010, Accepted 29th July 2010
DOI: 10.1039/c0cp00626b

A recently proposed "DFT + dispersion" treatment (Rajchel *et al.*, *Phys. Rev. Lett.*, 2010, **104**, 163001) is described in detail and illustrated by more examples. The formalism derives the dispersion-free density functional theory (DFT) interaction energy and combines it with the dispersion energy from separate DFT calculations. It consists of the self-consistent polarization of DFT monomers restrained by the exclusion principle *via* the Pauli blockade technique. Within the monomers a complete exchange-correlation potential should be used, but between them only the exact exchange operates. The application to a wide range of molecular complexes from rare-gas dimers to hydrogen-bonds to π-electron interactions shows good agreement with benchmark values.

1. Introduction

Density functional theory (DFT) based methods provide the most important viable approach to large systems of nano- and biotechnological relevance. Their success in the determination of structure, energetics and other static properties of dense matter is well known.[2–4]

However, the treatment of weak noncovalent interactions by DFT remains plagued by spurious and erratic results. This is a consequence of the fact that the stabilization in these complexes is determined by dispersion interactions, not accounted for by standard DFT functionals.[5,6] Consequently, exchange-correlation potentials derived from local and semi-local models, combined to satisfy empirical data, often feature artifacts when applied to systems with large non-local correlation effects.

Considerable effort has recently been invested to incorporate the dispersion effect into the DFT framework, and the results are promising.[7–13] At the same time, for many practical applications, remarkable progress has been achieved by using *a posteriori* dispersion corrections, and/or semi-empirical models, added on the top of regular DFT calculations (DFT + D)[8] in the spirit of the classic self-consistent field (SCF) + dispersion models of Ahlrichs *et al.*[14] and Wu *et al.*[6]

In order to make a DFT + dispersion strategy successful, one needs two ingredients: a dispersion-free DFT interaction energy[1] and the model for the dispersion energy. The first, the DFT dispersion component, may be obtained *via* the symmetry-adapted perturbation theory (SAPT) approach, but also from other approximate DFT treatments.[7,8,15,16] The second ingredient, the dispersion-free DFT interaction energy, is commonly obtained as the supermolecular DFT interaction energy. However, in contrast to the SCF interaction energy, the composition of the DFT interaction energy is neither understood nor controlled. In particular, an exchange-correlation functional is always an approximation, to some extent delocalized and never exactly dispersion-free, and the problem of double-counting obscure dispersion terms arises. In addition, the exchange-correlation potential compromises the demands of many users and various training sets, and thus is prone to erroneous behavior.[17]

A rigorous approach requires a DFT interaction energy that *a priori* neglects non-local long-range interaction energy terms (dispersion) but allows for accurate mutual exchange and mutual polarization effects—an analogue of the SCF interaction energy at the DFT level of theory. Such a DFT interaction energy could be confidently and rigorously supplemented with a dispersion component obtained also at the DFT level of theory using SAPT[18,19] or other formalisms.[7,8,16] The goal of this work has been to define an accurate DFT + dispersion treatment which is based on the derivation of "dispersion-free" interaction energy arising between DFT monomers to which *a posteriori* DFT dispersion energy is added. The former, the dispersion-free DFT interaction energy, leaves out any intermolecular correlation terms—thus avoiding artifactual exchange and doubly counted dispersion terms. The latter may be obtained from *e.g.* TDDFT and/or SAPT calculations. The basic formulation of the method and selected results for model systems: rare-gas dimers and H-bonded systems, have already been presented by Rajchel *et al.*[1]

To this end a novel hybrid DFT approach for calculations of van der Waals complexes has been proposed by Rajchel *et al.*[1] It uses the formalism of Gutowski and Piela,[20] termed Pauli blockade Hartree–Fock (PB-HF) combined with the bifunctional formulation of DFT of Rajchel *et al.*[21] At the first stage, the subsystems' sets of orbitals are separated by the symmetrical orthogonalization of the orbitals residing

[a] *Department of Chemistry, Oakland University, Rochester, Michigan 48309-4477, USA. E-mail: lrajchel@tiger.chem.uw.edu.pl; Fax: +48 22 8222309; Tel: +48 22 8220211 ext. 234*
[b] *Faculty of Chemistry, University of Warsaw, 02-093 Warszawa, Pasteura 1, Poland. E-mail: chalbie@tiger.chem.uw.edu.pl*
[c] *Department of Chemistry, Durham University, South Road, Durham DH1 3LE, United Kingdom*
[d] *Department of Chemistry, Oakland University, Rochester, Michigan 48309-4477, USA*

at different monomers. At the second stage, one iteratively evaluates the interaction energy between two DFT monomers described by Kohn–Sham (KS) determinants. That is, the monomers are mutually polarized until self-consistency in both fields is reached under the constraints of the Pauli exclusion principle (Pauli blockade technique). Various exchange-correlation DFT potentials may be used within the monomers (see below), but the intermonomer exchange-correlation potential is reduced to only the exact exchange, and thus neglects the dispersion contribution. In the third stage, the dispersion component is added *a posteriori*, from SAPT(DFT) calculations. In such a way, the erratic behavior of the approximate exchange functionals around the equilibrium separations is no longer an issue, while the missing long-range attraction caused by the dispersion is added without the problem of double counting.

It is worth noting that the above approach bears a resemblance to the range-separation idea in DFT,[22–24] differing in that it is based on the separation of monomers rather than ranges.

In the following section, the "dispersion-free" PB(DFT) is derived as a particular case for the PB treatment of DFT reported by us recently.[21] In section 3 we report the numerical results of our method for representative van der Waals and H-bonded systems, and discuss the overall performance of the method.

2. Theory

2.1 Pauli blockade method

Supermolecular energy in terms of DFT can be defined as the difference between the total energies of the dimer AB and the individual monomers A and B, separated to infinity:

$$E_{\mathrm{int}}^{\mathrm{DFT}} = E_{\mathrm{AB}}^{\mathrm{DFT}} - E_{\mathrm{A}}^{\mathrm{DFT}} - E_{\mathrm{B}}^{\mathrm{DFT}}. \tag{1}$$

The interaction energy calculated in this way contains the correlation contribution, however the long-range correlation effects are not taken into account correctly within the standard density functionals.

It was demonstrated by Gutowski and Piela[20] that the Hartree–Fock (HF) supermolecular interaction energy may be exactly recovered by solving the HF equations for monomers in the presence of the external perturbation consisting of the electrostatic potential and the non-local exchange potential generated by the second monomer. They have also proposed a convenient computational scheme in terms of the mutually orthogonalized A and B monomers' occupied orbitals, $\{\tilde{a}_i\}_{i\in\mathrm{A}}$ and $\{\tilde{b}_k\}_{k\in\mathrm{B}}$ (the quantities expressed in the orthonormalized orbitals are henceforth marked with $\sim$). With such orbitals, satisfying

$$\forall_{i\in\mathrm{A}}\forall_{k\in\mathrm{B}} : \left\langle \tilde{a}_i \mid \tilde{b}_k \right\rangle = 0, \tag{2}$$

the supermolecular interaction energy in the HF method can be written as

$$E_{\mathrm{int}}^{\mathrm{HF}} = \Delta\tilde{E}_{\mathrm{A}} + \Delta\tilde{E}_{\mathrm{B}} + \tilde{E}_{\mathrm{elst}} + \tilde{E}_{\mathrm{exch}}, \tag{3}$$

where

$$\Delta\tilde{E}_{\mathrm{A}} = \tilde{E}_{\mathrm{A}}^{\mathrm{HF}} - E_{\mathrm{A}}^{\mathrm{HF}} \tag{4}$$

is the difference between the final and isolated monomer A HF energy,

$$\tilde{E}_{\mathrm{elst}} = \int_{\mathbb{R}^3} v_{\mathrm{A}}^{\mathrm{ne}}(\mathbf{r})\tilde{\rho}_{\mathrm{B}}(\mathbf{r})\mathrm{d}^3\mathbf{r} + \int_{\mathbb{R}^3} v_{\mathrm{B}}^{\mathrm{ne}}(\mathbf{r})\tilde{\rho}_{\mathrm{A}}(\mathbf{r})\mathrm{d}^3\mathbf{r} + \\ + 4\sum_{i\in\mathrm{A}}\sum_{k\in\mathrm{B}}\left\langle \tilde{a}_i\tilde{b}_k \mid \tilde{a}_i\tilde{b}_k \right\rangle + V_{\mathrm{int}}^{\mathrm{nn}}, \tag{5}$$

is the electrostatic interaction (with $\mathbf{r}$ denoting spatial coordinates),

$$\tilde{\rho}_{\mathrm{A}}(\mathbf{r}) = 2\sum_{i\in\mathrm{A}}|\tilde{a}_i(\mathbf{r})|^2 \tag{6}$$

is the monomer A density,

$$v_{\mathrm{A}}^{\mathrm{ne}}(\mathbf{r}) = -\sum_{\alpha\in\mathrm{A}}\frac{Z_\alpha}{|\mathbf{r}-\mathbf{R}_\alpha|} \tag{7}$$

is the monomer A nuclear potential with α representing the coordinates of monomer A′s nuclei, each described by its position $\mathbf{R}_\alpha$ and charge Z_α,

$$V_{\mathrm{int}}^{\mathrm{nn}} = \sum_{\alpha\in\mathrm{A}}\sum_{\beta\in\mathrm{B}}\frac{Z_\alpha Z_\beta}{|\mathbf{R}_\alpha-\mathbf{R}_\beta|} \tag{8}$$

is the intermonomer nuclear repulsion energy (constant for a fixed geometry), and finally

$$\tilde{E}_{\mathrm{exch}} = -2\sum_{i\in\mathrm{A}}\sum_{k\in\mathrm{B}}\left\langle \tilde{a}_i\tilde{b}_k \mid \tilde{b}_k\tilde{a}_i \right\rangle, \tag{9}$$

is the exchange interaction. The monomer A orbitals are the eigenfunctions of the following modified Fock operator:

$$\hat{\tilde{f}}_{\mathrm{A}} + \hat{\tilde{v}}_{\mathrm{B}}^{\mathrm{elst}} + \hat{\tilde{v}}_{\mathrm{B}}^{\mathrm{exch}}, \tag{10}$$

where $\hat{\tilde{f}}_{\mathrm{A}}$ is the standard Fock operator build of the $\{\tilde{a}_i\}_{i\in\mathrm{A}}$ orbital set, and the two remaining terms are electrostatic and the non-local exchange potentials generated by monomer B, respectively. Monomer B orbitals are obtained analogously.

The procedure introduced by Gutowski and Piela[20] can be generalized to the case where the two subsystems are described by KS orbitals. To this end we note that the total density of the system can be represented as the sum of the monomer densities obtained from the orthogonalized orbitals:

$$\rho_{\mathrm{AB}} = \tilde{\rho}_{\mathrm{AB}} = \tilde{\rho}_{\mathrm{A}} + \tilde{\rho}_{\mathrm{B}}, \tag{11}$$

where the monomer A density is calculated as in (6) but with orbitals being the solutions of the following modified KS equation:

$$\left(\hat{\tilde{f}}_{\mathrm{A}}^{\mathrm{KS}}(\mathbf{r}) + \Delta\tilde{v}_{\mathrm{A}}^{\mathrm{xc}}(\mathbf{r}) + \hat{\tilde{v}}_{\mathrm{B}}^{\mathrm{elst}}(\mathbf{r})\right)\tilde{a}_i(\mathbf{r}) = \epsilon_{\mathrm{A},i}\tilde{a}_i(\mathbf{r}) \tag{12}$$

and satisfying (2). In eqn (12), $\hat{\tilde{f}}_{\mathrm{A}}^{\mathrm{KS}}$ is the standard KS operator built of $\{\tilde{a}_i\}_{i\in\mathrm{A}}$ orbitals,

$$\Delta\tilde{v}_{\mathrm{A}}^{\mathrm{xc}}(\mathbf{r}) = v_{\mathrm{AB}}^{\mathrm{xc}}(\mathbf{r}) - \tilde{v}_{\mathrm{A}}^{\mathrm{xc}}(\mathbf{r}), \tag{13}$$

where $\Delta\tilde{v}_{\mathrm{A}}^{\mathrm{xc}}(\mathbf{r})$ is the non-additivity of the monomer A exchange-correlation (xc) potential, and $\hat{\tilde{v}}_{\mathrm{B}}^{\mathrm{elst}}(\mathbf{r})$ is the electrostatic potential of eqn (10). With ρ_{AB} decomposed in such way,

the total KS interaction energy may be written as a functional of $\tilde{\rho}_A$ and $\tilde{\rho}_B$ densities:

$$E_{int}^{PB}[\tilde{\rho}_A;\tilde{\rho}_B] = \Delta\tilde{E}_A[\tilde{\rho}_A] + \Delta\tilde{E}_B[\tilde{\rho}_B] + E_{elst}[\tilde{\rho}_A;\tilde{\rho}_B] + \Delta E_{xc}[\tilde{\rho}_A;\tilde{\rho}_B]. \quad (14)$$

The terms of (14) are as follows. Monomer A deformation is

$$\Delta\tilde{E}_A[\tilde{\rho}_A] = E_A[\tilde{\rho}_A] - E_A[\rho_A^0], \quad (15)$$

and ρ_A^0 is the density of the unperturbed A monomer, *i.e.* the density composed of orbitals $\{a_i^0\}_{i\in A}$ satisfying the unperturbed KS equations,

$$f^{KS,0}(\mathbf{r})a_i^0(\mathbf{r}) = \varepsilon_{A,i}^0 a_i^0(\mathbf{r}). \quad (16)$$

The total energy of monomer A is expressed by the standard KS functional,

$$E_A[\tilde{\rho}_A] = T^s[\tilde{\rho}_A] + V_A^{ne}[\tilde{\rho}_A] + J[\tilde{\rho}_A] + E^{xc}[\tilde{\rho}_A] + V_A^{nn}. \quad (17)$$

The functional (17) includes the non-interacting kinetic energy:

$$T^s[\tilde{\rho}_A] = -\sum_{i\in A}\langle\tilde{a}_i|\Delta_{\mathbf{r}}|\tilde{a}_i\rangle, \quad (18)$$

nuclear-electron attraction energy:

$$V_A^{ne}[\tilde{\rho}_A] = \int_{\mathbb{R}^3} v_A^{ne}(\mathbf{r})\tilde{\rho}_A(\mathbf{r})d^3\mathbf{r}, \quad (19)$$

coulombic energy:

$$J[\tilde{\rho}_A] = \frac{1}{2}\int_{\mathbb{R}^3}\int_{\mathbb{R}^3}\frac{\tilde{\rho}_A(\mathbf{r}_1)\tilde{\rho}_A(\mathbf{r}_2)}{r_{12}}d^3\mathbf{r}_1 d^3\mathbf{r}_2, \quad (20)$$

and exchange-correlation (xc) energy:

$$E^{xc}[\tilde{\rho}_A] = \int_{\mathbb{R}^3} F^{xc}(\tilde{\rho}_A(\mathbf{r});\{\nabla_{\mathbf{r}}\tilde{\rho}_A(\mathbf{r});\ldots\})d^3\mathbf{r} \quad (21)$$

which is evaluated through the numerical integration of the F^{xc} integrand on a grid of points around monomer A. The last term of (17) is the monomer A nuclear–nuclear repulsion energy. Similar expressions can be written for monomer B. The electrostatic part of the interaction energy has the same form as in eqn (5) and in terms of densities it can be easily rewritten as

$$E_{elst}[\tilde{\rho}_A;\tilde{\rho}_B] = \int_{\mathbb{R}^3} v_B^{ne}(\mathbf{r})\tilde{\rho}_A(\mathbf{r})d^3\mathbf{r} + \int_{\mathbb{R}^3} v_A^{ne}(\mathbf{r})\tilde{\rho}_B(\mathbf{r})d^3\mathbf{r} + \int_{\mathbb{R}^3}\int_{\mathbb{R}^3}\frac{\tilde{\rho}_A(\mathbf{r}_1)\tilde{\rho}_B(\mathbf{r}_2)}{r_{12}}d^3\mathbf{r}_1 d^3\mathbf{r}_2 + V_{int}^{nn}. \quad (22)$$

Finally, the exchange-correlation interaction is calculated in a supermolecular manner,

$$\Delta E_{xc}[\tilde{\rho}_A;\tilde{\rho}_B] = E^{xc}[\tilde{\rho}_A + \tilde{\rho}_B] - E^{xc}[\tilde{\rho}_A] - E^{xc}[\tilde{\rho}_B]. \quad (23)$$

Inserting monomer densities calculated using eqn (6) with orbitals satisfying (2) and (12) into (14) one restores the DFT supermolecular interaction energy (1). The expression (14) is potentially exact, *i.e.* it yields the exact interaction energy, provided that the exact xc potential is used.

Technically, the orbitals satisfying (12) are found in a self-consistent iterative process and the orthogonality condition (2) is imposed by the brute force incorporation of the penalty operator and the successive Löwdin orthogonalization. Depicting iteration numbers in square brackets, the n^{th} iterative step for monomer A reads

$$\left(\hat{\tilde{f}}_A^{KS[n-1]} + \Delta\hat{\tilde{v}}_A^{xc[n-1]} + \hat{\tilde{v}}_B^{elst[n-1]} + \eta\hat{\tilde{R}}_B^{[n-1]}\right)a_i^{[n]} = \varepsilon_{A,i}^{[n]}a_i^{[n]}, \quad (24)$$

where the penalty operator is

$$\hat{\tilde{R}}_B^{[n]} = \sum_{k\in B}\left|\tilde{b}_k^{[n]}\right\rangle\left\langle\tilde{b}_k^{[n]}\right| \quad (25)$$

and it is obvious that its action on monomer A′s occupied orbitals annihilates them once the orbitals are orthogonal. $\eta > 0$ is a scaling parameter not affecting the final solutions. The equivalent of (24) for monomer B is obtained through the interchange of the A and B subscripts. The orbitals obtained in each iteration are orthogonalized, yielding an orthonormal

$$\left\{\left\{\tilde{a}_i^{[n]}\right\}_{i\in A};\left\{\tilde{b}_k^{[n]}\right\}_{k\in B}\right\} \quad (26)$$

set. The iterations start with the unperturbed orbitals obtained in eqn (16) and its analogue for monomer B.

The zeroth-order interaction energy may be viewed as an analog of the well known HF-based Heitler–London (HL) interaction energy. Specifically, we define the DFT-based HL interaction energy as

$$E_{int}^{HL} = E_{AB}[\tilde{\rho}_A^0;\tilde{\rho}_B^0] - E[\rho_A^0] - E[\rho_B^0], \quad (27)$$

where the densities $\tilde{\rho}_A^0$ and $\tilde{\rho}_B^0$ are obtained as in (6) from the orbitals generated through the orthogonalization of the unperturbed orbitals $\{\{a_i^0\}_{i\in A};\{b_k^0\}_{k\in B}\}$. This definition is equivalent to that proposed by Cybulski and Seversen.[25]

For the proof and the detailed discussion of DFT-based PB method, the reader is referred elsewhere.[21]

2.2 Dispersion-free approximation

Eqn (14) shows how the DFT interaction energy can be evaluated without referring to supermolecule concepts, using exclusively appropriately perturbed KS equations solved for monomers. The decomposition of the DFT interaction energy allows us to modify it in such a way that we can eliminate the correlation effects between two subsystems, so that we obtain a dispersionless interaction energy between the two systems. To this end, we describe the interacting monomers with the full xc potentials while allowing only the exact exchange potential to operate between them. Mathematically, this involves the replacement of the ΔE_{xc} term (23) in (14) with the exchange interaction which in terms of one-electron reduced density matrices (1-DMs) for the closed-shell system reads (*cf.* ref. 26)

$$E_{exch}[\tilde{\rho}_A;\tilde{\rho}_B] = -\frac{1}{2}\int_{\mathbb{R}^3}\int_{\mathbb{R}^3}\frac{\tilde{\rho}_A(\mathbf{r}_1;\mathbf{r}_2)\tilde{\rho}_B(\mathbf{r}_2;\mathbf{r}_1)}{r_{12}}d^3\mathbf{r}_1 d^3\mathbf{r}_2. \quad (28)$$

The 1-DM resulting from a single Slater determinant is

$$\tilde{\rho}_A(\mathbf{r}_1;\mathbf{r}_2) = 2\sum_{i\in A}\tilde{a}_i(\mathbf{r}_1)\tilde{a}_i^*(\mathbf{r}_2) \quad (29)$$

with the density (6) simply being the diagonal part of 1-DM,

$$\tilde{\rho}_A(\mathbf{r}) \equiv \tilde{\rho}_A(\mathbf{r};\mathbf{r}). \quad (30)$$

Thus, the dimer energy bifunctional incorporating the exact exchange takes the form

$$\mathscr{E}_{\mathrm{AB}}[\tilde{\rho}_{\mathrm{A}};\tilde{\rho}_{\mathrm{B}}] = E_{\mathrm{A}}[\tilde{\rho}_{\mathrm{A}}] + E_{\mathrm{B}}[\tilde{\rho}_{\mathrm{B}}] + E_{\mathrm{elst}}[\tilde{\rho}_{\mathrm{A}};\tilde{\rho}_{\mathrm{B}}] + E_{\mathrm{exch}}[\tilde{\rho}_{\mathrm{A}};\tilde{\rho}_{\mathrm{B}}]. \quad (31)$$

The idea of reducing the intermolecular potential to the exchange-only part was successfully used in the model helium dimer calculations by Heßelmann and Jansen,[27] and Allen and Tozer.[28] Now we perform the search for the extremals of the bifunctional (31) with respect to $\tilde{\rho}_{\mathrm{A}}$ and $\tilde{\rho}_{\mathrm{B}}$ under the constraint of the mutual orthogonality between the monomers' occupied orbitals. The orthogonality constraint ensures that the density additivity condition (11) is maintained and the intersystem Pauli exclusion principle is fulfilled. To this end, we perform the variational optimization in two steps using the PB method (see ref. 20 and 21): first, the bifunctional extremal search is performed without the imposition of the intermonomer orthogonality constraint, and secondly, the penalty operator is added in the resulting iterative scheme. The minimization of the bifunctional (31) leads to a system of coupled equations for optimum orbitals:

$$\begin{cases} \left(\hat{f}_{\mathrm{A}}^{\mathrm{KS}}(\mathbf{r}) + \hat{\tilde{v}}_{\mathrm{B}}^{\mathrm{elst}}(\mathbf{r}) + \hat{\tilde{v}}_{\mathrm{B}}^{\mathrm{exch}}(\mathbf{r})\right)\tilde{a}_i(\mathbf{r}) = \epsilon_{\mathrm{A},i}\tilde{a}_i(\mathbf{r}) \\ \left(\hat{f}_{\mathrm{B}}^{\mathrm{KS}}(\mathbf{r}) + \hat{\tilde{v}}_{\mathrm{A}}^{\mathrm{elst}}(\mathbf{r}) + \hat{\tilde{v}}_{\mathrm{A}}^{\mathrm{exch}}(\mathbf{r})\right)\tilde{b}_k(\mathbf{r}) = \epsilon_{\mathrm{B},k}\tilde{b}_k(\mathbf{r}) \end{cases}, \quad (32)$$

where the action of the exchange operator on an arbitrary one-electron function x reads

$$\hat{\tilde{v}}_{\mathrm{A}}^{\mathrm{exch}}(\mathbf{r})x(\mathbf{r}) = -\frac{1}{2}\int_{\mathbb{R}^3}\frac{\tilde{\rho}_{\mathrm{A}}(\mathbf{r};\mathbf{r}')}{|\mathbf{r}-\mathbf{r}'|}x(\mathbf{r}')\mathrm{d}^3\mathbf{r}'. \quad (33)$$

In the second step of the PB procedure, the iterative process of solving eqn (32) with the aid of the penalty operator is formulated in full analogy with (24). The interaction energy at the n^{th} iteration is obtained upon the insertion of the densities calculated with orthogonalized orbitals resulting from (26) into (31) and subtracting the unperturbed monomer energies:

$$\begin{aligned}\mathscr{E}_{\mathrm{int}}^{\mathrm{PB}[n]} &= \mathscr{E}_{\mathrm{AB}}[\tilde{\rho}_{\mathrm{A}}^{[n]};\tilde{\rho}_{\mathrm{B}}^{[n]}] - E_{\mathrm{A}}[\rho_{\mathrm{A}}^0] - E_{\mathrm{B}}[\rho_{\mathrm{B}}^0] \\ &= \Delta\tilde{E}_{\mathrm{A}}^{[n]} + \Delta\tilde{E}_{\mathrm{B}}^{[n]} + E_{\mathrm{elst}}[\tilde{\rho}_{\mathrm{A}}^{[n]};\tilde{\rho}_{\mathrm{B}}^{[n]}] + E_{\mathrm{exch}}[\tilde{\rho}_{\mathrm{A}}^{[n]};\tilde{\rho}_{\mathrm{B}}^{[n]}]. \end{aligned} \quad (34)$$

In the above equation, the A monomer deformation is

$$\Delta\tilde{E}_{\mathrm{A}} = E_{\mathrm{A}}[\tilde{\rho}_{\mathrm{A}}^{[n]}] - E_{\mathrm{A}}[\rho_{\mathrm{A}}^0], \quad (35)$$

and analogously for monomer B. The interaction energy at the zero iteration is therefore

$$\mathscr{E}_{\mathrm{int}}^{\mathrm{HL}} = \mathscr{E}_{\mathrm{AB}}[\tilde{\rho}_{\mathrm{A}}^0;\tilde{\rho}_{\mathrm{B}}^0] - E[\rho_{\mathrm{A}}^0] - E[\rho_{\mathrm{B}}^0]. \quad (36)$$

Henceforth, the energy (36) will be referred to as the dispersion-free HL interaction energy. The definition of the analog of the HL energy at the DFT level (27), which is simply the zero iteration obtained with monomer densities unperturbed by the interaction, depends on a particular functional, as shown by Cybulski and Severssen[25] and by Rajchel *et al.*[21] The dispersion-free HL interaction energy (36), in contrast to other definitions, rigorously excludes the dispersion interaction. It contains the well-defined electrostatic and exchange interaction contributions, in this case between the unperturbed isolated DFT monomers. It is closely related to the first-order energy in the symmetry-based perturbation theory based in SAPT(DFT).

$\mathscr{E}_{\mathrm{int}}^{\mathrm{PB}}$ represents the final PB energy calculated with (34) using self-consistent orbitals satisfying (32). It results from the mutual electric polarization of DFT monomers, and, owing to the Pauli blockade procedure, it contains exchange contributions. It is related to the induction terms of the SAPT formalism with two important advantages over the latter: PB sums all electric polarization terms to infinity and accounts for accompanying exchange effects in a consistent manner within the DFT formalism.

In the original HF-based formulation,[20] the PB procedure simply restores the supermolecular HF interaction energy, and obviously neglects any kind of electron correlation. For the DFT analog, both monomers are described with the full KS operator, but are coupled using HF Coulomb and exchange operators [$\hat{\tilde{v}}_{\mathrm{B}}^{\mathrm{elst}}$and $\hat{\tilde{v}}_{\mathrm{B}}^{\mathrm{exch}}$ in eqn (32), respectively] built from KS orbitals. Such an approach accounts for intramonomer local electron correlation leaving out the intermonomer non-local contributions. $\mathscr{E}_{\mathrm{int}}^{\mathrm{PB}}$ represents the "non-dispersion" part of the interaction energy that includes the electrostatic, exchange, and induction components. For rare-gas dimers it is purely repulsive (see section 3).

The computational cost of the dispersion-free approach scales as N^3, where N is the number of basis functions.

2.3 Pauli blockade plus dispersion

The total interaction energy, termed PBD for the Pauli blockade plus dispersion, is obtained by adding to $\mathscr{E}_{\mathrm{int}}^{\mathrm{PB}}$ the dispersion component obtained at the DFT level of theory, either from SAPT or by other accurate techniques:

$$E_{\mathrm{int}}^{\mathrm{PBD}} = \mathscr{E}_{\mathrm{int}}^{\mathrm{PB}} + E_{\mathrm{disp}}. \quad (37)$$

In this work we used the second-order dispersion components from SAPT(DFT).[29,30]

$$E_{\mathrm{int}}^{\mathrm{PBD}} = \mathscr{E}_{\mathrm{int}}^{\mathrm{PB}} + E_{\mathrm{disp}}^{(2)} + E_{\mathrm{exch-disp}}^{(2)}. \quad (38)$$

For the sake of comparison we also calculated the SAPT interaction energies using its most efficient hybrid version, SAPTδ, *i.e.* through the second order and corrected with the so called "Hartree–Fock delta term",[31] δ_{HF}:

$$E_{\mathrm{int}}^{\mathrm{SAPT}\delta} = E^{(1)} + E^{(2)} + \delta_{\mathrm{HF}}. \quad (39)$$

It includes all leading electrostatic, exchange, induction, and dispersion contributions, all evaluated at the DFT level of theory. It should be stressed, however, that the δ_{HF} correction comes from HF rather than DFT calculations. It provides a rough approximation of higher than second-order induction with exchange terms which are necessary to correct the otherwise divergent perturbation expansion. More explicitly, the HF supermolecular interaction energy and δ_{HF} satisfy

$$E_{\mathrm{int}}^{\mathrm{HF}} = E_{\mathrm{elst}}^{(10)} + E_{\mathrm{exch}}^{(10)} + E_{\mathrm{ind,resp}}^{(20)} + E_{\mathrm{exch-ind,resp}}^{(20)} + \delta_{\mathrm{HF}}, \quad (40)$$

where $E_{\mathrm{elst}}^{(10)}$ and $E_{\mathrm{exch-ind}}^{(20)}$ are first-order electrostatic and exchange SAPT-HF energies, and $E_{\mathrm{ind,resp}}^{(20)}$ and $E_{\mathrm{exch-ind,resp}}^{(20)}$ denote second-order induction and exchange-induction SAPT-HF contributions calculated within the coupled-HF formalism.[32,33] In this approach, all the third-order

dispersion-exchange-induction effects and dispersion-induction coupling are neglected.

3. Results and discussion

To test the efficiency of the PBD approach we performed calculations for two general classes of noncovalent interactions: van der Waals complexes of closed-shell atoms and ions and H-bonded systems. We applied four DFT functionals of the meta-GGA PBE hierarchy: PBEREV[34] and PW91[35] (local exchange plus correlation), and PBE0[36] and B3LYP[37] (a hybrid of local and exact exchange plus correlation). All calculations have been carried out with the aug-cc-pVTZ basis sets.

3.1 Closed-shell atoms and ions

We performed calculations for several diatomic systems composed of closed-shell atoms and ions. Ar_2, $ArNa^+$ and $ArCl^-$ have already been shown in ref. 1. Here we provide additional examples of $HeLi^+$, He_2, and Ne_2 which are typical closed shells and which provide a stringent test since their intra-monomer dynamic correlation is demanding for electronic structure methods. These results are compared with SAPTδ

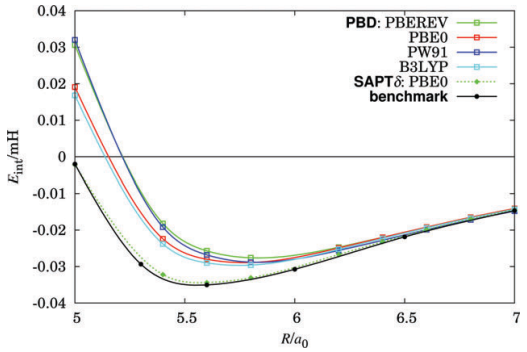

Fig. 1 Comparison of PBD and SAPTδ interaction energies for He_2. Benchmark results are taken from ref. 41.

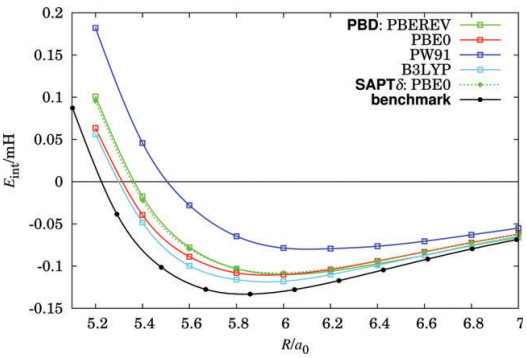

Fig. 2 Comparison of PBD and SAPTδ interaction energies for Ne_2. Benchmark results are taken from ref. 42.

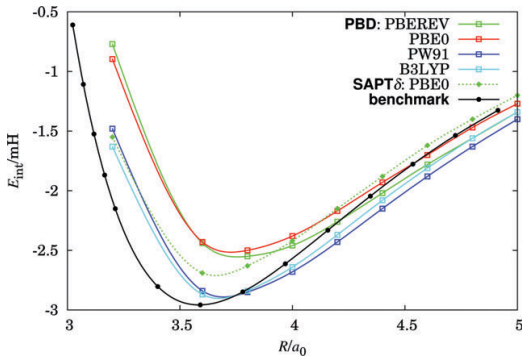

Fig. 3 Comparison of PBD and SAPTδ interaction energies for $HeLi^+$. Benchmark results are taken from ref. 43.

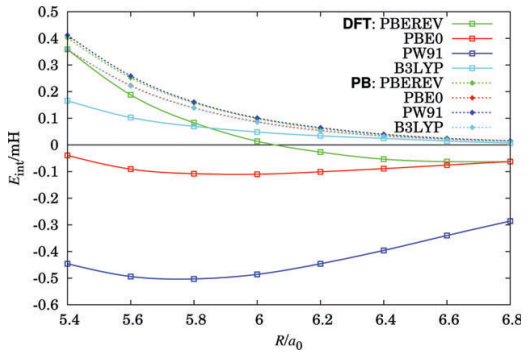

Fig. 4 Comparison of PB and supermolecular DFT interaction energies for Ne_2.

and benchmark values which typically originate from high-level supermolecular calculations.

Overall, our potentials are in good agreement with the benchmark curves for all systems under consideration, *cf.* Fig. 1–3. As anticipated, the best performance is for the PBE0 potential.

One can compare the PBD interaction potentials with the potentials obtained from straightforward supermolecular calculations using the same functionals corrected for basis-set supersposition error (BSSE). For the sake of brevity we illustrate this comparison only for Ne_2 (Fig. 4), but qualitatively the results for the other two complexes ($HeLi^+$, He_2), as well as for the complexes in ref. 1 (Ar_2, $ArNa^+$ and $ArCl^-$) are similar. One can see in Fig. 4 that the supermolecular interaction energies reproduce neither the accurate benchmarks (they are far too shallow) nor the "dispersion-free" part as they feature a small attraction and shallow unphysical minima in the long range. Therefore, they are not appropriate for combining with the pure dispersion term as is done in many "DFT + dispersion" approaches.[8,9,38–40] By way of contrast, the "dispersion-free" PB potentials based on the same DFT schemes (*cf.* Fig. 4) are purely repulsive, revealing proper asymptotic exponential behavior, and thus can be adequately corrected by adding the dispersion contribution.

3.2 Hydrogen-bonded and other molecular complexes

A set of hydrogen-bonded systems from Boese *et al.*,[44] Jurečka *et al.*[45] and Halkier *et al.*[46] supplemented with two typical van der Waals molecular complexes, the methane and ethylene dimers, have been used as a testing set. The selection covers a wide range of qualitatively different interactions: predominantly π–π, H-bonds with a large dispersion component (ammonia and HCl dimers), and finally strong H-bonds involving a shared proton characterized by a relatively large induction contribution. The PBE0 functional and aug-cc-pVTZ basis set have been used.

A comparison between perturbation and supermolecular results requires consistent treatment of monomer geometry in both approaches. In our comparison we performed PBD and SAPTδ calculations between monomers in their optimal dimer geometries. The databases of supermolecular interaction potentials[44,45] include the effects of monomer deformations within interaction energies. For a suitable comparison with the PBD and SAPTδ data we recomputed the monomer deformation effects at the CCSD(T) level from the monomer geometries of ref. 44 and subtracted them from the supermolecular interaction energies. These energies are reported as a benchmark in Table 1.

Both the total interaction energies as well as the components are displayed, and compared with calculations by the SAPT method and the benchmark values from appropriate references (denoted in the right-most column of Table 1). The total induction energy is the sum of the induction and exchange-induction contributions,

$$E^{(2)}_{\mathrm{ind-tot}} = E^{(2)}_{\mathrm{ind}} + E^{(2)}_{\mathrm{exch-ind}}. \qquad (41)$$

PBD agrees favourably with benchmark results and with SAPTδ. In certain classes of interactions (see discussion below), PBD yields more attractive interaction energies than both benchmark and SAPTδ.

The results in Table 1 allow one to compare the total induction effect in the PB method with that in SAPTδ. To do this, $\mathscr{E}^{\mathrm{PB}}_{\mathrm{def}}$ can be compared with the sum: $E^{(2)}_{\mathrm{ind-tot}} + \delta_{\mathrm{HF}}$. The PB induction is consistently more attractive than that from SAPTδ. The discrepancies appear to be largest for the strong H-bonds with a shared proton, such as OH^-–H_2O, as well as for ammonia–hydrogen halides where the induction effect leads to a significant stretching of the proton donor.

Table 2 Comparison of asymptotic corrections (in %) for PB and SAPT components of interaction energies

System	$\delta E\mathscr{E}^{\mathrm{HL}}_{\mathrm{int}}$	$\delta E^{(1)}$	$\delta E\mathscr{E}^{\mathrm{PB}}_{\mathrm{def}}$	$\delta E^{(2)}_{\mathrm{ind-tot}}$
NH_4^+–H_2O	8.8	16.2	−4.2	−0.5
H_3O^+–H_2O	−7.5	−8.8	−1.7	−1.0
OH^-–H_2O	5.2	1.0	0.3	−1.6
$(H_2O)_2$	27.0	124.5	−7.8	0.8
$(HF)_2$	21.8	857.0	−4.0	−0.2
$(HCl)_2$	−2.9	−11.7	−3.0	0.4
$(NH_3)_2$	3.2	158.8	−1.8	0.1
H_3N–HF	−3.3	−14.2	−0.9	−0.7
$(CH_4)_2$	−0.9	−41.8	5.9	24.9
$(C_2H_4)_2$	−5.7	−54.2	−21.4	−4.5

Table 2 allows us to investigate the need for the asymptotic correction (AC). A contribution of AC to PB and SAPT energy components,

$$\delta E = \frac{E_{\mathrm{AC}} - E}{E_{\mathrm{AC}}} \cdot 100\%, \qquad (42)$$

where E_{AC} and E denote energies calculated with and without AC, as shown in Table 1. For all calculations throughout this paper, the correction scheme of Grüning *et al.*[47] has been used. It is interesting that $\mathscr{E}^{\mathrm{HL}}_{\mathrm{int}}$ is much less sensitive than $E^{(1)}$ in the presence of AC. This can be explained in view of the fact that both $\mathscr{E}^{\mathrm{HL}}_{\mathrm{int}}$ and $E^{(1)}$ involve the mutual cancellation of the electrostatic and exchange effects of which only the exchange

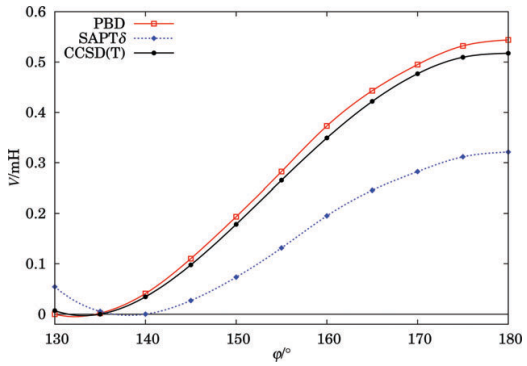

Fig. 5 Comparison of interaction energies for the H_2O–HF dimer with respect to the bending angle.

Table 1 Comparison of interaction energies and their components from PBD calculations with SAPT(DFT) and benchmark values (in mH). Equilibrium geometries are from indicated references. PBE0 potentials with aug-cc-pVTZ basis set are used for monomers

System	$\mathscr{E}^{\mathrm{HL}}_{\mathrm{int}}$	$E^{(1)}$	$\mathscr{E}^{\mathrm{PB}}_{\mathrm{def}}$	$E^{(2)}_{\mathrm{ind-tot}}$	δ_{HF}	$E^{\mathrm{PBD}}_{\mathrm{int}}$	$E^{\mathrm{SAPT}\delta}_{\mathrm{int}}$	Benchmark
NH_4^+–H_2O	−9.68	−9.11	−19.36	−12.19	−6.22	−35.02	−33.49	−33.3[44]
H_3O^+–H_2O	23.60	25.19	−103.72	−56.14	−38.37	−93.26	−82.46	−83.0[44]
OH^-–H_2O	11.70	13.02	−61.19	−29.65	−21.53	−63.77	−52.43	−52.4[44]
$(H_2O)_2$	−1.02	−0.89	−3.92	−2.16	−1.45	−8.56	−8.12	−9.00[45]
$(HF)_2$	−0.69	−0.05	−4.08	−2.43	−1.19	−7.59	−6.48	−7.22[46]
$(HCl)_2$	1.65	1.77	−2.20	−1.02	−0.98	−3.48	−3.16	−3.10[46]
$(NH_3)_2$	−0.48	−0.11	−1.55	−0.84	−0.52	−5.34	−4.78	−5.05[45]
NH_3–H_2O	−0.15	0.23	−6.61	−3.26	−2.44	−11.50	−10.21	−10.3[44]
H_3N–HF	1.08	2.47	−18.17	−9.30	−6.41	−23.94	−20.09	−20.8[44]
H_3N–HCl	8.35	9.05	−18.53	−7.32	−8.59	−18.28	−14.96	−14.3[44]
$(CH_4)_2$	0.70	0.58	−0.07	−0.01	−0.04	−0.85	−0.95	−0.81[45]
$(C_2H_4)_2$	1.71	1.35	−0.34	−0.11	−0.23	−2.11	−2.47	−2.58[45]

may have a wrong asymptotic behaviour. This attests to the robust character of $\delta_{\mathrm{int}}^{\mathrm{HL}}$.

Another test has been carried out for the bending potential of the H_2O–HF complex. The water and HF geometries and the intersystem distance were taken from ref. 46. The potential $V(\varphi)$, where φ is the angle between the water plane and the line connecting oxygen and the HF hydrogen atoms, is the interaction energy scaled so that it is zero at the minimum. As can be seen in Fig. 5, the PBD method gives a remarkably similar potential to CCSD(T), while SAPTδ underestimates the barrier by about 40%.

4. Summary and conclusions

A new DFT approach to calculations of van der Waals complexes has been derived, and tested for a variety of systems ranging from noble gas dimers to different, weakly and strongly H-bonded dimers.

The new formalism is based on the concept of interacting separated monomers.[21] The monomers are described within the DFT formalism. Their densities interact under the constraint of the antisymmetry principle and under the exact exchange intermolecular potential until self-consistency is reached. The resulting interaction energy represents the dispersion-free part of the total interaction energy. The new formalism provides a consistent definition of the "non-dispersion" part of the interaction energy at the DFT level of theory. The total interaction energy is obtained by *a posteriori* adding the DFT dispersion contribution from SAPT or other formalisms. It should be stressed that the PB treatment *does not* require any extra empirical and adjustable parameters (besides those that are already used by the DFT description of monomers).

It has been demonstrated that for rare gas dimers, hydrocarbon dimers, and both weak and strong H-bonded dimers including ionic interactions, the PB combined with monomer description of PBE0 provides results that agree well with the benchmark values.

The PB technique may be used for clusters of atoms and/or molecules and is not restricted to closed-shell systems. It may be combined with different functionals to describe the monomers. Similarly, it may be combined with a variety of formalisms to calculate the dispersion part.

Acknowledgements

Financial support from NSF (Grant No. CHE-0719260) is gratefully acknowledged. We acknowledge the computational resources purchased through the NSF MRI program (Grant No. CHE-0722689).

References

1 Ł. Rajchel, P. S. Żuchowski, M. M. Szczęśniak and G. Chałasiński, *Phys. Rev. Lett.*, 2010, **104**, 163001.
2 W. Koch and M. C. Holthausen, *A Chemist's Guide to Density Functional Theory*, Wiley-VCH, Weinheim, 2001.
3 R. G. Parr and W. Yang, *Density-Functional Theory of Atoms and Molecules*, Oxford University Press, USA, 1989.
4 J. P. Perdew and S. Kurt, vol. 620, Density Functionals for Non-relativistic Coulomb Systems in the New Century, *A Primer in Density Functional Theory*, Springer, Berlin, 2003.
5 S. Tsuzuki and H. P. Lüthi, *J. Chem. Phys.*, 2001, **114**, 3949.
6 X. Wu, M. C. Vargas, S. Nayak, V. Lotrich and G. Scoles, *J. Chem. Phys.*, 2001, **115**, 8748.
7 B. I. Lundqvist, Y. Andersson, H. Shao, S. Chan and D. C. Langreth, *Int. J. Quantum Chem.*, 1995, **56**, 247.
8 S. Grimme, *J. Comput. Chem.*, 2004, **25**, 1463.
9 J.-D. Chai and M. Head-Gordon, *Phys. Chem. Chem. Phys.*, 2008, **10**, 6615.
10 O. A. von Lilienfeld, I. Tavernelli, U. Rothlisberger and D. Sebastiani, *Phys. Rev. Lett.*, 2004, **93**, 153004.
11 Y. Zhao and D. G. Truhlar, *J. Chem. Phys.*, 2006, **125**, 194101.
12 J. Toulouse, I. C. Gerber, G. Jansen, A. Savin and J. G. Ángyán, *Phys. Rev. Lett.*, 2009, **102**, 096404.
13 B. G. Janesko, T. M. Henderson and G. E. Scuseria, *J. Chem. Phys.*, 2009, **130**, 081105.
14 R. Ahlrichs, R. Penco and G. Scoles, *Chem. Phys.*, 1977, **19**, 119.
15 M. A. Neumann and M.-A. Perrin, *J. Phys. Chem. B*, 2005, **109**, 15531.
16 A. D. Becke and E. R. Johnson, *J. Chem. Phys.*, 2007, **127**, 124108.
17 E. R. Johnson, A. D. Becke, C. D. Sherrill and G. A. DiLabio, *J. Chem. Phys.*, 2009, **131**, 034111.
18 A. J. Misquitta, B. Jeziorski and K. Szalewicz, *Phys. Rev. Lett.*, 2003, **91**, 033201.
19 A. Heßelmann and G. Jansen, *Chem. Phys. Lett.*, 2003, **367**, 778.
20 M. Gutowski and L. Piela, *Mol. Phys.*, 1988, **64**, 337.
21 Ł. Rajchel, P. S. Żuchowski, M. M. Szczęśniak and G. Chałasiński, *Chem. Phys. Lett.*, 2010, **486**, 160.
22 Y. Tawada, T. Tsuneda, S. Yanagisawa, T. Yanai and K. Hirao, *J. Chem. Phys.*, 2004, **120**, 8425.
23 J. G. Ángyán, I. C. Gerber, A. Savin and J. Toulouse, *Phys. Rev. A: At., Mol., Opt. Phys.*, 2005, **72**, 012510.
24 M. J. G. Peach, T. Helgaker, P. Sałek, T. W. Keal, O. B. Lutnæs, D. J. Tozer and N. C. Handy, *Phys. Chem. Chem. Phys.*, 2006, **8**, 558.
25 S. M. Cybulski and C. E. Seversen, *J. Chem. Phys.*, 2003, **119**, 12704.
26 R. McWeeny, *Methods of Molecular Quantum Mechanics*, Academic Press Limited, London, 2nd edn, 1989.
27 A. Heßelmann and G. Jansen, *Phys. Chem. Chem. Phys.*, 2003, **5**, 5010.
28 M. J. Allen and D. J. Tozer, *J. Chem. Phys.*, 2002, **117**, 11113.
29 A. J. Misquitta, R. Podeszwa, B. Jeziorski and K. Szalewicz, *J. Chem. Phys.*, 2005, **123**, 214103.
30 G. Jansen and A. Heßelmann, *J. Phys. Chem. A*, 2001, **105**, 11156.
31 S. Rybak, B. Jeziorski and K. Szalewicz, *J. Chem. Phys.*, 1991, **95**, 6576.
32 A. J. Sadlej, *Mol. Phys.*, 1980, **39**, 1249.
33 B. Jeziorski, R. Moszyński and K. Szalewicz, *Chem. Rev.*, 1994, **94**, 1887.
34 Y. Zhang and W. Yang, *Phys. Rev. Lett.*, 1998, **80**, 890.
35 J. P. Perdew, J. A. Chevary, S. H. Vosko, K. A. Jackson, M. R. Pederson, D. J. Singh and C. Fiolhais, *Phys. Rev. B: Condens. Matter*, 1992, **46**, 6671.
36 C. Adamo and V. Barone, *J. Chem. Phys.*, 1999, **110**, 6158.
37 (*a*) A. Becke, *J. Chem. Phys.*, 1993, **98**, 5648; (*b*) P. J. Stephens, F. J. Devlin, C. F. Chabalowski and M. J. Frisch, *J. Phys. Chem.*, 1994, **98**, 11623.
38 M. Elstner, P. Hobza, T. Frauenheim, S. Suhai and E. Kaxiras, *J. Chem. Phys.*, 2001, **114**, 5149.
39 Q. Wu and W. Yang, *J. Chem. Phys.*, 2002, **116**, 515.
40 U. Zimmerli, M. Parrinello and P. Koumoutsakos, *J. Chem. Phys.*, 2004, **120**, 2693.
41 T. Korona, H. L. Williams, R. Bukowski, B. Jeziorski and K. Szalewicz, *J. Chem. Phys.*, 1997, **106**, 5109.
42 R. Hellmann, E. Bich and E. Vogel, *Mol. Phys.*, 2008, **106**, 133.
43 P. Soldán, E. P. F. Lee, J. Lozeille, J. N. Murrell and T. G. Wright, *Chem. Phys. Lett.*, 2001, **343**, 429.
44 A. D. Boese, J. M. L. Martin and W. Klopper, *J. Phys. Chem. A*, 2007, **111**, 11122.
45 P. Jurečka, J. Šponer, J. Černý and P. Hobza, *Phys. Chem. Chem. Phys.*, 2006, **8**, 1985.
46 A. Halkier, W. Klopper, T. Helgaker, P. Jørgensen and P. R. Taylor, *J. Chem. Phys.*, 1999, **111**, 9157.
47 M. Grüning, O. V. Gritsenko, S. J. A. van Gisbergen and E. J. Baerends, *J. Chem. Phys.*, 2001, **114**, 652.

Chapter 5

Summary and Conclusions

5.1 Supermolecular DFT Interaction Energy

In the first part of the Thesis, we have provided a rigorous derivation of the supermolecular DFT interaction energy in terms of mutual monomer polarization via the PB method. Numerical calculations for model systems and functionals of different types have proved that the formalism leads to interaction energies rapidly converging to the supermolecular interaction energies. The accuracy achieved is better than 0.1% and appears to be limited only by the size of the grid. Our formalism appears thus to be a viable and useful alternative of solving the KS equations in terms of separated-monomer orbitals rather than supermolecular orbitals. This fact has several important practical implications.

On the one hand, the presented formalism offers possibilities of using different functionals to describe the monomers and to describe the interaction. On the other, it would be of interest to combine our approach for the DFT that is capable to reproduce the dispersion energy, e.g. of range-separated family of functionals.

The bifunctional formulation provides a platform for deriving a choice of DFT treatments which use different functionals (or even theories) for different subsystems. The results may thus be of interest for those who use subsystem formulation in the context of embedding potentials [47–50].

Our formalism may also be useful when interpreting different interaction energy decomposition schemes that have recently been proposed within the DFT approach [30, 51–53].

5.2 Dispersion-Free DFT

A new DFT approach to calculations of van der Waals complexes has been derived, and tested for a variety of systems ranging from noble gas diatomics to weakly

and strongly H-bonded dimers.

The new formalism is based on the concept of interacting separated monomers presented in Chapter 2. The monomers are described within the DFT formalism. Their densities interact under the constraint of the antisymmetry principle and under the exact exchange intermolecular potential until self-consistency is reached. The resulting interaction energy represents the dispersion-free part of the total interaction energy. The new formalism provides a consistent definition of the non-dispersion part of the interaction energy at the DFT level of theory. The total interaction energy is obtained by *a posteriori* adding the DFT dispersion contribution from SAPT or other formalisms. It should be stressed that the PB treatment *does not* require any extra empirical and adjustable parameters (besides those that are already used by the DFT description of monomers).

It has been demonstrated that for rare gas dimers, hydrocarbon dimers, and both weak and strong H-bonded dimers including ionic interaction, the exact exchange constraint of mutual polarization of monomer densities combined with the DFT description of monomers provides results that agree well with the benchmark values.

The PB technique may be used for clusters of atoms and/or molecules and is not restricted to closed-shell systems. It may be combined with different functionals to describe the monomers. Similarly, it may be combined with a variety of formalisms to calculate the dispersion part. Finally, it should be stressed that the PB approach is not the only method to impose the Pauli principle upon the electrons of interacting monomers and the other efficient techniques are currently being coded in [54].

The DFT-based road to the open-shell systems is similar to that sketched in Chapter 3 or in Section 1.4. Also, the open-shell unrestricted KS (UKS) coupled dispersion energy code is on the way [55].

Appendix A

Acronyms

1-DM	one-electron reduced density matrix
AC	asymptotic correction
BSSE	basis-set superposition error
CAS-D	CASSCF + dispersion
CASSCF	complete active space SCF
CCSD(T)	coupled-cluster singles, doubles and non-iterated triples
CHF	coupled HF
CKS	coupled KS
DCBS	dimer-centred basis set
DFT-D	DFT + dispersion
DFT	density functional theory
DF	density functional
DIIS	direct inversion of the iterative subspace
HF	Hartree-Fock
HHF	Hartree-Hartree-Fock
HL	Heitler-London
KS	Kohn-Sham

MB-SAPT	many-body SAPT
MP2	MP theory of the second order
MP	Møller–Plesset
MRCI	multireference configuration interaction
MRCI	multireference configuration interaction
PB-HF	HF-based PB
PB-UHF	UHF-based PB
PBD	PB plus dispersion
PB	Pauli blockade
SAPT-DFT	DFT-based SAPT
SAPT-HF	HF-based SAPT
SAPT	symmetry-adapted perturbation theory
SAPT	symmetry-adapted perturbation theory
SCF-D	SCF + dispersion
SCF	self-consistent field
SF-EOM	spin-flip equation of motion
UHF	unrestricted HF
UKS	unrestricted KS
xc	exchange-correlation

Appendix B

Notation

Here we present a brief summary of the notation used throughout the Thesis.

A, B, ... denote monomers of the system, N_{A} and $\mathscr{M}_{\mathrm{A}}$ are the numbers of monomer A's electrons and its occupied orbitals, respectively, their subscriptless equivalents referring to the quantities for the whole system, e.g.

$$N = N_{\mathrm{A}} + N_{\mathrm{B}} \tag{B.1}$$

for a dimer. A and B are sets of occupied orbital indices ascribed to A and B monomers. We choose

$$A = \{1; 2; \ldots; \mathscr{M}_{\mathrm{A}}\} \tag{B.2}$$

and

$$B = \{\mathscr{M}_{\mathrm{A}} + 1; \mathscr{M}_{\mathrm{A}} + 2; \ldots; \mathscr{M}_{\mathrm{A}} + \mathscr{M}_{\mathrm{B}}\}. \tag{B.3}$$

Additionally, we will use the set

$$AB = A \cup B. \tag{B.4}$$

Analogously, the sets:

$$\mathcal{A} = \{1; 2; \ldots; \mathscr{N}_{\mathrm{A}}\} \tag{B.5}$$

and

$$\mathcal{B} = \{\mathscr{N}_{\mathrm{A}} + 1; \mathscr{N}_{\mathrm{A}} + 2; \ldots; \mathscr{N}_{\mathrm{A}} + \mathscr{N}_{\mathrm{B}}\} \tag{B.6}$$

collect all A and B monomer nuclear indices with $\mathscr{N}_{\mathrm{A}}$ being the number of monomer A nuclei. Vectors $\mathbf{r}_i$ and $\mathbf{R}_\alpha$ denote electron and nuclei positions, respectively, and

$$\begin{cases} r_{ij} = |\mathbf{r}_i - \mathbf{r}_j| \\ R_{\alpha\beta} = |\mathbf{R}_\alpha - \mathbf{R}_\beta| \end{cases}. \tag{B.7}$$

The atomic units are used unless indicated otherwise.

Appendix C

Implementation

The methods described in Chapters 2 through 4 have been implemented in the development version of the Molpro package [5]. Below we sketch some technical issues concerning the numerical implementation together with exemplary input file.

C.1 DCBS

All calculations are performed in the DCBS, i.e. the basis set for any monomer is the sum of the basis sets for separate monomers. Let M_A and M_B denote basis dimensions for monomers A and B. Then the DCBS has the dimension

$$M = M_\mathrm{A} + M_\mathrm{B}. \tag{C.1}$$

Let $\mathbf{u}_\mathrm{A}$ and $\mathbf{u}_\mathrm{A}$ denote basis orbitals centred on monomers A and B, respectively:

$$\mathbf{u}_\mathrm{A} = \begin{bmatrix} \chi_{\mathrm{A},1} \\ \chi_{\mathrm{A},2} \\ \vdots \\ \chi_{\mathrm{A},M_\mathrm{A}} \end{bmatrix} = \begin{bmatrix} \chi_1 \\ \chi_2 \\ \vdots \\ \chi_{M_\mathrm{A}} \end{bmatrix}, \quad \mathbf{u}_\mathrm{B} = \begin{bmatrix} \chi_{\mathrm{B},1} \\ \chi_{\mathrm{B},2} \\ \vdots \\ \chi_{\mathrm{B},M_\mathrm{B}} \end{bmatrix} = \begin{bmatrix} \chi_{M_\mathrm{A}+1} \\ \chi_{M_\mathrm{A}+2} \\ \vdots \\ \chi_{M} \end{bmatrix}. \tag{C.2}$$

The DCBS has the following structure:

$$\mathbf{u} = \begin{bmatrix} \mathbf{u}_\mathrm{A} \\ \mathbf{u}_\mathrm{B} \end{bmatrix} = \begin{bmatrix} \chi_1 \\ \vdots \\ \chi_M \end{bmatrix}. \tag{C.3}$$

HF (1.13) or KS (2.1) equations for the unperturbed monomers yield the molecular orbitals expanded in the DCBS

$$\begin{cases} \mathbf{a} = (\mathbb{C}_\mathrm{A})^\mathrm{T}\,\mathbf{u} \\ \mathbf{b} = (\mathbb{C}_\mathrm{B})^\mathrm{T}\,\mathbf{u} \end{cases}, \tag{C.4}$$

where $\mathbb{C}_{\mathrm{A}}^{0}$ is the matrix of A monomer molecular orbital coefficients and

$$\mathbf{a} = \begin{bmatrix} a_1 \\ a_2 \\ \vdots \\ a_{\mathscr{M}_{\mathrm{A}}} \end{bmatrix}, \mathbf{b} = \begin{bmatrix} b_{\mathscr{M}_{\mathrm{A}}+1} \\ b_{\mathscr{M}_{\mathrm{A}}+2} \\ \vdots \\ b_{\mathscr{M}} \end{bmatrix} \tag{C.5}$$

are vectors composed of A and B monomer molecular orbitals. Eqs. (C.4) can be written explicitly as

$$\begin{cases} a_i = \sum_{p=1}^{M} (\mathbb{C}_{\mathrm{A}})_{pi}\, \chi_p \\ b_k = \sum_{p=1}^{M} (\mathbb{C}_{\mathrm{B}})_{pk}\, \chi_p \end{cases} . \tag{C.6}$$

C.2 Orthogonalization

Let $\mathbb{S}$ denote an overlap matrix in DCBS:

$$S_{pq} = \langle \chi_p | \chi_q \rangle \,. \tag{C.7}$$

One can readily see that the $\mathbb{S}$ matrix is composed of four blocks, corresponding to the orbitals of monomers A and B:

$$\mathbb{S} = \begin{bmatrix} \mathbb{S}_{\mathrm{AA}} & \mathbb{S}_{\mathrm{AB}} \\ \mathbb{S}_{\mathrm{BA}} & \mathbb{S}_{\mathrm{BB}} \end{bmatrix}, \tag{C.8}$$

where the blocks have the following dimensions: $\mathbb{S}_{\mathrm{AA}}$ — $M_A \times M_A$, $\mathbb{S}_{\mathrm{AB}}$ — $M_A \times M_B$, $\mathbb{S}_{\mathrm{BA}}$ — $M_B \times M_A$, and $\mathbb{S}_{\mathrm{BB}}$ — $M_B \times M_B$. Moreover,

$$\mathbb{S}_{\mathrm{AB}} = \mathbb{S}_{\mathrm{BA}}^{\dagger}. \tag{C.9}$$

Monomers A and B have $\mathscr{M}_{\mathrm{A}}$ and $\mathscr{M}_{\mathrm{B}}$ occupied orbitals, respectively. Now we create the union of occupied orbitals of A and B monomers:

$$\mathbb{D} = \begin{bmatrix} \mathbb{C}_{\mathrm{A}}^{\mathrm{occ}} & \mathbb{C}_{\mathrm{B}}^{\mathrm{occ}} \end{bmatrix}, \tag{C.10}$$

where $\mathbb{C}_{\mathrm{A}}^{\mathrm{occ}}$ and $\mathbb{C}_{\mathrm{B}}^{\mathrm{occ}}$ are $M \times \mathscr{M}_{\mathrm{A}}$ and $M \times \mathscr{M}_{\mathrm{B}}$ parts of $\mathbb{C}_{\mathrm{A}}$ and $\mathbb{C}_{\mathrm{B}}$ matrices containing occupied orbitals only. Similarly, the $\mathbb{C}_{\mathrm{A}}^{\mathrm{vir}}$ matrix contains only monomer A's virtual orbitals and is of $M \times (M - \mathscr{M}_{\mathrm{A}})$ dimension. Thus, the $\mathbb{C}_{\mathrm{A}}$ matrix is partitioned as

$$\mathbb{C}_{\mathrm{A}} = \begin{bmatrix} \mathbb{C}_{\mathrm{A}}^{\mathrm{occ}} & \mathbb{C}_{\mathrm{A}}^{\mathrm{vir}} \end{bmatrix}, \tag{C.11}$$

and the same holds for the $\mathbb{C}_{\mathrm{B}}$ matrix. Therefore $\mathbb{D}$ is a $M \times \mathscr{M}$ matrix, where

$$\mathscr{M} = \mathscr{M}_{\mathrm{A}} + \mathscr{M}_{\mathrm{B}} \tag{C.12}$$

is the total number of occupied orbitals of the system. Now we have to find the overlap matrix ($\mathbb{T}$) resulting from $\mathbb{D}$ (C.10) matrix which will be used subsequently to orthogonalise the dimer orbitals. Since $\mathbb{D}$ matrix contains the coefficients of occupied orbitals of A and B monomers, the $\mathbb{T}$ matrix will consist of four blocks:

$$\mathbb{T} = \begin{bmatrix} \mathbb{T}_{\mathrm{AA}} & \mathbb{T}_{\mathrm{AB}} \\ \mathbb{T}_{\mathrm{BA}} & \mathbb{T}_{\mathrm{BB}} \end{bmatrix}. \tag{C.13}$$

The $\mathbb{T}_{\mathrm{AA}}$ ($\mathscr{M}_{\mathrm{A}} \times \mathscr{M}_{\mathrm{A}}$) block's elements are calculated as

$$(\mathbb{T}_{\mathrm{AA}})_{ij} = \langle a_i | a_j \rangle = \sum_{p=1}^{M} \sum_{q=1}^{M} (\mathbb{C}_{\mathrm{A}})^*_{pi} \, (\mathbb{C}_{\mathrm{A}})_{qj} \, S_{pq}. \tag{C.14}$$

However, since the monomer orbitals are canonical, we get

$$(\mathbb{T}_{\mathrm{AA}})_{ij} = \delta_{ij}. \tag{C.15}$$

Eqs. (C.14) and (C.15) can be cast into matrix form as

$$\mathbb{T}_{\mathrm{AA}} = (\mathbb{C}_{\mathrm{A}}^{\mathrm{occ}})^{\dagger} \mathbb{S} \mathbb{C}_{\mathrm{A}}^{\mathrm{occ}} = \mathbb{I}_{\mathscr{M}_{\mathrm{A}}}, \tag{C.16}$$

where $\mathbb{I}_n$ denotes $n \times n$ identity matrix. Similarly,

$$\mathbb{T}_{\mathrm{BB}} = (\mathbb{C}_{\mathrm{B}}^{\mathrm{occ}})^{\dagger} \mathbb{S} \mathbb{C}_{\mathrm{B}}^{\mathrm{occ}} = \mathbb{I}_{\mathscr{M}_{\mathrm{B}}}. \tag{C.17}$$

The $\mathbb{T}_{\mathrm{AB}}$ block has dimension $\mathscr{M}_{\mathrm{A}} \times \mathscr{M}_{\mathrm{B}}$ and its elements are calculated as

$$(\mathbb{T}_{\mathrm{AB}})_{ik} = \langle a_i | b_k \rangle = \sum_{p=1}^{M} \sum_{q=1}^{M} (\mathbb{C}_{\mathrm{A}})^*_{pi} \, (\mathbb{C}_{\mathrm{B}})_{qk} S_{pq}. \tag{C.18}$$

Eq. (C.18) in the matrix form reads

$$\mathbb{T}_{\mathrm{AB}} = (\mathbb{C}_{\mathrm{A}})^{\dagger} \mathbb{S} \mathbb{C}_{\mathrm{B}}. \tag{C.19}$$

It is straightforward to see that

$$\mathbb{T}_{\mathrm{BA}} = \mathbb{T}_{\mathrm{AB}}^{\dagger} = (\mathbb{C}_{\mathrm{B}})^{\dagger} \mathbb{S} \mathbb{C}_{\mathrm{A}} \tag{C.20}$$

and it is a $\mathscr{M}_{\mathrm{B}} \times \mathscr{M}_{\mathrm{A}}$ block. Finally, the $\mathscr{M} \times \mathscr{M}$ matrix of overlap integrals in the molecular orbitals basis has the form

$$\mathbb{T} = \begin{bmatrix} \mathbb{I}_{\mathscr{M}_{\mathrm{A}}} & (\mathbb{C}_{\mathrm{A}}^{\mathrm{occ}})^{\dagger} \mathbb{S} \mathbb{C}_{\mathrm{B}}^{\mathrm{occ}} \\ (\mathbb{C}_{\mathrm{B}}^{\mathrm{occ}})^{\dagger} \mathbb{S} \mathbb{C}_{\mathrm{A}}^{\mathrm{occ}} & \mathbb{I}_{\mathscr{M}_{\mathrm{B}}} \end{bmatrix}. \tag{C.21}$$

Next, using the $\mathbb{T}$ matrix we create the $\mathbb{T}^{-1/2}$ matrix and we apply Löwdin's orthogonalisation to the occupied orbitals contained in union $\mathbb{D}$:

$$\widetilde{\mathbb{D}} = \mathbb{D}\mathbb{T}^{-1/2}. \tag{C.22}$$

Since we use Löwdin-type orthogonalisation, the orbitals can still be ascribed to monomers A and B, so we can write

$$\widetilde{\mathbb{D}} = \begin{bmatrix} \widetilde{\mathbb{C}}_{\mathrm{A}}^{\mathrm{occ}} & \widetilde{\mathbb{C}}_{\mathrm{B}}^{\mathrm{occ}} \end{bmatrix}. \tag{C.23}$$

Since we have orthogonalised only occupied orbitals, the transformed orbital matrix reads

$$\widetilde{\mathbb{C}}_{\mathrm{A}} = \begin{bmatrix} \widetilde{\mathbb{C}}_{\mathrm{A}}^{\mathrm{occ}} & \mathbb{C}_{\mathrm{A}}^{\mathrm{vir}} \end{bmatrix}, \tag{C.24}$$

and similarly for $\widetilde{\mathbb{C}}_{\mathrm{B}}$.

C.3 Matrix Elements

Matrix elements of the Coulomb operator in the DCBS are given by

$$\begin{cases} \left(\mathbb{J}_{\mathrm{A}}\right)_{pq} = \langle \chi_p | \hat{\jmath}_{\mathrm{A}} | \chi_q \rangle = 2 \sum\limits_{i \in A} \sum\limits_{r,s=1}^{M} \left(\mathbb{C}_{\mathrm{A}}\right)_{si} \left(\mathbb{C}_{\mathrm{A}}\right)^*_{ri} (pq|rs) \\ \left(\mathbb{K}_{\mathrm{A}}\right)_{pq} = \langle \chi_p | \hat{k}_{\mathrm{A}} | \chi_q \rangle = \sum\limits_{i \in A} \sum\limits_{r,s=1}^{M} \left(\mathbb{C}_{\mathrm{A}}\right)_{ri} \left(\mathbb{C}_{\mathrm{A}}\right)^*_{si} (pr|sq) \end{cases}, \tag{C.25}$$

where we have used the following notation for two-electron integrals:

$$(pq|rs) = \int_{\mathbb{R}^3} \int_{\mathbb{R}^3} \frac{\chi_p^*(\mathbf{r}_1)\chi_q(\mathbf{r}_1)\chi_r^*(\mathbf{r}_2)\chi_s(\mathbf{r}_2)}{r_{12}} \, d^3\mathbf{r}_1 \, d^3\mathbf{r}_2. \tag{C.26}$$

Introducing the closed-shell density matrix,

$$\mathbb{P}_{\mathrm{A}} = 2\mathbb{C}_{\mathrm{A}}^{\mathrm{occ}} (\mathbb{C}_{\mathrm{A}}^{\mathrm{occ}})^{\dagger} \tag{C.27}$$

the matrix elements (C.25) are readily found to be

$$\begin{cases} \left(\mathbb{J}_{\mathrm{A}}\right)_{pq} = \sum\limits_{r,s=1}^{M} \left(\mathbb{P}_{\mathrm{A}}\right)_{sr} (pq|rs) \\ \left(\mathbb{K}_{\mathrm{A}}\right)_{pq} = \dfrac{1}{2} \sum\limits_{r,s=1}^{M} \left(\mathbb{P}_{\mathrm{A}}\right)_{rs} (pr|sq) \end{cases}. \tag{C.28}$$

The general expression for the density matrix, valid also for the open shells, reads

$$\mathbb{P} = \mathbb{C}\mathbb{O}\mathbb{C}^{\dagger}, \tag{C.29}$$

where

$$\mathbb{O} = \begin{bmatrix} k_1 & 0 & \dots & 0 \\ 0 & k_2 & \dots & 0 \\ \vdots & \vdots & \ddots & \vdots \\ 0 & 0 & \dots & k_M \end{bmatrix} \tag{C.30}$$

is the matrix containing orbital occupation numbers, i.e. $k_i = O_{ii}$ is the number of electrons of ith orbital.

The DCBS representation of the penalty operator reads

$$\widetilde{\mathbb{R}}_{\mathrm{A}} = \mathbb{S}\mathbb{C}_{\mathrm{A}}^{\mathrm{occ}}(\mathbb{C}_{\mathrm{A}}^{\mathrm{occ}})^{\dagger}\mathbb{S}. \tag{C.31}$$

C.4 Matrix Operations and DIIS

The iterative process of solving the Eqs. (2.32) (or similar ones for the dispersion-free DFT or the UHF variant of the PB method) is performed with the use of the above defined matrices replacing respective operators appearing in those Eqs. by the BLAS and LAPACK routines [56]. To accelerate the convergence, the direct inversion of the iterative subspace (DIIS) procedure of Pulay [57] is used with the following definition of the matrix scalar product:

$$\langle \mathbb{A} | \mathbb{B} \rangle = \sqrt{\mathrm{Tr}\,(\mathbb{A}^{\dagger}\mathbb{B})}. \tag{C.32}$$

C.5 DFT Integration

We restrict our attention to the functionals that depend on the density and its gradient, as is the case for the most commonly used functionals. The xc functional is calculated as

$$E^{\mathrm{xc}} = \int_{\mathbb{R}^3} F^{\mathrm{xc}}(\rho;\zeta)\, d^3\mathbf{r}, \tag{C.33}$$

where

$$\zeta = |\nabla_{\mathbf{r}}\rho| = \sqrt{\nabla_{\mathbf{r}}\rho \cdot \nabla_{\mathbf{r}}\rho}. \tag{C.34}$$

The integral (C.33) is evaluated numerically through the summation on a grid of points around the molecule. The xc potential (v^{xc}) itself is not calculated — it suffices to evaluate its matrix elements according to

$$\langle \chi_p | v^{\mathrm{xc}} | \chi_q \rangle = \int_{\mathbb{R}^3} \chi_p \frac{\partial F^{\mathrm{xc}}}{\partial \rho} \chi_q \, d^3\mathbf{r} + \int_{\mathbb{R}^3} \frac{\partial F^{\mathrm{xc}}}{\partial \zeta} \frac{\rho_\alpha}{\zeta} \nabla_\alpha (\chi_p \chi_q)\, d^3\mathbf{r}, \tag{C.35}$$

where we have used repeated suffix summation convention and

$$\rho_\alpha = \frac{\partial \rho}{\partial \alpha}, \nabla_\alpha = \frac{\partial}{\partial \alpha}, \alpha \in \{x; y; z\}. \tag{C.36}$$

Again, the integrals (C.35) are evaluated on the numerical grid.

Bibliography

[1] M. Pitoňák, P. Neogrády, J. Řezáč, P. Jurečka, M. Urban, and P. Hobza, J. Chem. Theory Comput. **4**, 1829 (2008).

[2] S. Maeda and K. Ohno, J. Phys. Chem. A **111**, 4527 (2007).

[3] B. Jeziorski, R. Moszyński, and K. Szalewicz, Chem. Rev. **94**, 1887 (1994).

[4] S. F. Boys and F. Bernardi, Mol. Phys. **19**, 553 (1970).

[5] H.-J. Werner, P. J. Knowles, R. Lindh, F. R. Manby, M. Schütz, et al., *Molpro, version 2009.2, a package of ab initio programs*, URL http://www.molpro.net.

[6] R. Bukowski, W. Cencek, P. Jankowski, M. Jeziorska, B. Jeziorski, S. A. Kucharski, V. F. Lotrich, A. J. Misquitta, R. Moszyński, K. Patkowski, et al., *SAPT2008: an ab initio program for many-body symmetry-adapted perturbation theory calculations of intermolecular interaction energies*, URL http://www.physics.udel.edu/~szalewic/SAPT/SAPT.html.

[7] G. Chałasiński and M. M. Szczęśniak, Chem. Rev. **94**, 1723 (1994); G. Chałasiński and M. M. Szczęśniak, Chem. Rev. **100**, 4227 (2000).

[8] A. Szabo and N. S. Ostlund, *Modern Quantum Chemistry: Introduction to Advanced Electronic Structure Theory* (Dover Publications, 1996).

[9] R. McWeeny, *Methods of Molecular Quantum Mechanics* (Academic Press Limited, 1989), 2nd ed., p. 128.

[10] S. Rybak, B. Jeziorski, and K. Szalewicz, J. Chem. Phys. **95**, 6576 (1991).

[11] K. Kitaura and K. Morokuma, Int. J. Quant. Chem. **10**, 325 (1976).

[12] A. J. Stone and M. Alderton, Mol. Phys. **56**, 1047 (1985).

[13] M. Gutowski and L. Piela, Mol. Phys. **64**, 337 (1988).

[14] G. Chałasiński and M. M. Szczęśniak, Mol. Phys. **63**, 205 (1988).

[15] S. Kristyán and P. Pulay, Chem. Phys. Lett. **229**, 175 (1994); J. M. Pérez-Jordá and A. D. Becke, Chem. Phys. Lett. **233**, 134 (1995); E. J. Meijer and M. Sprik, J. Chem. Phys. **105**, 8684 (1996); T. van Mourik and R. J. Gdanitz, J. Chem. Phys. **116**, 9620 (2002).

[16] S. Grimme, J. Comp. Chem. **25**, 1463 (2004); S. Grimme, J. Antony, S. Ehrlich, and H. Krieg, J. Chem. Phys. **132**, 154104 (2010).

[17] Y. Zhao, N. E. Schultz, and D. G. Truhlar, J. Chem. Phys. **123**, 161103 (2005); D. G. Truhlar and Y. Zhao, J. Chem. Phys. **125**, 194101 (2006).

[18] B. I. Lundqvist, Y. Andersson, H. Shao, S. Chan, and D. C. Langreth, Int. J. Quant. Chem. **56**, 247 (1995); Y. Andersson, D. C. Langreth., and B. I. Lundqvist, Phys. Rev. Lett. **76**, 102 (1996); O. A. von Lilienfeld, I. Tavernelli, U. Rothlisberger, and D. Sebastiani, Phys. Rev. Lett. **93**, 153004 (2004); J.-D. Chai and M. Head-Gordon, Phys. Chem. Chem. Phys. **10**, 6615 (2008).

[19] A. D. Becke and E. R. Johnson, J. Chem. Phys. **123**, 154101 (2005); A. D. Becke and E. R. Johnson, J. Chem. Phys. **124**, 014104 (2006).

[20] Y. Tawada, T. Tsuneda, S. Yanagisawa, T. Yanai, and K. Hirao, J. Chem. Phys. **120**, 8425 (2004); J. G. Ángyán, I. C. Gerber, A. Savin, and J. Toulouse, Phys. Rev. A **72**, 012510 (2005).

[21] G. Jansen and A. Heßelmann, J. Phys. Chem. A **105**, 11156 (2001); A. J. Misquitta and K. Szalewicz, Chem. Phys. Lett. **357**, 301 (2002); A. J. Misquitta, B. Jeziorski, and K. Szalewicz, Phys. Rev. Lett. **91**, 033201 (2003); A. J. Misquitta, R. Podeszwa, B. Jeziorski, and K. Szalewicz, J. Chem. Phys. **123**, 214103 (2005).

[22] M. P. Hodges, A. J. Stone, and S. S. Xantheas, J. Phys. Chem. A **101**, 9163 (1997).

[23] E. M. Mas, R. Bukowski, and K. Szalewicz, J. Chem. Phys. **118**, 4386 (2003); E. M. Mas, R. Bukowski, and K. Szalewicz, J. Chem. Phys. **118**, 4404 (2003).

[24] R. Bukowski, K. Szalewicz, G. Groenenboom, and A. van der Avoird, J. Chem. Phys. **125**, 044301 (2006).

[25] R. Ahlrichs, R. Penco, and G. Scoles, Chem. Phys. **19**, 119 (1977).

[26] C. F. Kuntz, C. Hättig, and B. A. Hess, Mol. Phys. **89**, 139 (1996).

[27] Ł. Rajchel, P. S. Żuchowski, J. Kłos, M. M. Szczęśniak, and G. Chałasiński, J. Chem. Phys. **127**, 244302 (2007).

[28] K. Pernal, R. Podeszwa, K. Patkowski, and K. Szalewicz, Phys. Rev. Lett. **103**, 263201 (2009).

[29] W. Kohn and L. J. Sham, Phys. Rev. **140**, A1133 (1965).

[30] S. M. Cybulski and C. E. Seversen, J. Chem. Phys. **119**, 12704 (2003).

[31] Ł. Rajchel, P. S. Żuchowski, M. M. Szczęśniak, and G. Chałasiński, Chem. Phys. Lett. **486**, 160 (2010).

[32] A. J. Sadlej, Mol. Phys. **39**, 1249 (1980).

[33] A. Conway and J. N. Murrell, Mol. Phys. **23**, 1143 (1972).

[34] B. Jeziorski, M. Bulski, and L. Piela, Int. J. Quant. Chem. **10**, 281 (1976).

[35] M. Gutowski, G. Chałasiński, and J. van Duijneveldt-van de Rijdt, Int. J. Quant. Chem. **26**, 971 (1984).

[36] J. Kłos, P. S. Żuchowski, Ł. Rajchel, G. Chałasiński, and M. M. Szczęśniak, J. Chem. Phys. **129**, 134302 (2008).

[37] D. J. Tozer and N. C. Handy, J. Chem. Phys. **109**, 10180 (1998).

[38] M. Grüning, O. V. Gritsenko, S. J. A. van Gisbergen, and E. J. Baerends, J. Chem. Phys. **114**, 652 (2001).

[39] Ł. Rajchel, P. S. Żuchowski, M. Hapka, M. M. Szczęśniak, and G. Chałasiński (2010), arXiv:1006.2878 [physics.chem-ph].

[40] M. Dion, H. Rydberg, E. Schröder, D. C. Langreth, and B. I. Lundqvist, Phys. Rev. Lett. **92**, 246401 (2004).

[41] A. D. Becke and E. R. Johnson, J. Chem. Phys. **127**, 124108 (2007).

[42] G. J. Williams and A. J. Stone, J. Chem. Phys. **119**, 4620 (2003); A. J. Misquitta and A. J. Stone, Mol. Phys. **106**, 1631 (2008).

[43] Ł. Rajchel, P. S. Żuchowski, M. M. Szczęśniak, and G. Chałasiński, Phys. Rev. Lett. **104**, 163001 (2010).

[44] P. Jurečka, J. Šponer, J. Černý, and P. Hobza, Phys. Chem. Chem. Phys. **8**, 1985 (2006).

[45] A. Halkier, W. Klopper, T. Helgaker, P. Jørgensen, and P. R. Taylor, J. Chem. Phys. **111**, 9157 (1999).

[46] A. D. Boese, J. M. L. Martin, and W. Klopper, J. Phys. Chem. A **111**, 11122 (2007).

[47] R. Kevorkyants, M. Dulak, and T. A. Wesołowski, J. Chem. Phys. **124**, 024104 (2006).

[48] P. Cortona, Phys. Rev. B **44**, 8454 (1991).

[49] E. V. Stefanovich and T. N. Truong, J. Chem. Phys. **104**, 2946 (1996).

[50] T. Klüner, N. Govind, Y. A. Wang, and E. A. Carter, Phys. Rev. Lett. **86**, 5954 (2001).

[51] G. Frenking, K. Wichmann, N. Fröhlich, C. Loschen, M. Lein, J. Frunzke, and V. M. Rayón, Coord. Chem. Rev. **238-239**, 55 (2003).

[52] P. Reinhardt, J.-P. Piquemal, and A. Savin, J. Chem. Theory Comput. **4**, 2020 (2008).

[53] P. Su and H. Li, J. Chem. Phys. **131**, 014102 (2009).

[54] M. Modrzejewski, Master's thesis, University of Warsaw (2010).

[55] M. Hapka, Master's thesis, University of Warsaw (2010).

[56] E. Anderson, Z. Bai, C. Bischof, S. Blackford, J. Demmel, J. Dongarra, J. Du Croz, A. Greenbaum, S. Hammarling, A. McKenney, et al., *LAPACK Users' Guide* (Society for Industrial and Applied Mathematics, 1999).

[57] P. Pulay, Chem. Phys. Lett. **73**, 393 (1980).